**DOKUZ EYLÜL UNIVERSITY**

**GRADUATE SCHOOL OF NATURAL AND APPLIED SCIENCES**

# INVESTIGATION OF MECHANICAL PROPERTIES OF FRICTION SPOT WELDED SIMILAR AND HYBRID JOINTS BETWEEN ALUMINUM ALLOYS AND POLYMERS

**by**

**Mustafa BOZKURT**

**November, 2017**

**İZMİR**

# INVESTIGATION OF MECHANICAL PROPERTIES OF FRICTION SPOT WELDED SIMILAR AND HYBRID JOINTS BETWEEN ALUMINUM ALLOYS AND POLYMERS

**A Thesis Submitted to the**
**Graduate School of Natural and Applied Sciences of Dokuz Eylül University**
**InPartial Fulfillment of the Requirements for the Degree of Master of Science**
**inMechanical Engineering, Mechanics Program**

**by**

**Mustafa BOZKURT**

**November, 2017**
**İZMİR**

**M.Sc THESIS EXAMINATION RESULT FORM**

We have read the thesis entitled **"INVESTIGATION OF MECHANICAL PROPERTIES OF FRICTION SPOT WELDED SIMILAR AND HYBRID JOINTS BETWEEN ALUMINUM ALLOYS AND POLYMERS"** completed by **MUSTAFA BOZKURT** under supervision of **PROF. DR. ÇINAR EMİNE YENİ,** and **ASSOC. PROF. DR. SAMİ SAYER** and we certify that in our opinion it is fully adequate, in scope and in quality, as a thesis for the degree of Master of Science.

Prof. Dr. Çınar Emine YENİ

Supervisor

Assoc. Prof. Dr. Sami SAYER

Supervisor

Prof. Dr. Çiçek ÖZEŞ

(Jury Member)

Doç. Dr. Hasan ÖZTÜRK

(Jury Member)

Yrd. Doç. Dr. Aydın ÜLKER

(Jury Member)

Prof.Dr. Kadriye ERTEKİN
Director
Graduate School of Natural and Applied Science

## ACKNOWLEDGEMENTS

First of all, I would like to extend my sincere gratitude to my supervisor Prof. Dr. Çınar Emine YENİ and co-supervisor Assoc. Prof. Dr. Sami SAYER for their guidance, cooperation, support and interest throughout my master education and this thesis.

I wish to express my special thanks to Research Assistant Nahit ÖZTOPRAK for his contributions and great help during my thesis study.

I would like to thanks also Opaksan Company and Par-Mak Machining Company for their technical support.

Most importantly, I am also grateful to my family who has supported me throughout my education. My sincere thanks are for my wife, Nesibe BOZKURT, for her support, encouragement and patience in every step of our life together.

Mustafa BOZKURT

# INVESTIGATION OF MECHANICAL PROPERTIES OF FRICTION SPOT WELDED SIMILAR AND HYBRID JOINTS BETWEEN ALUMINUM ALLOYS AND POLYMERS

## ABSTRACT

The use of aluminum alloys and polymers in automotive and aerospace industries is increasing day by day within the scope of weight reduction studies. In addition to weight reduction studies in the manufacturing industry, the studies are being made on metal and plastic hybrid structures, which are light and have mechanical strength. In this study, similar and hybrid joints of aluminum, polycarbonate, 30 percent glass fiber reinforced polypropylene sheets were worked on using the welding apparatus, which were designed with reference to the friction stir spot welding method. Welding applications have been carried out by using three different plunge depths depending on material type and keeping other parameters constant. The effects of plunge depth on welding strength, macrostructure and dome structure formed after welding have been investigated by mechanical tests and dimensional measurements in welded specimens. According to the force distributions obtained from the tensile tests, it was seen that the maximum average strength was increased as the plunge depth increased in similar joint of aluminum and polycarbonate sheets.

**Keywords:** Friction stir spot welding, aluminum alloys, polymers

# ALUMİNYUM ALAŞIMLAR İLE POLİMERLER ARASINDAKİ BENZER VE HİBRİT SÜRTÜNME NOKTA KAYNAKLI BAĞLANTILARIN MEKANİK ÖZELLİKLERİNİN ARAŞTIRILMASI

## ÖZ

Otomotiv ve havacılık sanayinde ağırlık azaltma çalışmaları kapsamında alüminyum alaşımları ve polimerlerin kullanımı günden güne artmaktadır. Üretim endüstrisinde ağırlık azaltma çalışmalarına ek olarak hafif ve mekanik dayanıma sahip olan metal ve plastik hibrid yapılar üzerinde çalışmalar yapılmaktadır. Bu çalışmada alüminyum, polikarbonat ve yüzde 30 cam elyaf katkılı polipropilen levhaların bir katı hal kaynak yöntemi olan sürtünme karıştırma nokta kaynağı yöntemi referans alınarak tasarlanan kaynak aparatı kullanılarak benzer ve hibrid kaynakları üzerine çalışılmıştır. Kaynak uygulamaları, kaynak malzemesi tipine bağlı üç farklı dalma derinliği kullanılarak ve diğer parametreler sabit tutularak yapılmıştır. Kaynaklı numunelerde dalma derinliğinin kaynak dayanımına, makroyapıya ve kaynak sonrası oluşan kubbe yapısına etkisi mekanik testler ve boyutsal ölçümler ile incelenmiştir. Çekme testlerinden elde edilen kuvvet dağılımlarına göre alüminyum ve polikarbonat levhaların benzer kaynaklarında dalma derinliği arttıkça maksimum ortalama kuvvetin arttığı görülmüştür.

**Anahtar kelimeler:** Sürtünme karıştırma nokta kaynağı, alüminyum alaşımları, polimerler

**CONTENTS**

**Page**

## LIST OF FIGURES

**Page**

## LIST OF TABLES

**Page**

# CHAPTER ONE
# INTRODUCTION

In today's technology, automotive and aerospace industries work on producing light-weight and environmentally friendly; vehicles and airplanes by using light and high strength materials such as aluminum, magnesium alloys and polymer matrix composites instead of steels and classical iron based alloys. These light and high strength materials are already being used in important volumes in production especially in the automotive industry. In the future, using much larger volumes of these materials will be necessary in order to manufacture more efficient vehicles, reduce energy consumption and air pollution (Mallick, 2010, Miller et al., 2000, Cole & Sherman, 1995).

In recent years, many researchers, engineers, designers and companies have been closely interested in aluminum alloys and have evaluated them as promising structural materials for automotive industry and aerospace applications (Venukumar, Yalagi & Muthukumaran, 2013). In the transport applications, aluminum is an ideal material because of its advanced properties such as high strength to weight ratio, corrosion resistance, very good thermal and electrical conductivity. At the same time, it has a critical role in reducing $CO_2$ emissions that is today's social trouble in transportation and helping to improve the sustainability of the transport industry. Use of aluminum in vehicles structures, bodies, power trains makes it possible to manufacture vehicles that are lighter, safer, more efficient and higher performance. These lighter vehicles have lower fuel consumption. Due to these reasons given above, a wide variety of aluminum products such as aluminum profiles, sheets and tubes are used by the automotive and other industry manufacturers. According to researches, use of aluminum surpassed cast iron as the second most-used material in a North American vehicle, behind steel in 2006 and the usage percentage of aluminum based on industries has been published as transportation (32%), followed by containers and packaging (21%) and building and construction (13%) (Venukumar, Muthukumaran, Yalagi & Kailas, 2014).

Although aluminum alloys have advantageous properties, the welding process of aluminum affects negatively using it in automotive, aerospace and other industries. In the automotive industry, conventional methods used for joining of aluminum alloys are resistance spot welding (RSW) and self-piercing riveting. Currently, RSW is very common and used especially in the automotive industry for welding of overlapping vehicle body parts made from aluminum in a quick and cheap manner. However, there are many disadvantages of aluminum alloys sheets such as weld cracks, high heat input, porosity and high energy consumption in RSW applications. Because aluminum has better electrical and heat conductivity then steel, RSW of aluminum needs much more heat and higher amperage level. For that reason, alternative joining methods for aluminum weld was improved named as friction stir spot welding (FSSW) instead of RSW (Gean, Westgate, Kucza & Ehrstrom, 1999, Thornton, Krause & Davies, 1996, Khan, Kuntz, Su, Gerlich, North, & Zhou, 2007).

The usage of polymeric materials has become popular in several industries such as electronics, automotive, aerospace and packaging. Joining of polymers is a critical issue in the production of complex assemblies. In the manufacturing industries, a few joining methods for similar and dissimilar polymer structures are used, which are clinching, friction lap welding and friction stir spot welding. Among these used methods, FSSW allows to join polymers as well as polymers and metal sheets and produces weld with more joining strength when compared to other welding and joining methods (Lambiase, Paoletti & Di Ilio, 2015).

There is a challenging trend that is becoming more important day by day in the manufacturing industry related to joining of lightweight dissimilar materials, especially metals and polymers. Multi-material and hybrid structures plays a critical role in terms of lightweighting in the manufacturing industry. Hybrid structures and the alternative new joining methods of them are becoming increasingly popular for research and development studies of researchers, as well as engineers (Martinsen, Hu, Carlson, 2015).

Friction stir spot welding was developed by Mazda Motor Company as an alternative joining method to RSW in the automotive industry that has been developed from friction stir welding. This method was first used in the Mazda RX-8 rear door panel spot welding in 2003 and Mazda claimed that the energy consumption has been reduced by 99% using this method when it is compared to the conventional earlier processes. Development of FSSW plays an important role in terms of energy saving in manufacturing industry and attaining more quality aluminum alloys welds. At the same time, there are many investigations and studies about the availability of this method in welding of dissimilar materials such as polymers and metals (Mishra & Mahoney 2007).

Jeon, Hong, Kwon, Cho, Han (2012) have investigated the mechanical properties and material mixing patterns of friction stir spot welded joints of dissimilar aluminum alloys that are 3 mm thick, namely Al 5052-H32 and Al 6061-T6. These aluminum alloys are used generally in automotive industry applications. Four welding combinations, as similar or dissimilar joints were applied as shown in Table 1.1 below in this study.

Table 1.1 Material combinations for FSSW of selected aluminum alloys (Jeon et al., 2012)

| Type No. | Notation | Top material (upper sheet) | Bottom material (lower sheet) |
|---|---|---|---|
| 1 | T5B5 | Al 5052-H32 | Al 5052-H32 |
| 2 | T5B6 | Al 5052-H32 | Al 6061-T6 |
| 3 | T6B6 | Al 6061-T6 | Al 6061-T6 |
| 4 | T6B5 | Al 6061-T6 | Al 5052-H32 |

In the study, the process parameters including the z-axis force and torque were measured as a function of the tool displacement. The mechanical properties were evaluated by microhardness measurements of the joints and the material mixing zone was investigated by an electron probe micro-analyzer. Figure 1.1 shows cross-sectional views of welded samples. At the end of the study, 5052-H32 and 6061-T6 aluminum alloys were successfully joined by FSSW under the predefined

weld parameters without visible superficial porosity or macroscopic defects (Jeon et al., 2012).

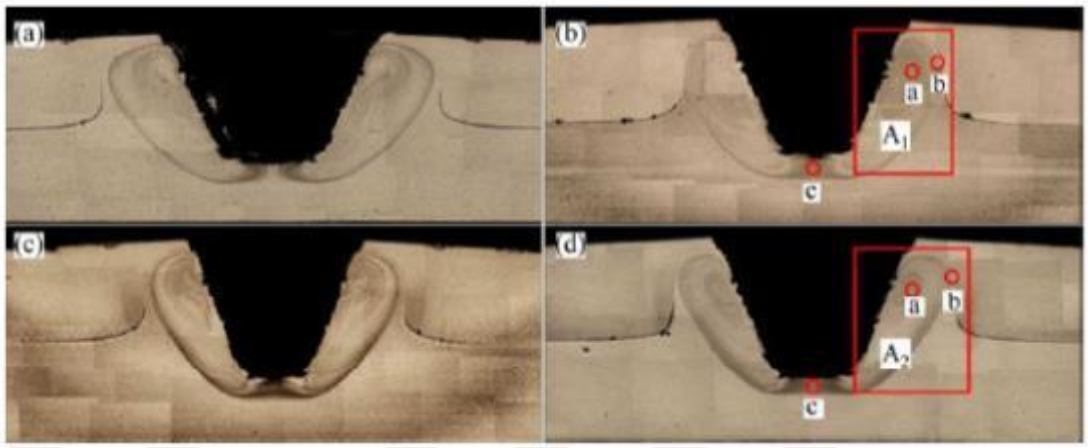


Figure 1.1 Cross-sectional optical micrographs of T5B5 (a), T5B6 (b), T6B6 (c) and T6B5 (d) joints (Jeon et al., 2012)

Zhang, Yang, Zhang, Zhou, Xu & Zou (2011), have studied the normal FSSW and walking FSSW of AA 5052-H112 1mm thick sheets. They have investigated the effect of rotational speed and dwell time on microstructure and mechanical properties of joints. In the study, the hardness profile of the welds were exhibited and it was seen that minimum hardness occurs in the heat affected zone of the welds. In addition, the results of cross-tension tests and tensile tests show that the weld joint strength decreases with increasing rotational speed and it is not affected significantly by the dwell time (Zhang et al., 2011).

Piccini and Svoboda (2015) have investigated the effect of tool penetration depth during welding process and the relative position of the materials used in the superimposed joints for the friction stir spot welding of 3 mm thick AA5052 sheets and 2 mm thick AA 6063 sheets. In the study, tool penetration depths between 0.05 and 1.25 mm were analyzed for welding sample combinations. Sample combinations were defined according to upper sheet type. In the analysis, the effect of penetration depth, macrostructural and dimension characterization, microhardness measurements and peel tests were conducted for different conditions. They reported that the fracture loads gained from peel test increases with the tool penetration depth for both material

positions and the fracture load is higher when AA 6063 is the upper material (Piccini & Svoboda, 2015).

Sudağ (2011), has studied friction stir spot welding of 3 mm thick AA 6061 and AA 7075 materials and has investigated the mechanical properties of welded specimens. In this study, tool rotational speed and process time were constant and the variable parameter is three different tool geometries for each sample group. Tensile strength and microhardness measurements were used to evaluate the mechanical properties of the welded samples and the parent metal, thermo mechanical affected zone, heat affected zone of welded section of samples were also observed by using microstructure and scanning electron microscope images. Best mechanical and metallurgical results were gained from the specimens which were joined using cylindrical tool geometry (Sudağ, 2011).

In 2015, Lambiase, Paoletti, Di Ilio have investigated the mechanical behaviour of friction stir spot welds of 3 mm thick polycarbonate sheets. The aim of this study is to analyze the influence of rotational speed and processing time on mechanical properties of FSSW joints of polycarbonate sheets. The variable parameters are rotational speed, tool plunge rate, pre-heating time, dwell time and waiting time. Mechanical evaluation of welded samples was carried out by means of single lap shear tests and the most critical factors that influence the mechanical behaviour of FSSW joints were determined. According to achieved results of the study, tool plunge rate, dwell time and waiting time are the most influencing parameters on the joint strength. Figure 1.2 shows sample of welded polycarbonate sheets using FSSW (Lambiase et al., 2015).

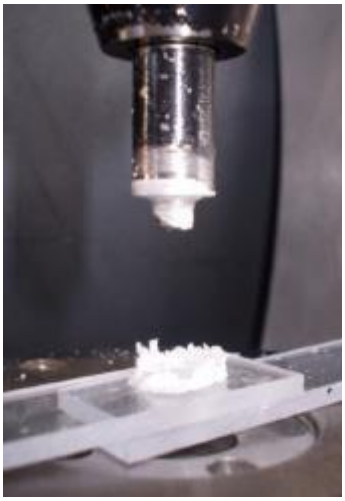

Figure 1.2 Schematic of FSSW of polycarbonate sheets (Lambiase et al., 2015)

Arıcı & Mert (2008) have studied the friction stir spot welding of polypropylene sheets with 5 mm thickness. They have investigated the effects of tool penetration depth and dwell time on the tensile shear strength of lap joints for polypropylene sheets. At the end of the study, an optimum combination of parameters that makes joint tensile failure load maximum was determined (Arıcı & Mert, 2008).

In this study, friction stir spot welding method have been applied to the joining of AA 5052-H32, polycarbonate and polypropylene GF%30 sheets as similar and hybrid joint combinations. The special welding apparatus based on friction stir spot welding method has been designed and manufactured. The mechanical, macrostructural properties of welded samples and weldebility of aluminum and polymers by using the method of FSSW has been investigated and evaluated.

# CHAPTER TWO

# FRICTION STIR WELDING AND FRICTION STIR SPOT WELDING METHOD

## 2.1 Friction Stir Welding

The friction stir welding (FSW) method is a solid state joining technique, invented by The Welding Institute (TWI) of UK in 1991. This welding technology produces weld between two sheet plates by the heating and plastic material displacement caused by a rapidly rotating tool and its linear motion along the welding line. Because of its solid-state joining properties, friction stir welding produces more quality structural joints when it is compared to conventional arc welds in aluminum, steel, nickel, copper, and titanium alloys. The advantages of this method over conventional arc welding methods are higher strength, increased fatigue life, lower distortion, less residual stress and less sensitivity to corrosion (Mishra & Mahoney, 2007).

Friction stir welding method uses a nonconsumable tool in order to create heat between tool and workpieces. In this welding method, a tool is used commonly, which has the shape of rode including a concave shoulder surface and a pin. The shoulder surface contacts with the workpieces and the pin plunges into the workpiece in welding process. Before welding operation, the workpieces are clamped to prevent relative motion between them and they are supported by a backing plate during friction stir welding. A critical point for the tool design is that the pin should be shorter than the thickness of the weld joint in order to prevent a contact between the pin and backing plate. Figure 2.1 shows the three-dimensional friction stir welding method schematically (Mishra & Mahoney, 2007, Schwartz, 2011 & Önol, 2010).

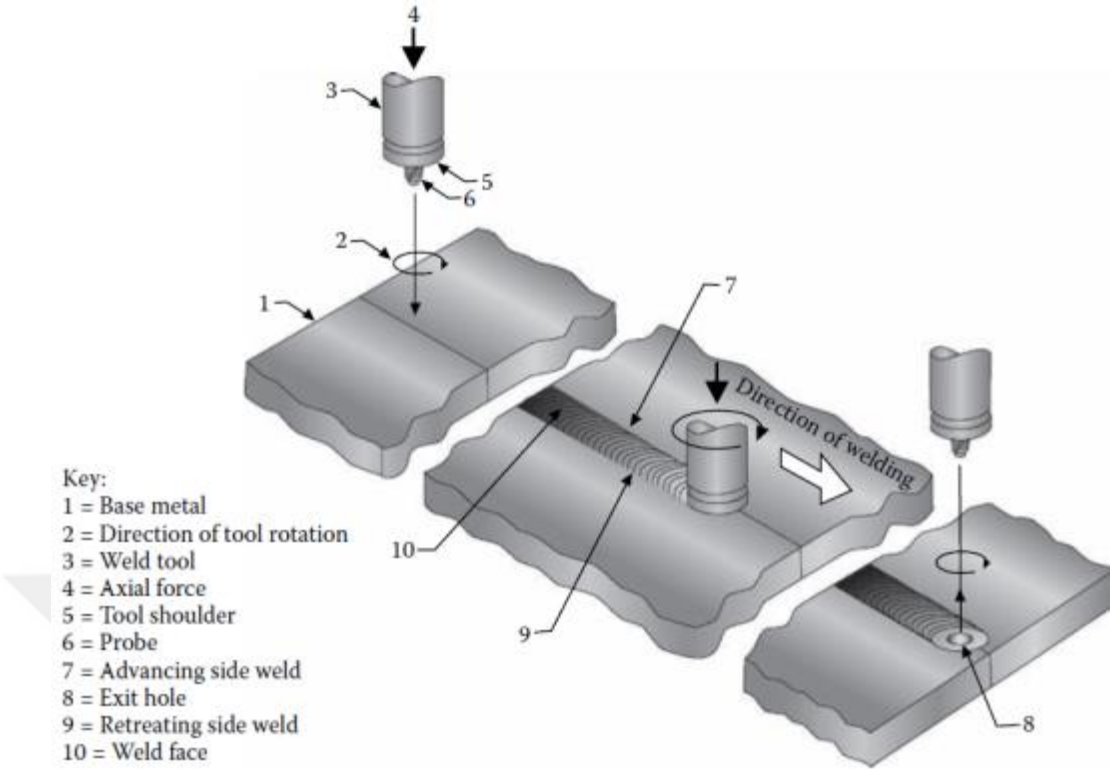


Figure 2.1 Schematic of FSW Method (Schwartz, 2011)

In the basic concept of the welding method, the consumable tool starts to rotate with predefined speed and then contacts and penetrates into the abutting edges of the workpieces being welded. Within this time period, the frictional heat is produced by rotational speed and plunge motion of the tool. The tool traverses along the welding line from starting point to the end point of the weld. While the tool rotates, it generates a large amount of frictional heat on the workpieces. Frictional heat softens the material surrounding the pin and provide movement of material flow around the pin in order to relocate the material from in front of to the backside of the rotating pin. Because no melting occurs in this process, the welding method is defined as a solid-state joining technology (Mishra & Mahoney, 2007, Schwartz, 2011 & Önol, 2010).

## 2.2 Friction Stir Spot Welding

Friction stir spot welding (FSSW), is a derivative of friction stir welding (FSW), which was developed by the Mazda Motor Company and Kawasaki Heavy Industry. Firstly, this new welding technology was applied in the Mazda RX-8 rear door panel

spot welding in 2003 (Sakano et al., 2001 & Iwashita, 2003). It was reported that FSSW method provides a great reduction in equipment investment and energy consumption when it is compared to resistance spot welding (RSW). This welding method has a great usage potential in the manufacturing industries instead of spot joining processes such as resistance spot welding and riveting (Hancock, 2004).

The main difference of friction stir spot welding from friction stir welding is that FSSW does not include traverse movement after plunging a rotating noncomsumable tool in to the welding sheets (Mishra & Mahoney, 2007).

The FSSW method includes three main phases that are plunging, stirring, and retraction. Figure 2.2 shows schematically the three-dimensional friction stir spot welding method. The welding process starts with plunging the tool into the welding sheets until the shoulder contacts the top surface of the upper workpiece with high rotational speed. At the next step, the stirring phase enables the mixing of the two workpiece materials under the compression pressure caused by the vertical motion of the welding tool.

At the stirring phase of welding, the bonding between two workpieces occurs due to the compression pressure and frictional heat that cause inter-diffusion of material across the interface at atomic level. The shoulder and the pin play important roles respectively for producing of the frictional heat and mixing of the material in welding zone. Finally, once a predefined penetration depth is reached, the tool retracts from the workpieces (Awang, 2007).

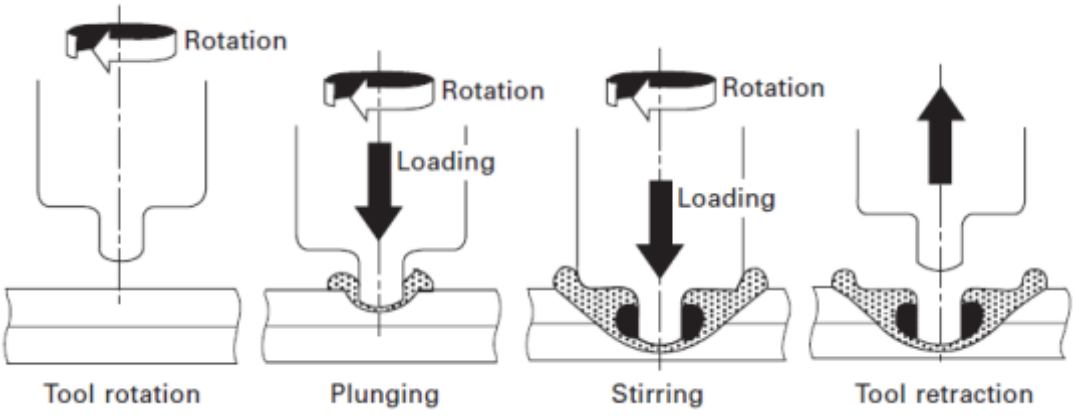


Figure 2.2 Schematic of FSSW (Mallick, 2010)

### *2.2.1 Types of Friction Stir Spot Welding*

Friction stir spot welding can be classified into five categories as indicated below;

- Pure spot friction stir welding,
- Refill friction stir spot welding,
- Swing friction stir spot welding,
- Stitch friction stir spot welding,
- Pinless friction stir spot welding (Okamoto, Hunt & Hirano, 2005, Yang, Fu & Li, 2014, Mishra & Mahoney, 2007).

#### *2.2.1.1 Pure Spot FSW*

Pure spot FSW is the most commonly used welding type in current industries and is also known as ‘’Plunge Type FSSW’’. A basic schematic illustration of the pure spot FSW process is indicated in Figure 2.3. This welding method is applied to a lap joint consisting of upper and lower sheets. During pure spot FSW, a rotating tool with a protruded pin is plunged into the material from the top surface of the upper sheet to a predetermined plunge depth. In this stage frictional heat is generated (with a certain dwell time), at the same time, a backing plate located below of the lower sheet contacts the lower workpiece to support the downward force. The generated frictional heat between the tool and workpieces softens the surrounding material and the rotating and moving pin causes plastic material flow in both circumferential and axial directions. In addition, the shoulder of the welding tool gives a strong compressive force to the welding sheets. Finally, the tool is retracted from the material and a solid-state bond is achieved between the upper and lower welding sheets (Mishra & Mahoney, 2007).

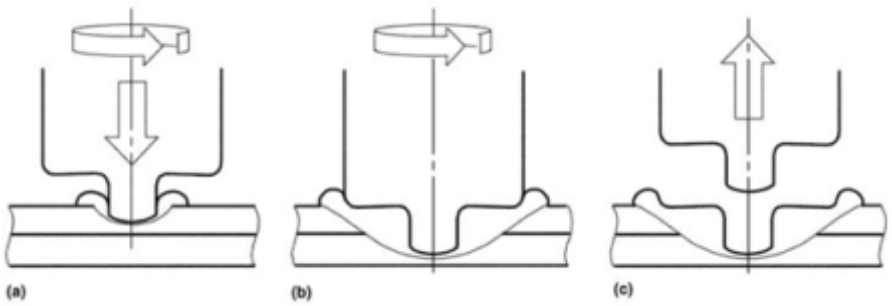


Figure 2.3 A schematic of a plunge type FSSW (a) plunging, (b) bonding, (c) drawing out (Mishra & Mahoney, 2007)

The appearance and cross-sectional configuration of a pure spot friction stir weld of sheets is shown in Figure 2.4. There is a hole at the upper surface of the weld and the bottom surface of weld has a flat surface. The welding hole is created by the pin of the tool and it reaches to lower workpiece without drilling on the bottom sheet (Mishra & Mahoney, 2007).

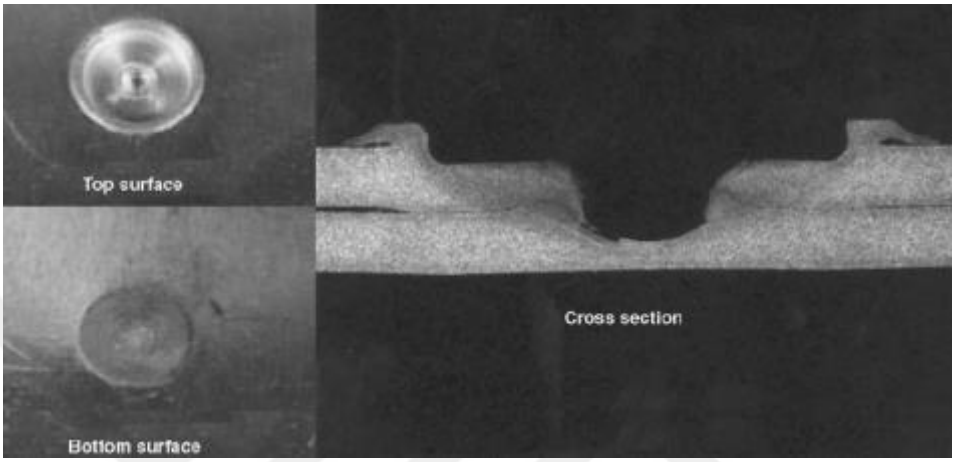


Figure 2.4 Cross-sectional configuration of a FSSW (Mishra & Mahoney, 2007)

### *2.2.1.2 Refill FSSW*

Refill FSSW (RFSSW), which is a patented method of GKSS (Germany) joins two sheets of material with the lap configuration of welding sheets. In this method, the weld region consists of a spot of material that has been plasticized and displaced during the weld process. In forming a weld spot, material back extrusion, material replacement and surface flushing steps are followed. Figure 2.5 shows the three-dimensional Refill FSSW method schematically (Mishra et al., 2007).

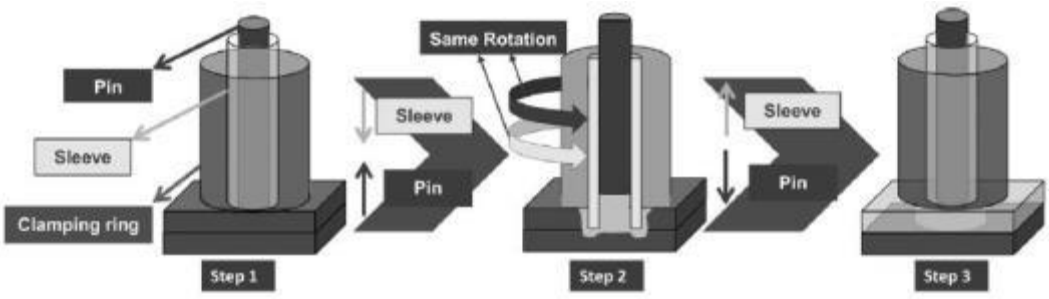


Figure 2.5 Schematic of three-dimensional refill FSSW method (Gonçalves, Santos, Canto, Amancio-Filho, 2015)

The refill FSSW method uses a three-piece weld tool system that includes a clamp ring, outer shoulder, and inner pin. Each of these three pieces are controlled by a separate actuation system such that each can be moved down or up independently and concentrically. The refill FSSW includes three main stages during the weld process that are initiation, full plunge and full retract as shown in Figure 2.6.

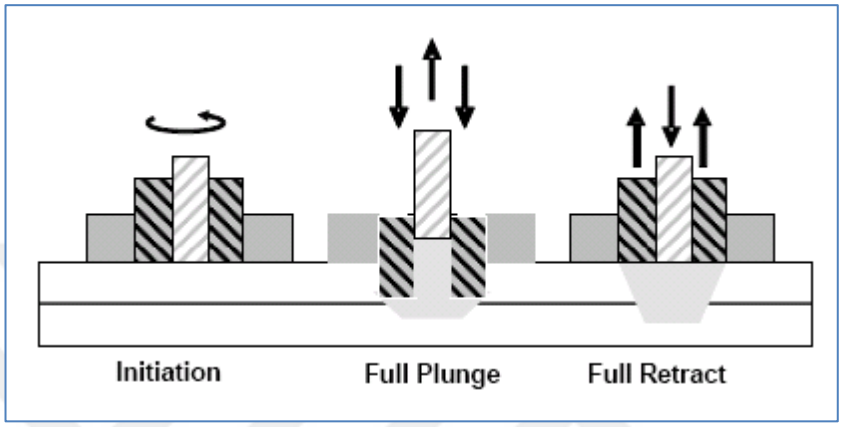


Figure 2.6 Cross-sectional configuration of refill FSSW process (Allen & Arbegast, 2005)

In the welding process, firstly the weld workpieces are overlapped and fixed against a backing bar by using a clamp ring under a constant pressure. In the initiation stage, both the pin and shoulder start to rotate concentrically in the same direction at a pre-set rotational speed and both of them are positioned on the top surface of the upper weld sheet. During this step, necessary frictional heat is generated for plunging between the tool and the sheets. In the full plunge stage, the shoulder plunges into the sheet material and at the same time the pin retracts upward. Finally, in the full retract stage the shoulder and the pin return to their original position and while they are returning to initial position, the displaced material is pushed back into the gap created by the shoulder (Mishra & Mahoney, 2007, Gonçalves, Santos, Canto & Amancio-Filho, 2015).

Although the above mentioned welding method is an innovative one it has a disadvantage caused by sticking issues. In the full plunge step, the larger diameter shoulder relocates an important volume of plasticized material and this requires the smaller diameter pin to retract to a greater distance in order to provide constant material volume exchange. The large motion of the pin draws the plasticized materials

into the cooler area of the shoulder and in addition the material adheres to the inner wall of the shoulder. This issue causes sticking and locking of the pin in the shoulder periodically in the weld process. To resolve the disadvantage of this explained process, a modified refill FSSW method was improved (Mishra & Mahoney, 2007).

The modified Refill FSSW process includes four stages. The main difference of this method is that a pin plunges into the material instead of the shoulder plunging into the material. In the first stage, the rotating pin and shoulder start to go towards the sheets with the same vertical velocity as shown in Figure 2.7. During stage-2, the pin plunges into the welding material up to a predefined depth and the space created by the motion of shoulder is filled with the displaced weld material. In Stage-3, the pin is retracted into the shoulder and at the same time the shoulder extrudes the displaced material from the previous stage, back into initial position. In the last stage, the pin and the shoulder are retracted to the initial position with the same vertical velocity and the weld process is completed (Mishra & Mahoney, 2007).

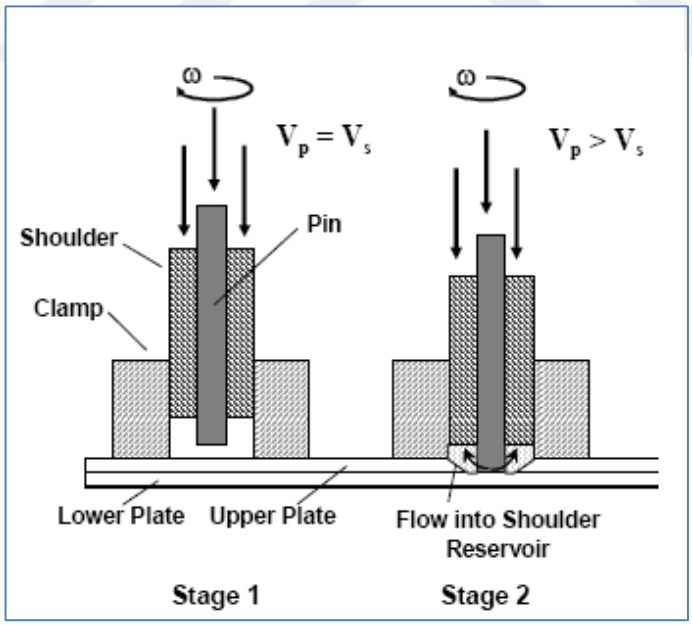

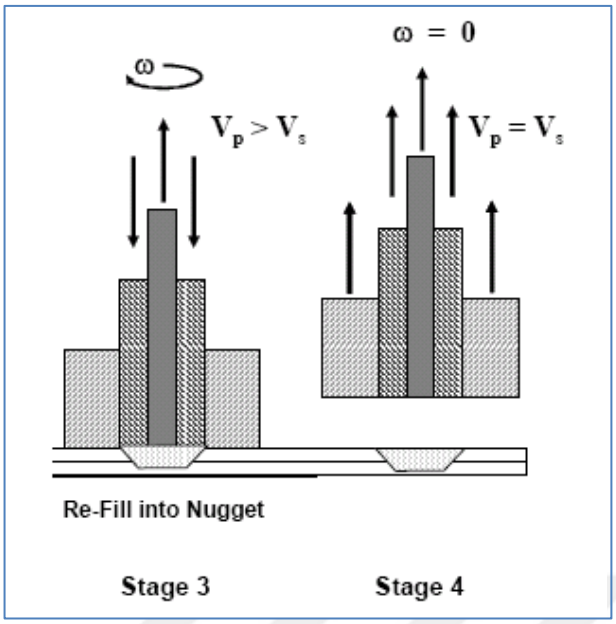


Figure 2.7 Schematic show of the modified refill FSSW process (Mishra & Mahoney, 2007)

Tier et al, (2013), have investigated the influence of plunge depth, rotational speed, plunge rate and time on the microstructure and shear strength of refill FSSW. In this study, refill FSSW of AA 5042-0 1.5 mm thick sheet material was used and the welds were performed using an prototype refill friction spot welding machine that is capable of applying forces up to 15 kN (vertical axis) and a maximum rotation speed of 3000 rpm. The welding tool has a three-piece system: an 18 mm diameter clamping ring, a 9 mm diameter threaded sleeve and a 5.2 mm diameter grooved pin, as shown in Figure 2.8. The critical property of the tool is that each of its pieces has an independent actuator system and this way they can be moved up and down independently to provide the refill process.

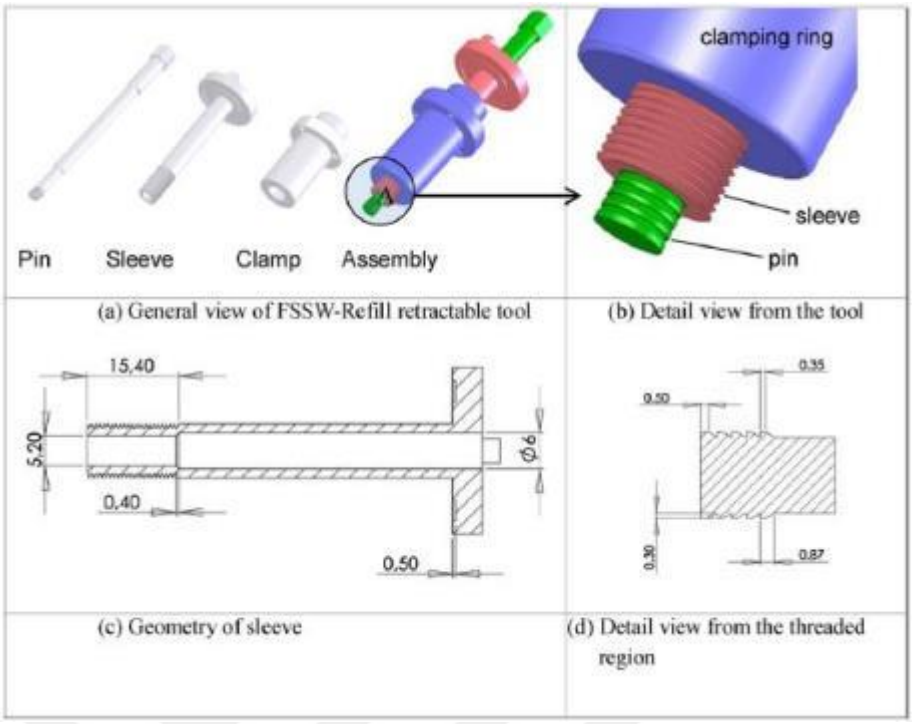


Figure 2.8 Schematic illustration of the three-piece retractable tool system in refill FSSW

Tier et al., (2013) have welded the aluminum sheets with the rotational speed range of 900 rpm to 1900 rpm, the test results of samples have shown high strength joint and low strength joint views. Figure 2.9 shows a high strength weld sample and Figure 2.10 shows a low strength weld sample, respectively.

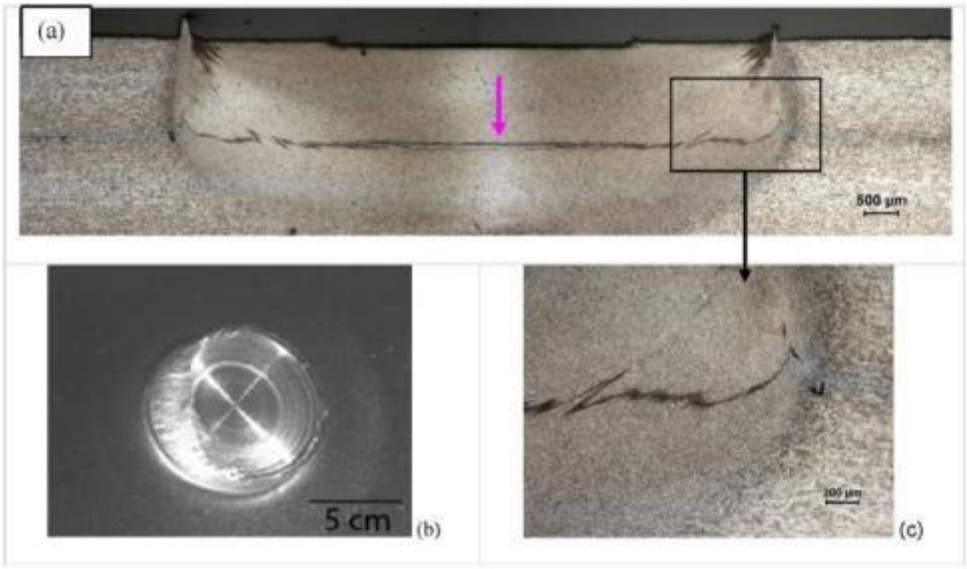


Figure 2.9 A high strength joint: (a) cross section of FSSW-Refill joint no. 02 processed at 900 rpm (6.21 kN); (b) “pull out” fracture; and (c) zoom from the interface at the lower right corner

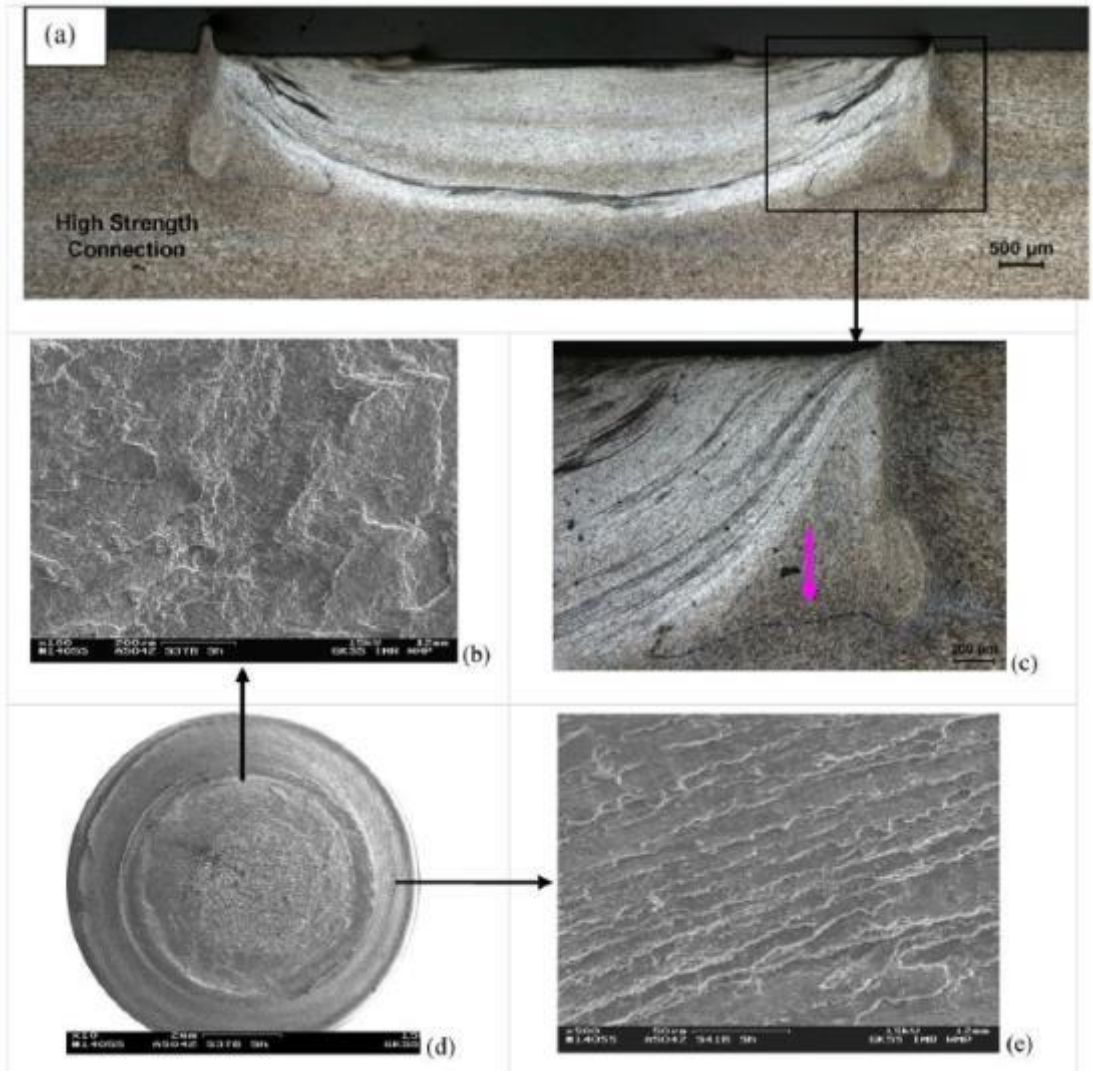


Figure 2.10 Low strength connection: (a) cross-section of connection no. 10 processed at 1900 rpm, 1.31 mm/s (4.53 kN); (b) SEM of fracture surface in the center of the weld; (c) zoom from the interface at lower right corner; (d) through welding fracture; and (e) SEM of fracture surface in the corner of the weld

Tier et al., (2013), have used the Statictica software package to correlate process parameters with the mechanical properties of the joints and it was explained that the most important parameters are the plunge depth and rotational speed in terms of mechanical properties.

*2.2.1.3 Swing FSSW*

Hitachi developed the technique of swing FSSW (Okamoto, Hunt & Hirano, 2005). This method, different from conventional FSSW, after the tool plunging into the sheet material, the tool goes up a little but this motion is accepted as negligible level, and then the tool moves with a small angle and a big radius like a swing motion. Figure 2.11 shows the schematic of this alternative method. The advantage of such a method is that the contact area of the weld is greater and the strength of weld is better (Mishra & Mahoney, 2007).

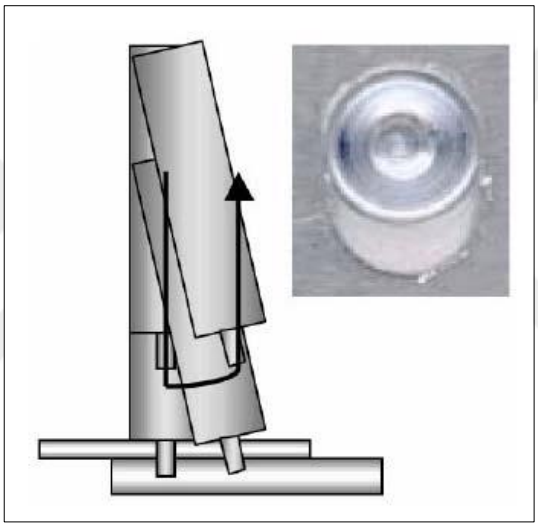

Figure 2.11 Schematic of swing FSSW (Mishra & Mahoney, 2007)

Figure 2.12 shows the weld path of the swing friction stir spot welding and this motion of the shoulder provides a larger weld spot.

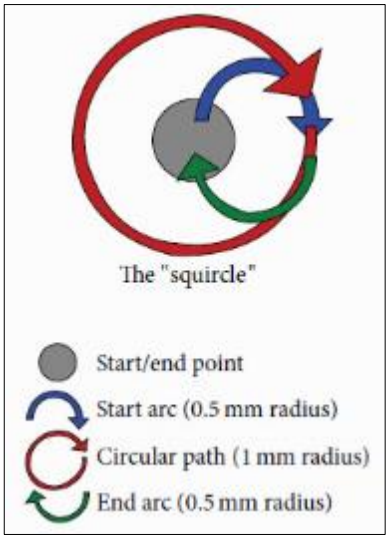


Figure 2.12 Schematic illustration of weld path of swing FSSW (Yang et al., 2014)

*2.2.1.4 Stitch FSSW*

Stitch friction stir spot welding is another version of FSSW from GKSS (Germany). In this method, after the tool plunge, it traverses a short linear distance parallel to the sheet surface as shown in Figure 2.13. The purpose of this method is to produce spot welds with larger joining areas and higher strength (Okamoto et al., 2005).

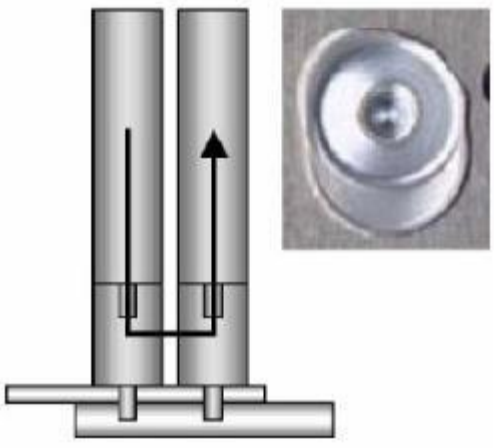

Figure 2.13 Illustration of stitch FSSW (Mishra & Mahoney, 2007)

Venukumar, Babya, Muthukumaran & Kailasb (2014), have applied a novel spot welding process named walking friction stir spot welding (WFSSW) for AA 6061-T6 joints in order to increase the strength of the joint. In this study, the tool movement is

over a distance of 15 mm and the method of this welding process is the same with stitch FSSW as shown in Figure 2.14 (Venukumar, Muthukumaran et al., 2014).

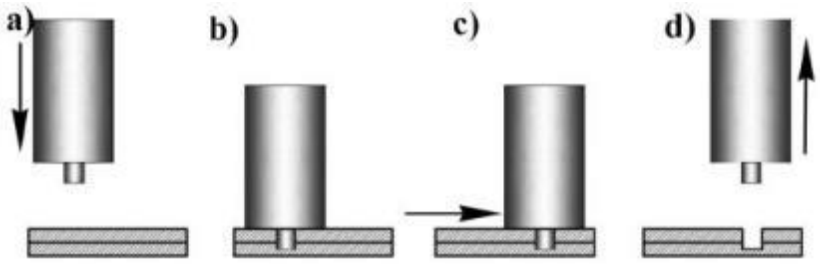


Figure 2.14 Schematic representation of WFSSW (Venukumar, Muthukumaran et al., 2014)

The welds were carried out for four different rotational speeds (900 rpm, 1120 rpm, 1400 rpm, 1800 rpm) and the best static shear strength was achieved at a tool rotational speed of 900 rpm as given in Figure 2.15.

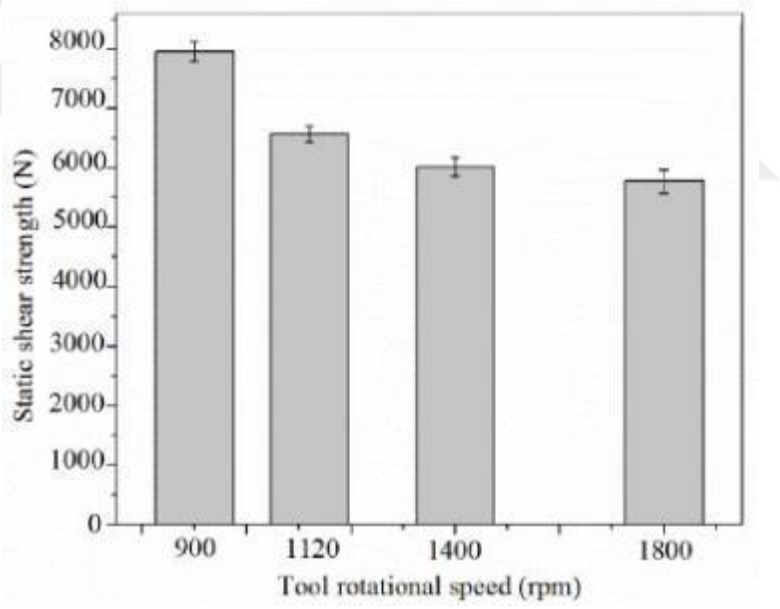


Figure 2.15 Static shear strength of WFSSW joints made by WFSSW (Venukumar, Muthukumaran et al., 2014)

Venukumar, Muthukumaran et al. (2014), have analyzed the microhardness distribution of WFSSW joint made at a tool rotational speed of 900 rpm in different regions of the weld. The hardness measurement results of aluminum alloy showed W-shape distribution as shown in Figure 2.16. It was observed that the hardness increase in SZ of joint is due to fine grains and precipitates.

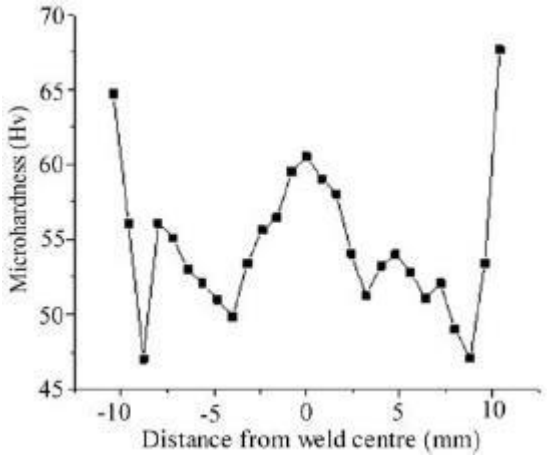


Figure 2.16 Hardness profile of WFSSW joint across the weld interface. (Venukumar, Muthukumaran et al., 2014)

Venukumar, Muthukumaran et al. (2014), have carried out macro and microstructural analysis in order to analyze the local material microstructure evolution and fatigue tests were also conducted. As a result of this study, the increasing in the rotational speed causes the generation of coarse grains and decreases the static shear strength. In addition, higher micro hardness and fine grain structure was observed in the stir zone.

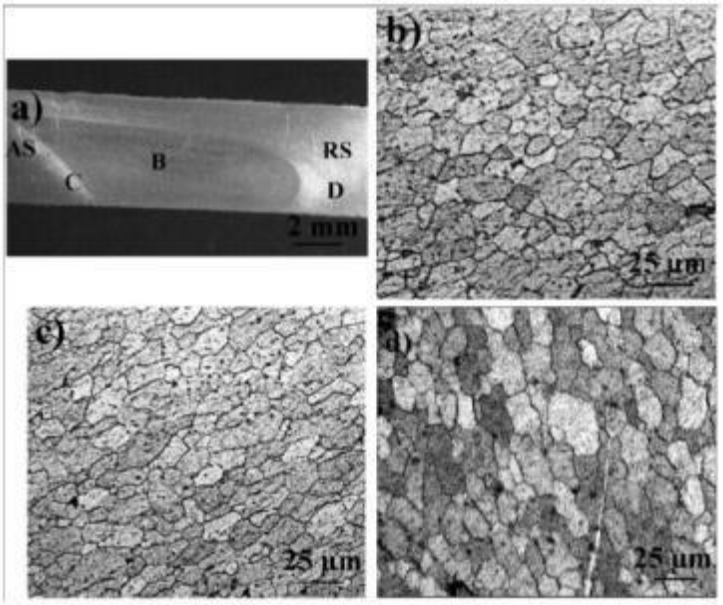


Figure 2.17 (a) Macroscopic appearance of the WFSSW joint; Microstructures in WFSSW (b) SZ (c) TMAZ (d) BM (Venukumar, Muthukumaran et al., 2014)

*2.2.1.5 Pinless FSSW*

The pinless version of FSSW was invented by Tazoki. In this method, the tools work without pin but there is a scroll groove on the shoulder surface. This process can be preferred due to its advantages of being a simpler process, having a better weld appearance and weld without keyhole. In addition to these advantages, recently, the obtained preliminary data have shown that this method can be used to produce high-strength welds with a short dwell time in several applications. Pinless FSSW method is schematically shown in Figure 2.18 (Yang et al., 2014).

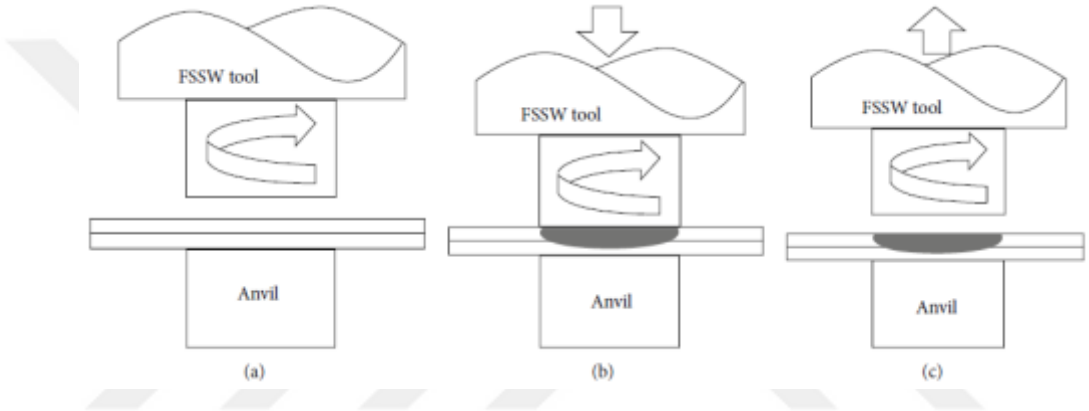


Figure 2.18 Illustration of the pinless FSSW process: (a) plunging, (b) stirring, and (c) retracting (Yang et al., 2014)

Tozaki, Uematsub & Tokajib (2010), have developed a new tool as shown in Figure 2.19, which has no pin but has a scroll groove (scroll tool) of 0.5 mm depth on its shoulder surface. This tool was used in FWWS of 2mm thick aluminum alloy 6061-T4 sheets and the potential of it was discussed in terms of weld structure and static strength of welds.

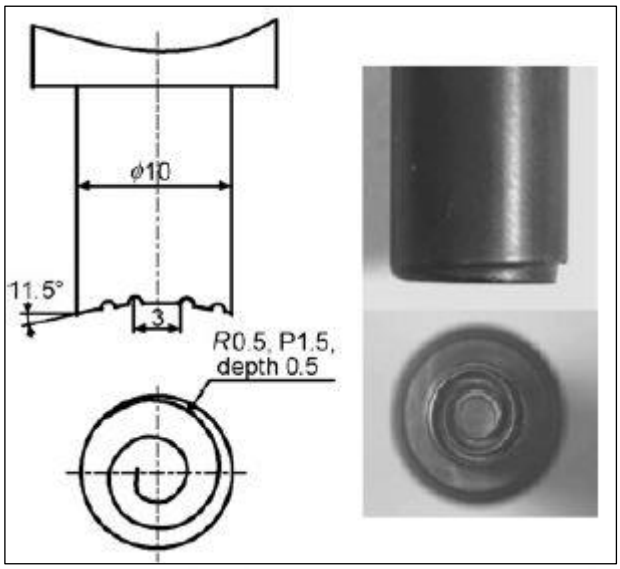


Figure 2.19 Configuration and photograph of newly developed tool. All dimensions are in mm

A newly developed tool was compared with two different tools in terms of welding potential and performance. First one is a conventional pin tool with a standard metric M3 left-hand threaded and the pin length is 3.7 mm. The other tool is a plain tool that has no probe or scroll groove. The shoulder is the same for all welding tools which is 10 mm diameter and concave shape with the angle of concavity of 11.5°. In this study, the tool rotational speeds of 2000 and 3000 rpm, the tool holding times of 1–7 s and the shoulder plunge depths of 0.5, 0.7 and 0.9 mm were used for the scroll tool and the plain tool. For the probe tool welding applications, the tool holding times of 0.2, 1, 2 and 3 s, the tool rotational speeds of 2000 and 3000 rpm and were used. The plunge rate is the same, 10 mm/min, in all cases. Figure 2.20 shows the macroscopic weld structures of a longitudinal section of the welds made by the pin tool and the scroll tool. In case of using the pin tool, a classical friction stir spot weld structure including a pin hole in the center of the weld zone can be seen. In case of using the scroll tool, there is no probe hole. It can be seen from longitudinal section of welded samples that the using of scroll tool has a advantage in terms of having weld structure without a hole.

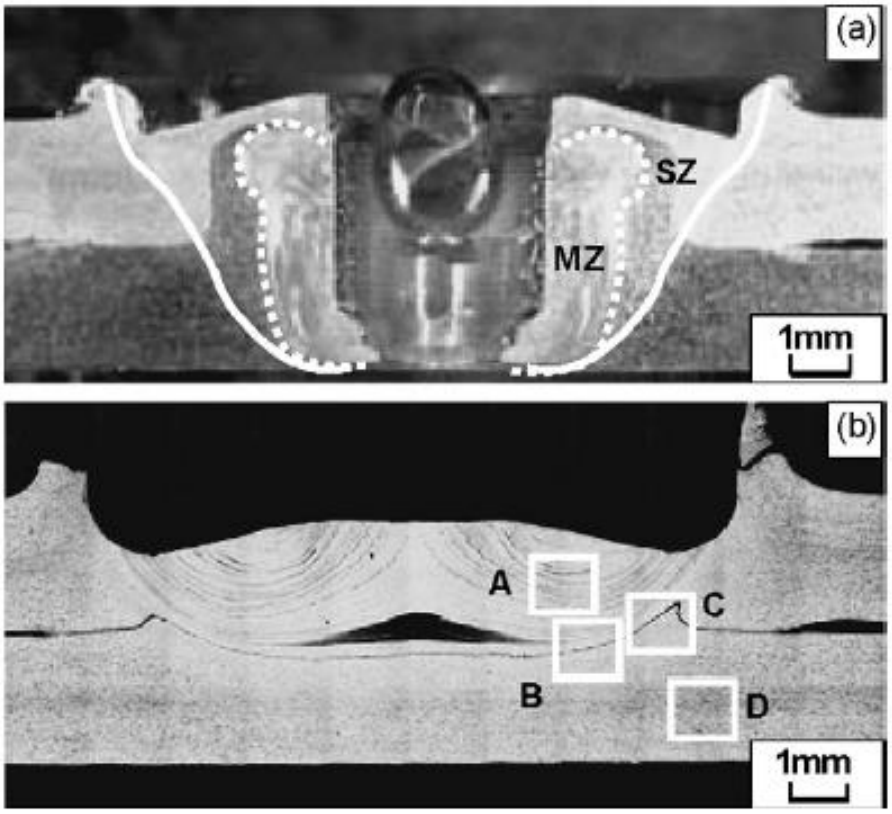


Figure 2.20 Weld structures of longitudinal section made by (a) probe tool (b) scroll tool

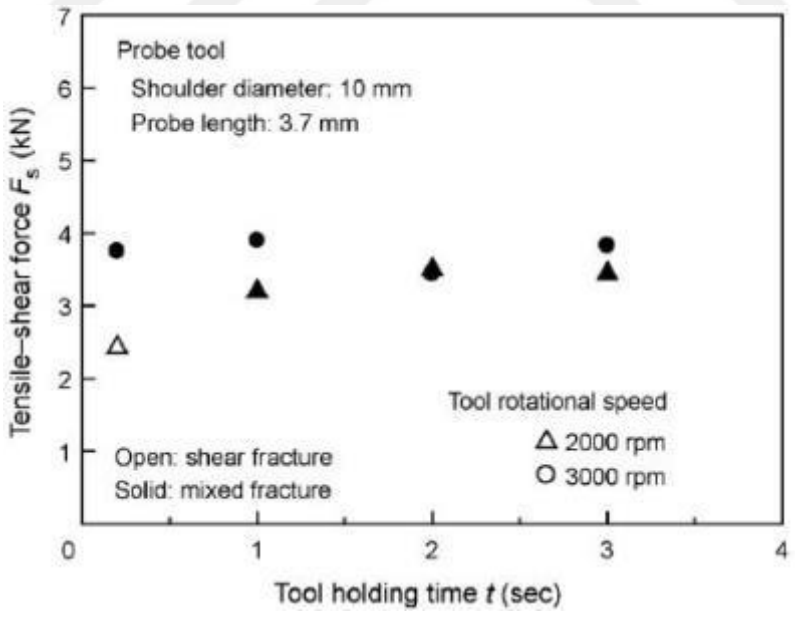


Figure 2.21 Tensile-shear strength of welds made by probe tool

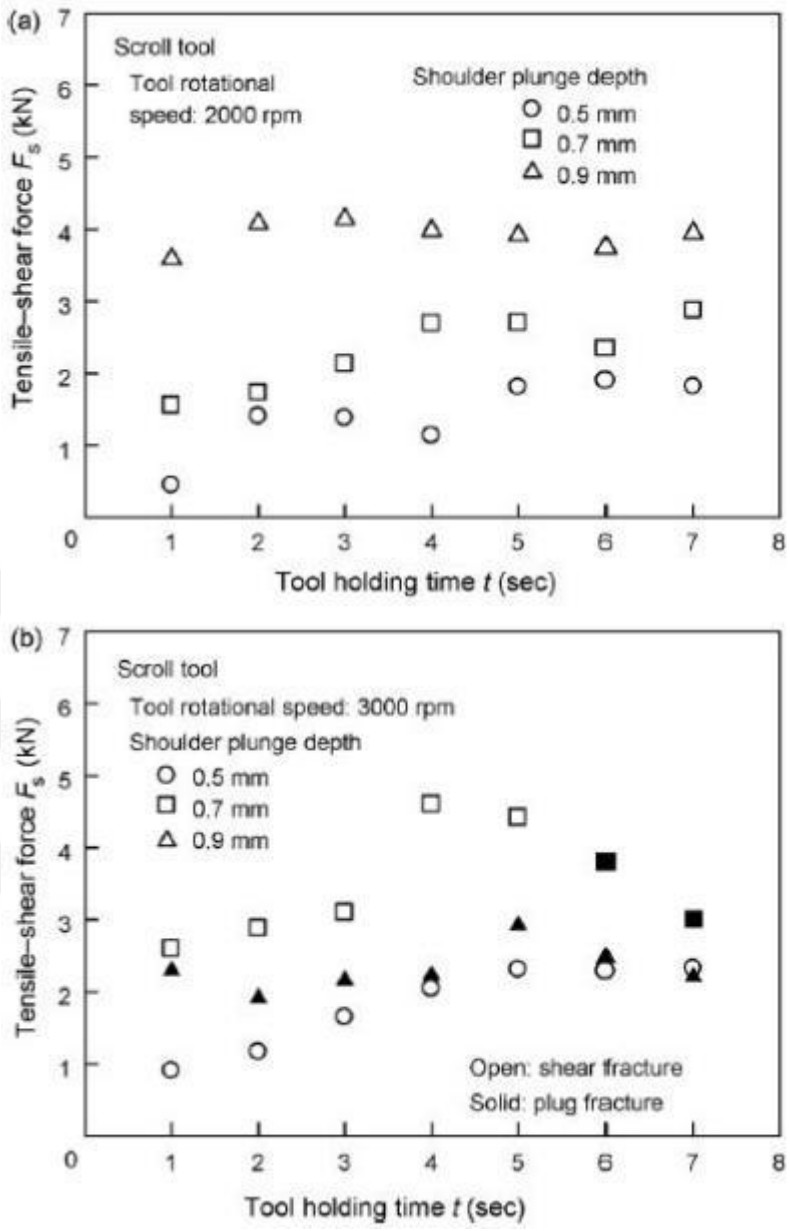


Figure 2.22 Tensile-shear strength of welds made by scroll tool

Figure 2.21 shows the tensile-shear strength of welds made by probe tool as a function of tool holding time and similarly, Figure 2.22 shows tensile-shear strength of welds made by scroll tool. In the final part of this study, experiments and observations showed that the scroll tool has comparable or superior performance to a conventional probe tool. The maximum tensile-shear strength of the welds was achieved by the scroll tool and it was found to be 4.6 kN that was higher than that of the welds made by the probe tool (Tozaki, Uematsub & Tokajik, 2010).

### *2.2.2 Process Parameters of Friction Stir Spot Welds*

Friction stir spot welding process can be characterized by four process parameters which are the tool rotational speed, plunge rate, plunge depth and dwell time. These parameters are determined depending on the materials being joined, sheet thickness and tool geometry. In the literature, these parameters were investigated in order to find optimal parameters related to joint mechanical properties of many different materials in several studies (Mallick, 2010).

The rotational speed is one of the dominant process parameter in FSSW. It is critical in welding process because the heat input into the weld zone is related to rotational speed. It is generally between 1000 and 3000 rpm in the applications based on the materials used (Mallick, 2010).

In the FSSW process, plunge rate directly affects the required welding force and is directly related with welding force. When the plunge rate is increased, the required welding force increases. In addition, plunge rate is in connection with the heat input into the weld zone. In the welding process, the tool and work pieces are heated up during the plunging of the weld tool in to the work pieces. The microstructure of joint is affected more rapidly in the beginning of the weld application with a higher plunge rate that gives a higher heating rate. If the plunge rate is fast, the material to be welded is less softened in the initial plunging step. In case of the plunge rate is fast in applications, tool wears more and its life is influenced by the plunge rate. According to previous studies, the plunge rate was found have a greater effect on tensile shear fracture load (Mishra & Mahoney, 2007; Jambhale, Kumar & Kumar, 2015).

In the FSSW process, the tool that includes the shoulder and the pin stays in rotation for a short time at its bottom location before the retraction step. This time is called as dwell time and it is the most dominant welding parameter for the weld strength. During weld process, it is expected that a longer dwell time causes a larger heat generation in the weld zone because the weld tool has more time in order to generate heat. There are few studies in the literature, which describe the effect of dwell time on FSSW. According to studies carried out in the past, it has been determined that

there seems to be an improvement of the tensile shear strength when the dwell time increases. This result can be explained as a long dwell time causes a larger welded area and a higher quantity of intermetallic compounds (Jambhale et al., 2015).

### *2.2.3 Tool Design of Friction Stir Spot Welds*

The tool design in the friction stir spot welding applications is the critical parameter for weld quality and is a very popular topic for researchers and engineers. The FSSW tool consists of basically the shoulder and the pin. The length and geometry of the pin and geometry and diameter of the shoulder are the topics for the studies that have been carried out in the past in order to achieve an optimal tool design.

#### *2.2.3.1 Pin Geometry of FSSW*

A number of studies on the pin geometry have been conducted in order to investigate its effect on FSSW. Bilici & Yükler (2012), have investigated the influence of tool geometry and process parameters on macrostructure and static strength of friction stir spot welded polyethylene sheets. In this study, six different pins with different shoulder geometries, different pin length, pin angle and concavity angle as shown in Figure 2.23 (straight cylindrical, tapered cylindrical, threaded cylindrical, triangular, square and hexagonal) were evaluated to identify the optimal geometry of the pin for joints.

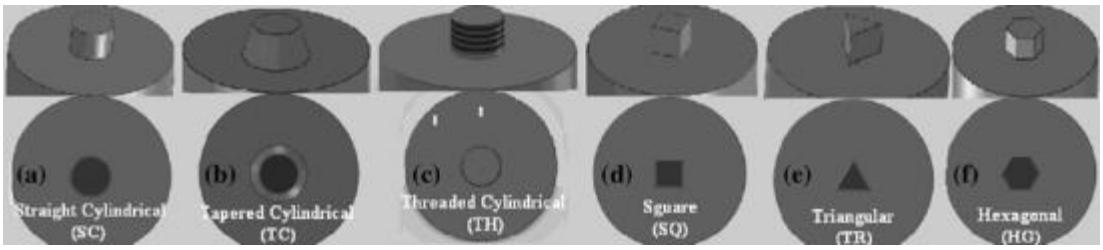


Figure 2.23 FSSW tool profiles (a) straight cylindrical, (b) tapered cylindrical, (c) threaded cylindrical, (d) square, (e) triangular and (f) hexagonal (Bilici et al., 2012)

Different tools were designed considering the dimensions as shown in Figure 2.24 and the tool geometry parameters and ranges were as illustrated in Table 2.1.

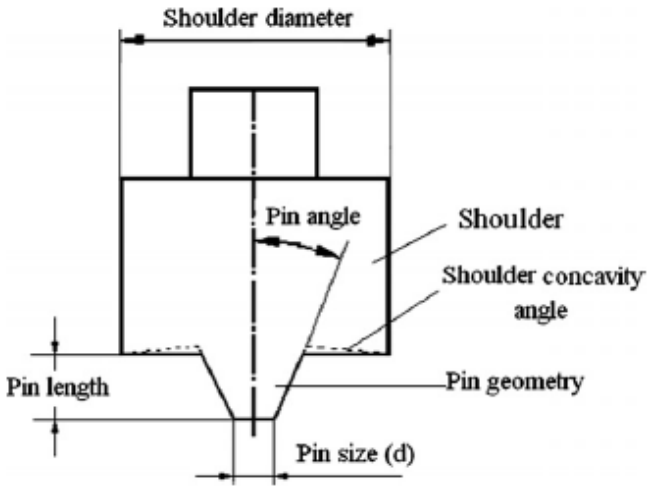


Figure 2.24 Friction stir spot welding tool design showing geometric parameters (Bilici et al., 2012)

Table 2.1 Tool geometry parameters and their ranges

| Dimensions | Units | Ranges |
|---|---|---|
| Pin diameter | millimeter (mm) | 5–11.25 |
| Pin angle | degrees | 0–25 |
| Pin length | millimeter (mm) | 4–7 |
| Shoulder diameter | millimeter (mm) | 15–35 |
| Shoulder concavity | angle degrees | 0–12 |
| Tool geometry | 6 type | 7.5 |

It is found that, the pin geometry significantly affects the thickness of the weld nugget and tensile strength of the welded joint. In addition, tapered cylindrical pin was found to produce the strongest spot welds at similar plunge depths when compared to others in terms of lap-shear tensile load as shown in Figure 2.25.

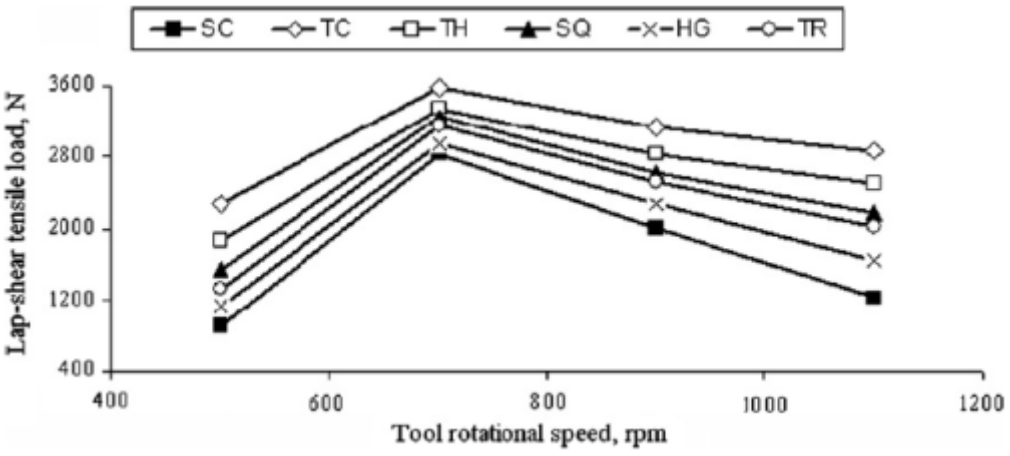


Figure 2.25 Effect of tool profile and tool rotational speed on weld strength (Bilici et al., 2012)

*2.2.3.2 Pin Lenght of FSSW*

The length of the pin is generally defined according to selected workpiece thickness, for example friction stir spot welding of thicker sheets require longer pins.

Tozaki et al. (2007), have investigated the effect of tool geometry on static strength and microstructure in friction stir spot welds of 6061 aluminum alloy sheets. In this study, tools with three different probe lengths were used, as shown in Figure 2.26, in order to weld the aluminum workpieces with different tool rotational speeds and tool holding times.

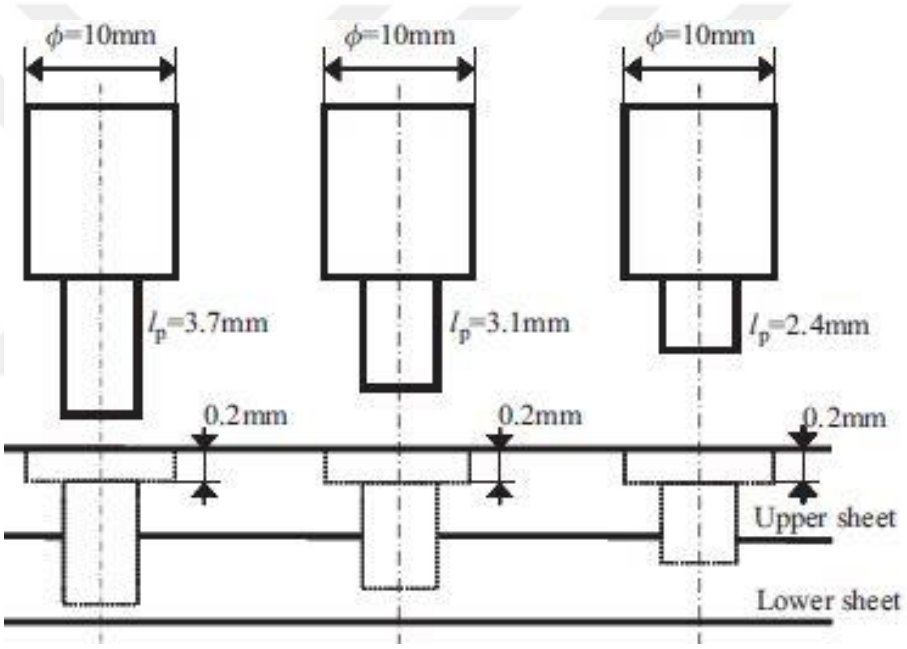


Figure 2.26 Geometry of tools used (Tozaki et al., 2007)

The weld microstructures were analyzed for welded samples that have different weld parameters and it was seen that the weld microstructures vary significantly depending on the pin length, tool rotational speed and tool holding time as shown in Figure 2.27. Tozaki et al. have observed in the scope of this study that the increasing of the pin length resulted in increasing stir zone of joint.

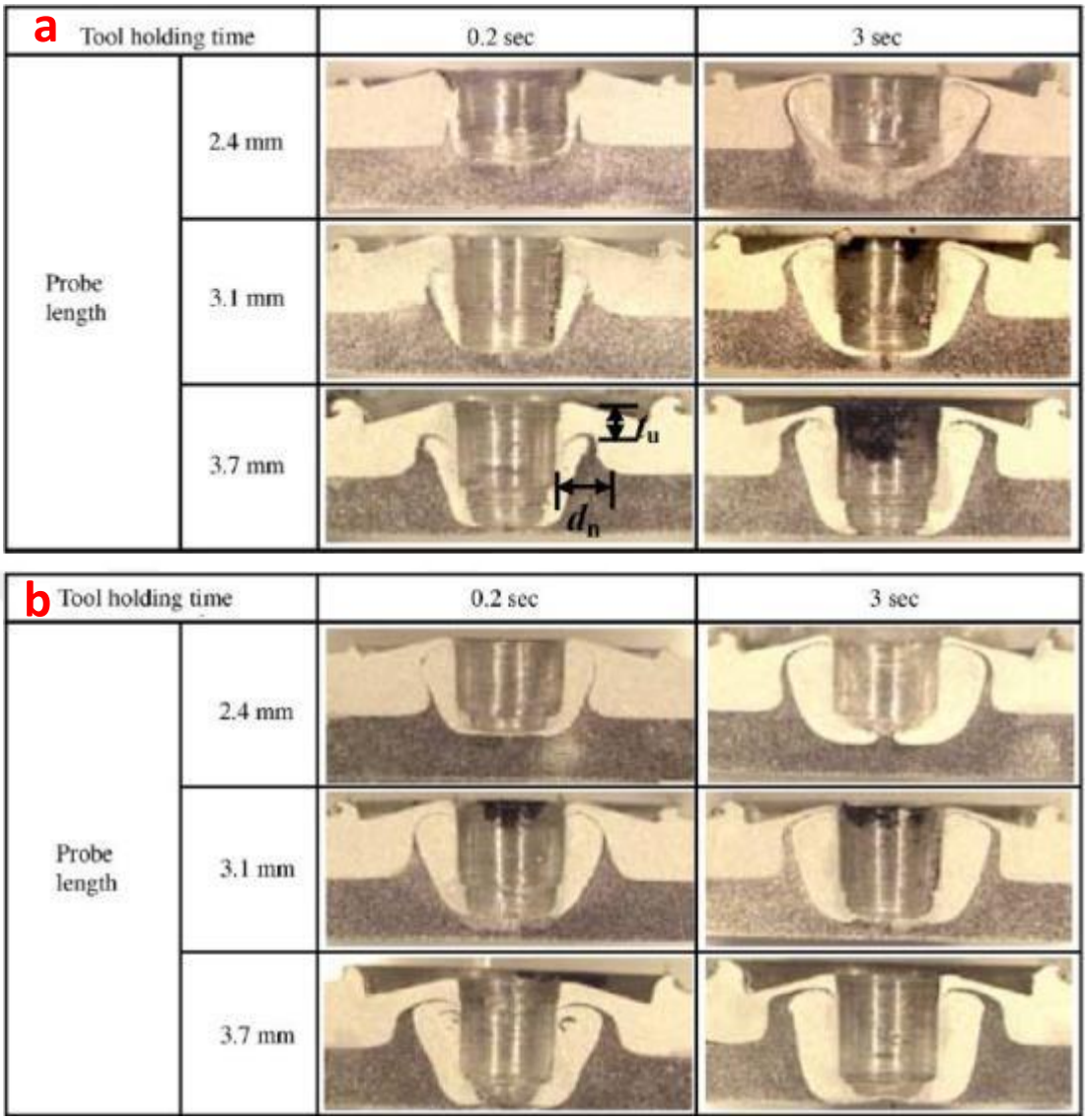


Figure 2.27 Microstructures of the cross-section of FSSW for different probe lengths and tool holding times at a tool rotational speed of (a) 2000 rpm and (b) 3000 rpm (Tozaki et al., 2007)

Tozaki et al. (2007), have explained that the tensile shear strength of the friction stir spot weld increases with increasing pin length without bothering the dwell time and rotational speed. Figure 2.28 show the tensile shear strength distribution. It was found out that increasing the size of the weld nugget provides more shear strength of weld associated with longer pin length.

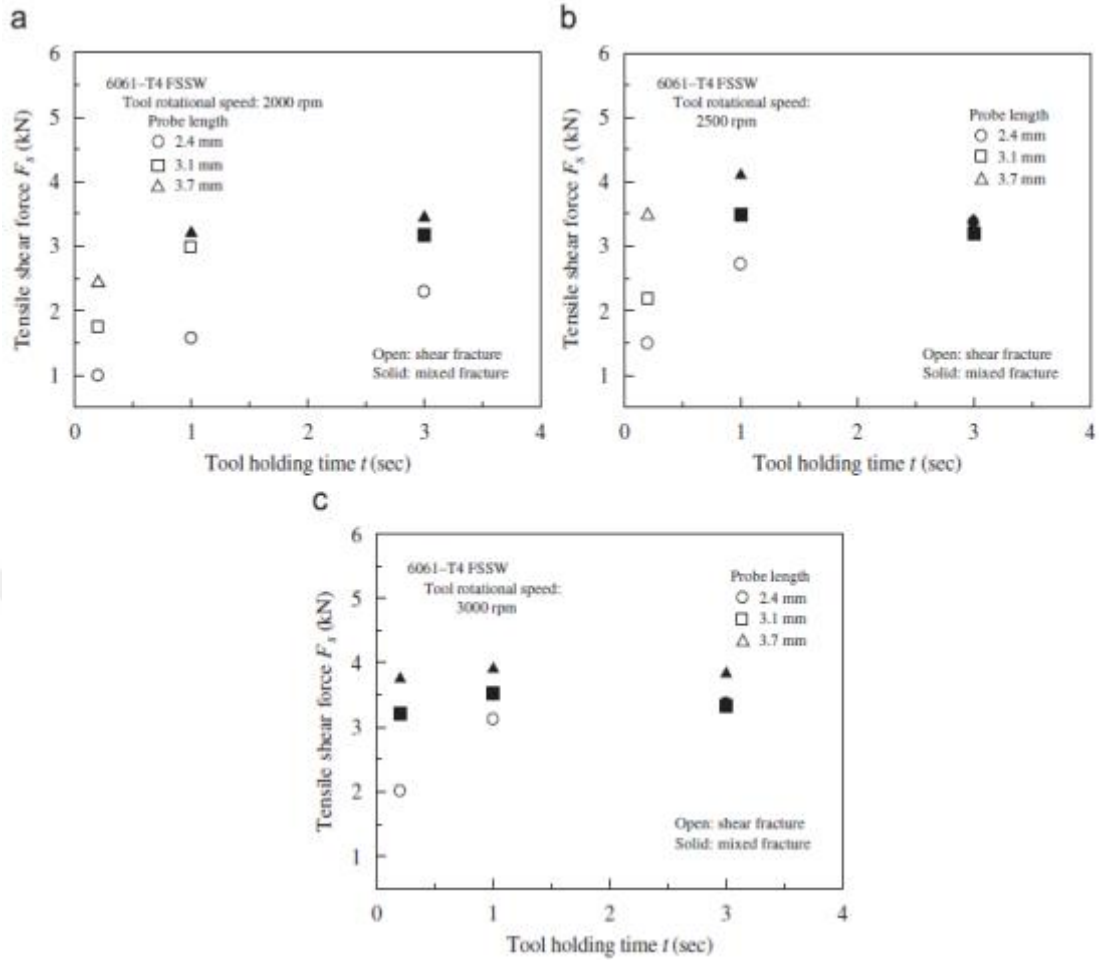


Figure 2.28 Tensile shear force as a function of tool holding time: (a) 2000 rpm, (b) 2500 rpm, (c) 3000 rpm

Bakavos and Prangnell (2009), have investigated the influence of pin length in the FSSW of thin (0.9 mm) 6111-T4 aluminum automotive closure panels. They have found that if the pin length penetrates into bottom sheet more than 20%, this affects the tensile shear strength of the weld negatively as given in Figure 2.29. In addition, in the same study a pinless tool was found to produce comparable welds with traditional tool with a pin.

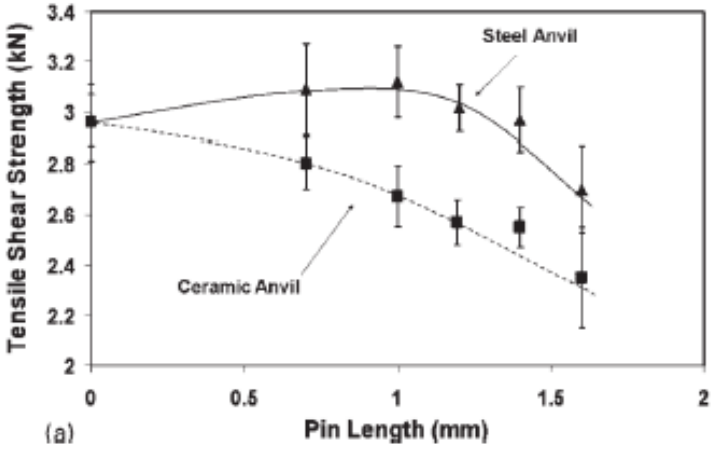


Figure 2.29 Effect of FSSW pin length (x-axis) and anvil insulation on 6111 aluminum alloy tensile shear strength (y-axis) (Bakavos et al., 2009)

*2.2.3.3 Shoulder Geometry of FSSW*

The shoulder of the friction stir spot welding tool generates largely the friction heat during the weld process, provides the forging force in the step of plunging into the weld specimen and conserves the plasticized material within the weld zone. There are many studies on the shape and form of the shoulder in order to investigate the effect of it on welding joints. The diameter of the shoulder is associated with heat generation, axial load and the volume of the weld zone.

Badarinarayan, Shi, Li & Okamoto (2009), have investigated the effect of tool geometry on partial metallurgical bond called the ‘’hook’’ which is formed in the weld region between the overlapped metal sheets. In this study, welds were made with three different shoulder profiles that are concave, convex and flat in order to compare the effect of them on the hook geometry and static strength as shown in Figure 2.30. As a result of this study, it is found that the tool geometry affects significantly the hook formation and the inherent concave shoulder profile provided a higher effective top sheet thickness that produced the highest weld strength.


Figure 2.30 Schematic of FSSW tool shoulder geometries a) concave, (b) flat, (c) convex (Badarinarayan et al., 2009)

Bakavos, Chen, Babout & Prangnell (2011), have worked on different shoulder geometries using pinless tool in the friction stir spot welding process. In this study, shoulder surface geometry was produced as variations of ‘’wiper’’ and ‘’scroll’’. For the wiper tool variations, six symmetrically arranged flutes were machined ending before the outer diameter of the shoulder. On the other hand, the scroll tool was designed as consisting of a machined fluted scroll that starts at the center of the shoulder and ends at the outer diameter. The variations of the shoulder are shown in Figure 2.31. As a result of the evaluations, it was explained that weld is more rapid and successful with fluted features machined on the shoulder surface.

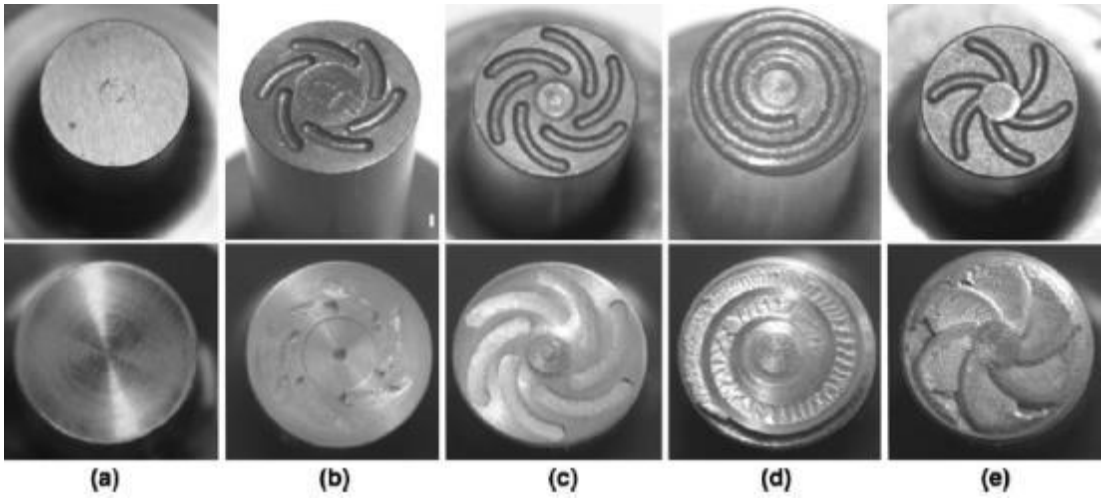


Figure 2.31 Different FSSW shoulder features shown before and after twenty welds: (a) featureless tool, (b) the short flute wiper tool , (c) the long flute wiper tool , (d) the fluted scroll tool, and (e) the proud wiper tool (Bakavos, Chen et al., 2011)

### *2.2.4 Mechanical Properties of Friction Stir Spot Welds*

There are a few test methods to determine the mechanical properties of spot welds. The commonly preferred testing methods to evaluate the mechanical properties and the quality of the spot welds are the overlap-shear test, cross-tension test, fatigue test and microhardness measurement. The overlap-shear and cross-tension test configurations are given in Figure 2.32. Overlap shear test applies shear loading at the joint interface of the sheets and is a fast, convenient and practical method for determination of weld mechanical property. In order to apply the shear load to the weld joint interface, small spacers are put at the gripped ends of the test specimens. This testing method can be seen in almost all current literature in evaluating the mechanical properties of spot welds. Cross-tension test applies a tensile load normal to the spot weld and a special fixture is used to grip the ends of the welded sheets in a mechanical testing machine (Schwartz, 2011).

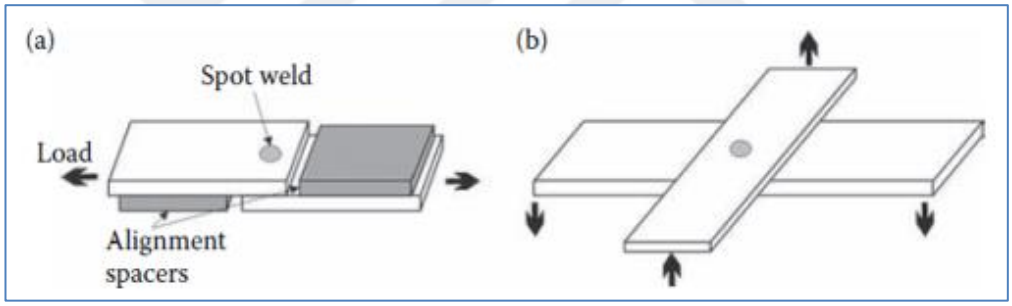


Figure 2.32 Test specimen configuration of (a) overlap shear (b) cross-tension test (Schwartz, 2011)

### *2.2.5 Material Flow of Friction Stir Spot Welds*

Leon & Shin (2016), have investigated the material flow behaviors during friction stir spot welding of lightweight aluminum and magnesium alloys using pin and pinless tools. In this study, they have used a cylindrical pin tool and pinless tools in order to characterize the behaviors of material flow during FSSW of lightweight alloys and the welding process was performed using a small scale computer numerically controlled milling machine in the displacement control mode. Figure 2.33 shows the details of the welding tools.

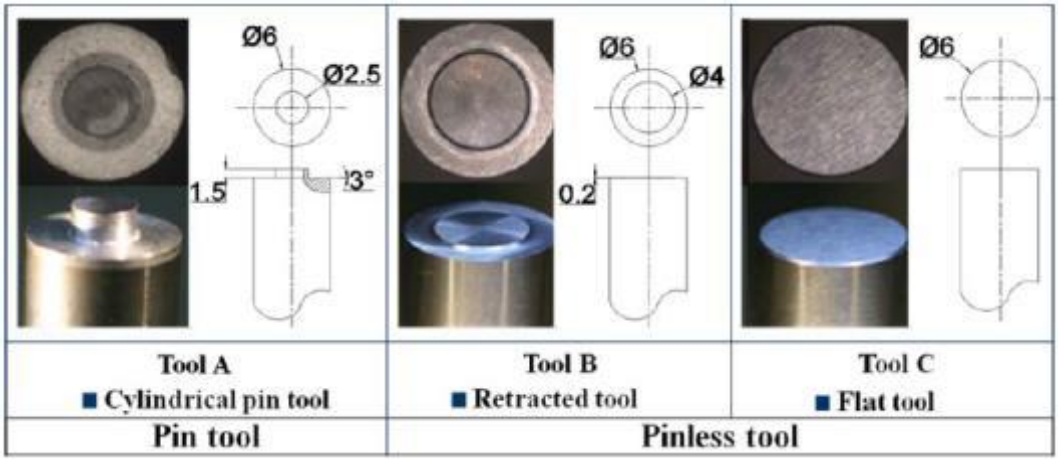


Figure 2.33 Shapes and dimensions of used tools (Leon et al, 2016)

For the experimental studies, the welded parts were cross-sectioned at the center of the weld zone to observe the material flow and cross-sectional views were observed using an optical microscope and the scanning electron microscope. In addition, because of the difficulties in the material flow observations in the case of similar material FSSW, a tracer material technique was used. In this technique, a silver paste was used to trace the material flow induced during friction stirring. Before the welding applications, Ag paste was applied in between the upper and lower sheets to determine the material flow (Leon et al, 2016).

Figure 2.34, Figure 2.35 and Figure 2.36 show the cross-sectional views of the welds performed using cylindrical pin tool (tool-A), retracted tool (tool-B) and flat tool (tool-C) respectively. These all views of the welded samples were analyzed and commented using the tracer material locations according to the original boundary interface between the upper and lower sheets.

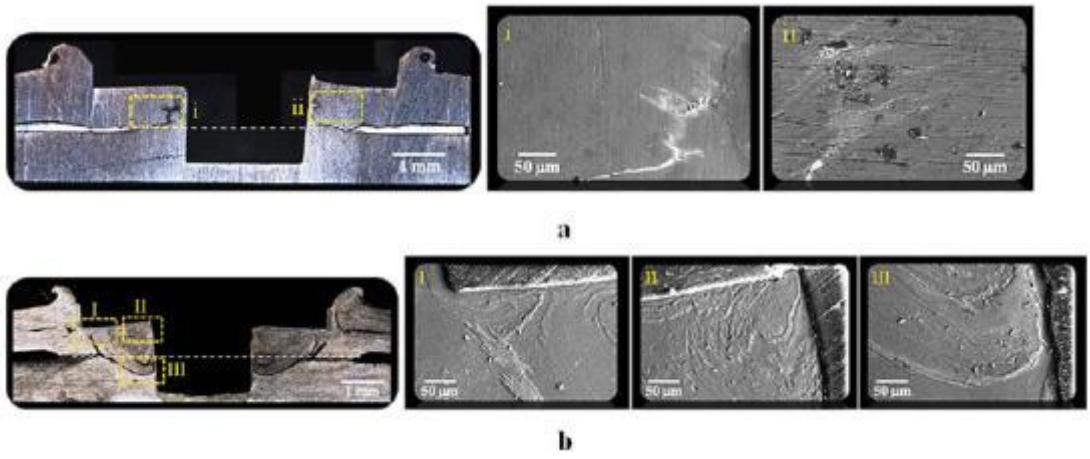


Figure 2.34 Cross-sectional views of weld part with tracer material using tool A, (a) similar Al welds; (b) Mg welds (Leon et al, 2016)

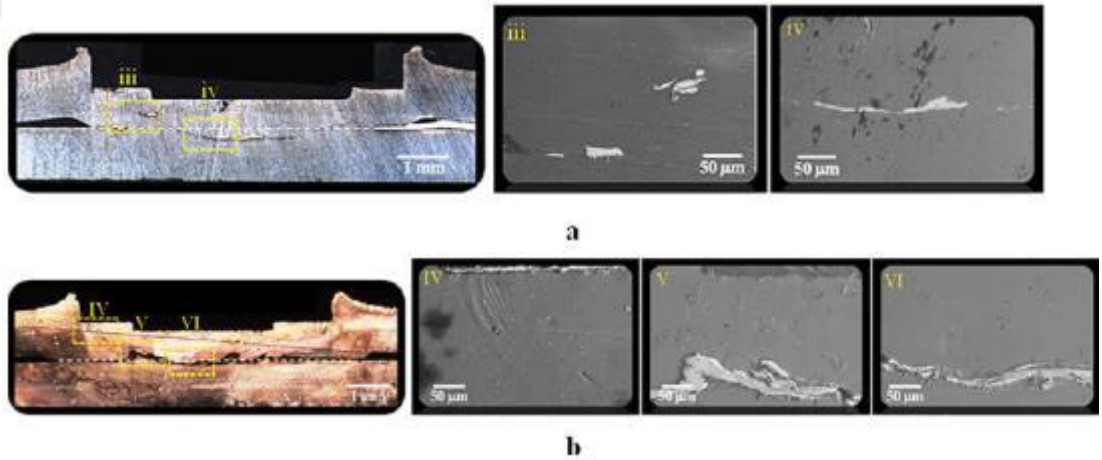


Figure 2.35 Cross-sectional views of weld part with tracer material using tool B, (a) similar Al welds; (b) Mg welds (Leon et al, 2016)

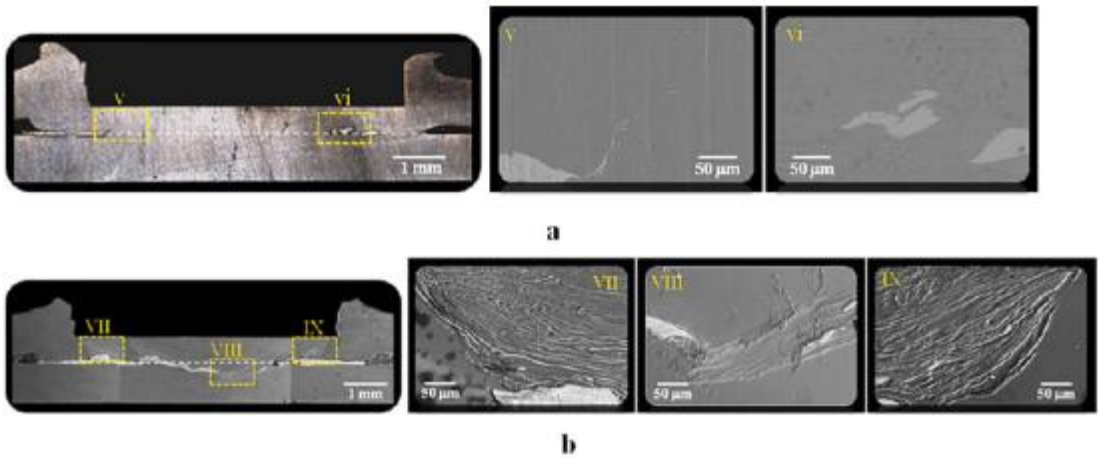


Figure 2.36 Cross-sectional views of weld part with tracer material using tool C, (a) similar Al welds; (b) Mg welds (Leon et al, 2016)

At the end of the study, the observed material flow during FSSW of similar lightweight alloys according to tool geometry was published schematically as shown in Figure 2.37. The arrows show the material flows obtained from cross-sectional analysis of welded samples. The solid line arrows indicate a high intensity flow and the dotted line arrows show a mild intensity material flow

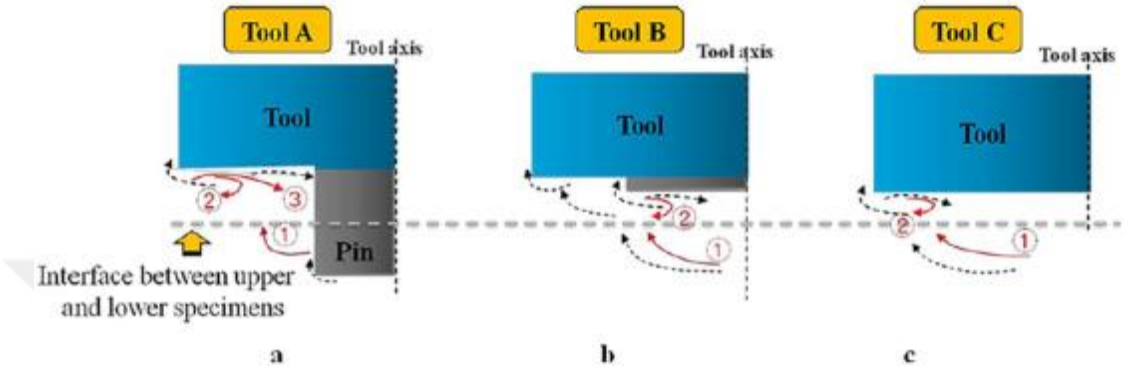


Figure 2.37 Schematic illustrations of material flow for (a) tool A, (b) tool B and (c) tool C (Leon et al, 2016)

### *2.2.6 Microstructure of Friction Stir Spot Welds*

The microstructural observation of friction stir spot welds provides valuable information regarding the metallurgy of the joint. It was explained in the previous studies that the welding area includes different zones according to heat affect and grain size in the friction stir spot welding. Microstructure evaluation of weld cross-section enables to observe the weld depth, grain size, hardness profile and texture (Mishra & Mahoney 2007).

Wang and Lee have investigated microstructures and failure mechanisms of friction stir spot welds of aluminum 6061-T6 sheets. In this study, three distinct regions were determined in the weld joint that are the stir zone (SZ), the thermomechanically affected zone (TMAZ) and the heat affected zone (HAZ). The cross sectional area of the weld zone was investigated and the zones were classified as given in Figure 2.38. The stir zone where the upper and lower sheets are bonded is near the outer area of the central hole and is gray. TMAZ has been generated by the motion

of the tool and friction heat during the welding process. HAZ is under the effect of friction heat during the weld process (Wang & Lee 2007).

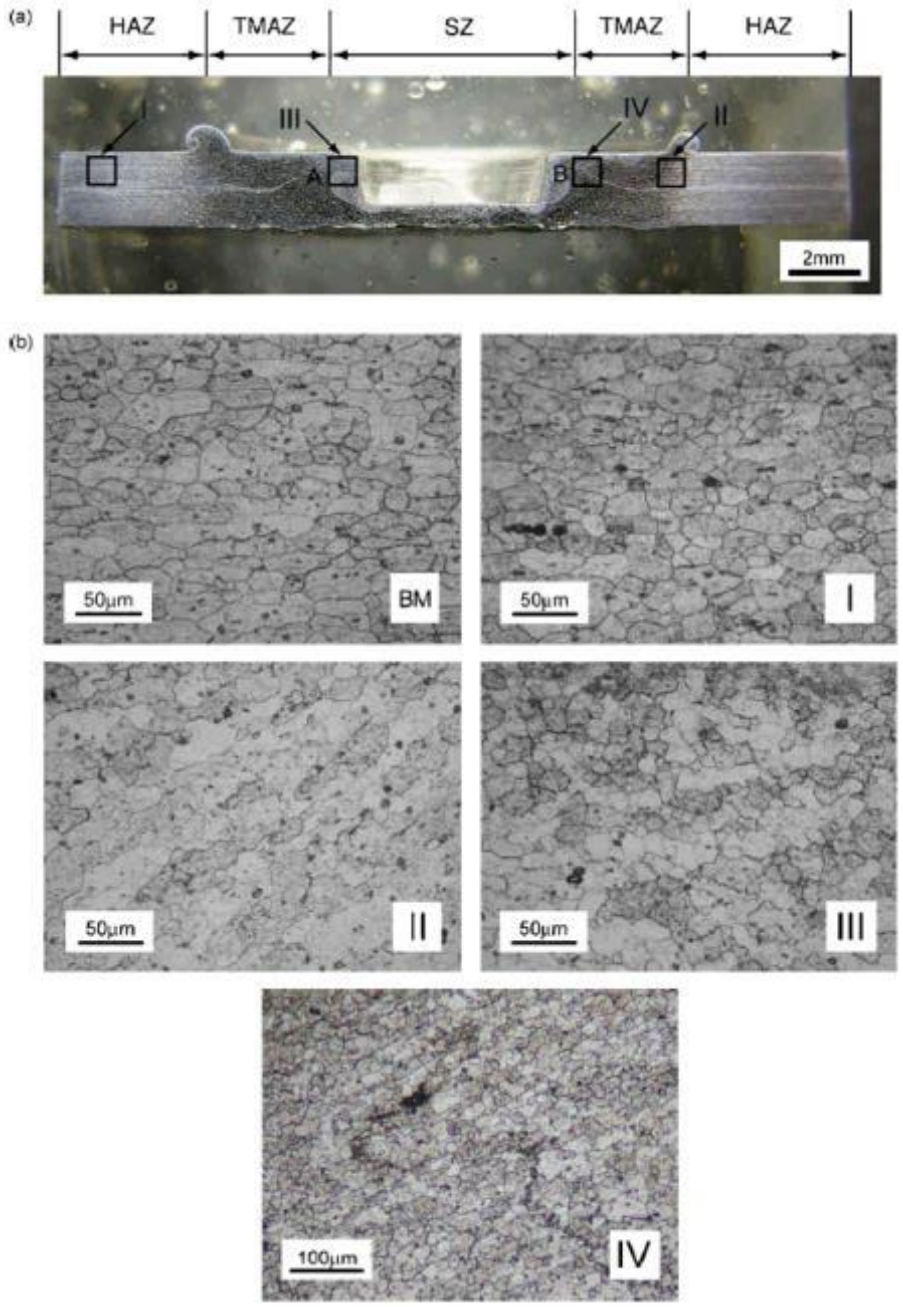


Figure 2.38 (a) A micrograph of the cross-section of a friction stir spot weld generated by the tool; (b) close-up views of regions I–IV (Wang & Lee 2007)

In this study, the four regions were selected in the cross-section view of the weld and their grain sizes were investigated by the researchers. The close up view of region-I shows that HAZ has less coarse grains compared to BM. A close-up view of

region II shows that there are finer and distorted grains in the TMAZ. Finally, close-up views of regions III and IV show that SZ includes very fine equiaxed grains. According to the microstructure evaluation, it was thought that the equiaxed grains in the SZ are probably formed due to stir and recrystallization (Wang & Lee 2007).

### 2.2.6 Advantages of Friction Stir Spot Welding

Friction stir spot welding was developed for joining of aluminum sheets as an alternative to conventional methods that are resistance spot welding (RSW) and self-piercing riveting (SPR) (Badarinarayan et al., 2009; Bilici et al., 2012; Mert & Mert, 2013).

RSW is a very common welding technique used in the automotive industry for joining sheet metal assemblies of vehicle bodies due to its advantages on welding efficiency and its suitability for automation (Bilici et al., 2012). However this method has some disadvantages and difficulties when it is used in the welding process of low melting points materials, such as aluminum or magnesium alloys. Some of these disadvantages include high energy consumption, short duration time of the welding electrodes, crack formation, welding deformation and the use of consumables (Mert et al., 2013).

The advantages of FSSW are categorized as four sections that are metallurgical benefits, cost and investment benefits, environmental benefits and energy benefits, when it is compared to conventional joining methods. Firstly, metallurgical benefits of friction stir spot welding are:

- Solid-phase weld process,
- Lower distortion,
- There is no loss of alloy material,
- Good dimensional stability and repeatability in applications,
- Fine recrystallized microstructure,
- Good mechanical properties in the welding area,
- High joint strength without porosity, solidification cracks,

- Usability instead of multiple parts joined by fasteners,
- Usability in welding of all all aluminum alloys.

The environmental advantages of FSSW are given as follows:

- No harmful gas emissions and environment friendly method,
- No shielding gas required for weld,
- Minimal surface cleaning required,
- No cleaning material consumption before weld application,
- Eliminates grinding wastes,
- Consumable materials saved in the weld application such as welding wire or any gases.

FSSW has a lower energy consumption compared to RSW. In this welding method, the energy is consumed only to rotate and drive the welding tool. The energy consumption is reduced by 99% for FSSW of aluminum and 80% for steel (Mishra et al., 2007).

The cost and investment advantages of FSSW are given as follows:

- Low weld cost,
- Lower equipment investment,
- Low maintenance investment because of using less equipment (Er, 2010).

# CHAPTER THREE
# MATERIAL AND METHOD

## 3.1 Aluminum Alloys

Aluminum and its alloys have wide usage areas in the automotive, aerospace, defense, and manufacturing industries because of their unique combinations of properties and therefore, these properties make them one of the most versatile, economical, and attractive metallic materials in engineering applications (Davis, 2001). The critical property of aluminum is its low density (2.69 $g/cm^3$), which is one-third of steel that makes it so attractive. For various applications, aluminum can be alloyed and strengthened by cold working, can be applied heat treatment to achieve high strength and a high strength to weight ratio. Its modulus of elasticity does not change much under cold working and heat treatment applications. These are the important points for preferring aluminum in the applications In addition, aluminum and its alloys can be produced in many forms such as extrusions, castings, forgings, stampings and machined component (Mallick, 2010). Aluminum is a noncorrosive element; because of this critical property, it is very suitable for production of food and beverage storage containers (Campbell, 2006).

Today, using of aluminum in vehicle structures, power trains and other components enables to produce lighter, safer vehicles that have higher performance. Figure 3.1 shows the increasing amount of aluminum usage in the North American light vehicle production (Mallick, 2010).

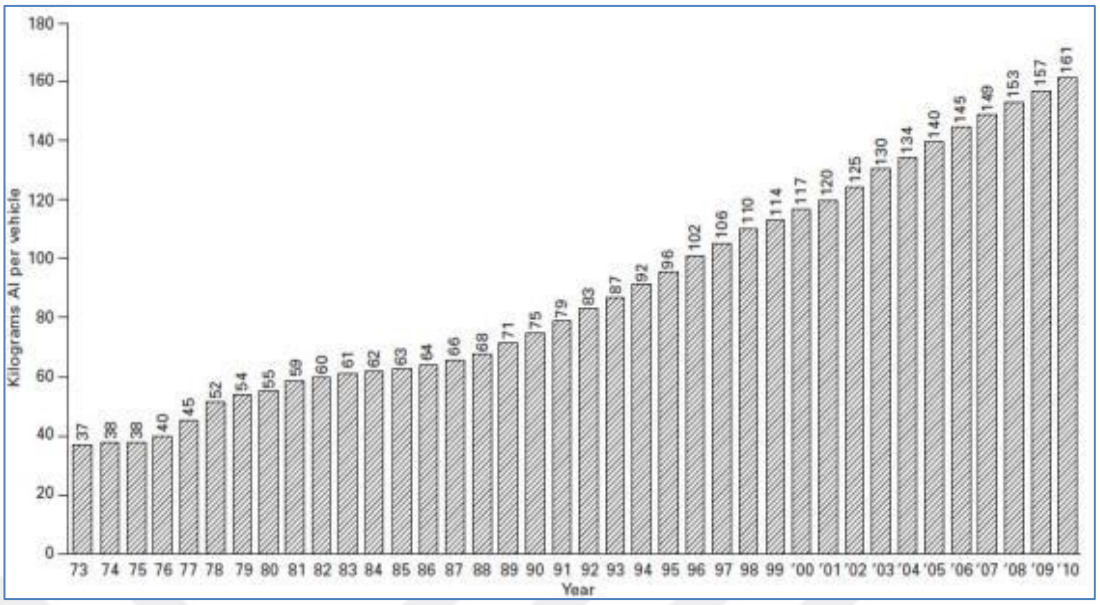


Figure 3.1 Schematic of North American light vehicle aluminum content (Mallick, 2010)

Aluminum alloys are used in many parts of a car body in relation to its properties. Some aluminum alloys and their application areas in the body of a typical sedan car are shown in Figure 3.2 (Mallick, 2010).

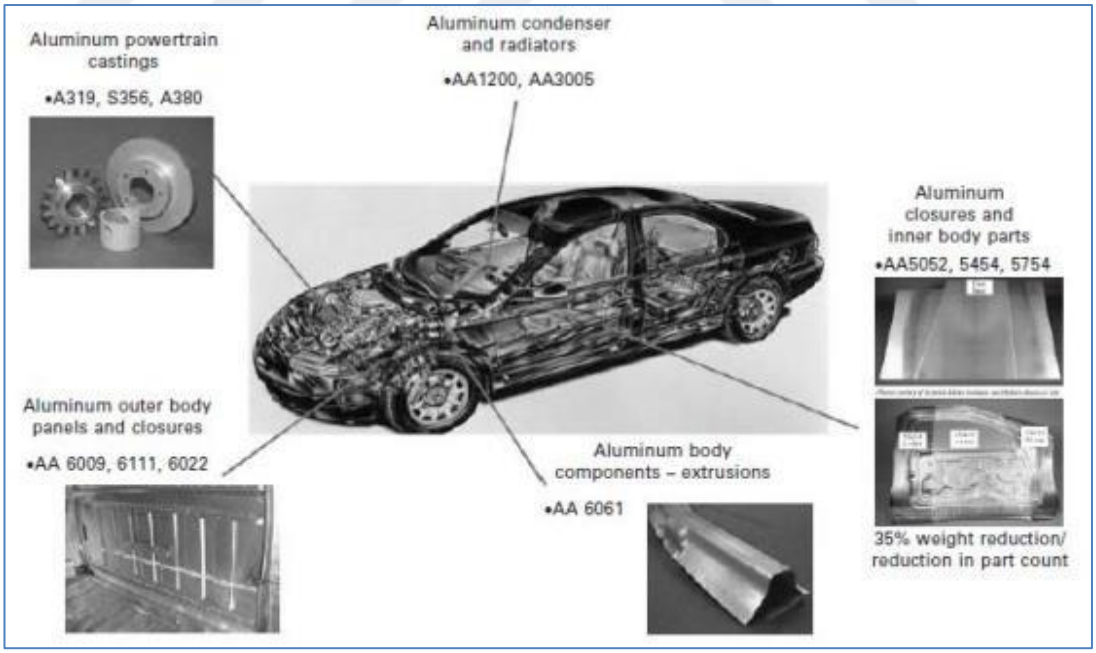


Figure 3.2 Aluminum alloys used in a typical sedan car (Mallick, 2010)

Today, aluminum alloys are classified as two major categories as wrought composition and cast composition. Furthermore, wrought aluminum alloys are divided into two categories: non-heat treatable and heat treatable alloys (Davis, 2001).

There is a definition method of wrought aluminum alloys by a four digit numerical. The first digit describes the group of aluminum alloys. The variations in the original basic alloy is described by the second digit. If it is zero, it is the original composition and if it is two, this shows that it is the second variation and so forth. The third digit defines the specific alloy being in the series and same thing applies for the fourth digit. Designation method for wrought aluminum alloys can be explained as shown in Table 3.1.

Table 3.1 Aluminum Alloy Designation System

| SERIES | MAIN ALLOYING ELEMENT |
|---|---|
| 1XXX | ALUMINUM (MINIMUM 99.00%) |
| 2XXX | COPPER |
| 3XXX | MANGANESE |
| 4XXX | SILICON |
| 5XXX | MAGNESIUM |
| 6XXX | MAGNESIUM and SILICON |
| 7XXX | ZINC |
| 8XXX | OTHER ELEMENTS |

### *3.1.1 Wrought Aluminum Alloys*

Wrought aluminum series are used in all essential engineering fields, automotive industry, defence industry, civil engineering, transport, electrical engineering, electronics, machinery, packing and their main properties are explained respectively below;

**1XXX: Pure AI.** The pure aluminum rate is 99% or higher in this series. The important properties of 1XXX series aluminum alloys can be given as follows:

* Typical ultimate tensile strength range is 70-185MPa,
* Strain hardenable,
*Excellent corrosion resistance,
* Easily joined by welding, brazing, soldering,
* High thermal and electrical conductivity,
* High formability and workability.

**2XXX: AI-Cu Alloys.** The major additional alloying element in the 2XXX series aluminum alloys is copper. The important properties of 2XXX series aluminum alloys can be given as follows:

* Typical ultimate tensile strength range is 185-430MPa,
* Heat treatable,
* High strength in the condition of room and elevated temperatures,
* Usually joined mechanically but some alloys are weldable,
* Corrosion resistance not as powerful as other alloys.

**3XXX: AI-Mn Alloys.** The major additional alloying element in the 3XXX series aluminum alloys is manganese. The important properties of 3XXX series aluminum alloys can be given as follows:

* Typical ultimate tensile strength range is 110-280MPa,
* High formability, corrosion resistance with medium strength,
* Readily joined by all commercial procedures,
* Hardened by strain hardening.

**4XXX: AI-Si Alloys.** The major additional alloying element in the 4XXX series aluminum alloys is silicon. The important properties of 4XXX series aluminum alloys can be given as follows:

* Typical ultimate tensile strength range is 170-380MPa,
* Some of them are heat treatable,
* Good flow characteristics, medium strength,
* Easily joined, especially by brazing and soldering.

**5XXX: AI-Mg Alloys**. The major additional alloying element in the 5XXX series aluminum alloys is magnesium. The important characteristics of the 5XXX series can be given as follows:

* Typical ultimate tensile strength range is 125-350MPa,
* Strain hardenable,
* Excellent corrosion resistance in marine atmospheres, toughness, weldability, moderate strength,

* Building and construction, automotive, cryogenic, marine applications.

**6XXX: AI-Mg-Si Alloys.** 6XXX series contain silicon and magnesium. The important properties of the 6XXX series can be given as follows:

* Typical ultimate tensile strength range: 125-400MPa,
* Heat treatable,
* High corrosion resistance, outstanding extrudability; moderate strength,
* Readily welded by gas metal arc welding and gas tungsten arc welding methods,
* Building & construction, highway, automotive, marine applications.

**7XXX: AI-Zn Alloys.** The major additional alloying element in the 7XXX series aluminum alloys is zinc. The important properties of each type of 7XXX series aluminum alloys can be given as follows:

* Typical ultimate tensile strength range: 220-605MPa,
* Heat treatable,
* Very high strength,
* Having special high toughness versions,
* Mechanically joined,
* Usage of in aerospace, automotive applications.

**8XXX: Alloys with AI-Other Elements (Not Covered by Other Series).** The major alloying elements are iron, nickel and lithium. The important properties of each type of 8XXX series aluminum alloys can be given as follows:

* Typical ultimate tensile strength range: 115-415MPa,
* Heat treatable,
* High strength, hardness and conductivity,
* Commonly used in aerospace, electrical industries (Davis, 2001 & Campbell, 2006).

### *3.1.2. AA 5052 Properties and Application Field*

This aluminum alloy has good workability, very good corrosion resistance, high fatigue strength, weldability, and moderate strength. These properties lead to its use in

many industries and applications such as marine applications, automotive parts, aircraft fuel/oil lines, railroad cars, hydraulic tubes, home appliances, agricultural applications, trucks and trailers fuel tanks, automotive and other transportation areas, pressure vessels, fan blades, tanks, electronic panels, electronic chassis, medium strength sheet metal parts, containers, cooking utensils, fasteners, hardware, highway signs, hospital and medical equipment, kitchen equipment, sheet metal-work, lighting, wire and riveting. In this study, AA 5052-H32 3 mm thick aluminum alloy sheet of Alcoa company was used. The chemical composition, physical properties and mechanical properties of this material are shown in Table 3.2, Table 3.3 and Table 3.4, respectively (Davis, 2001 & MatWeb, nd).

Table 3.2 Chemical Composition of AA 5052-H32 (Aalco, nd)

| Chemical Composition | | | | | | | |
|---|---|---|---|---|---|---|---|
| Element (%) | Si | Fe | Cu | Mn | Mg | Cr | Zn |
| min | | | | | 2.20 | 0.15 | |
| max | 0.25 | 0.40 | 0.10 | 0.10 | 2.80 | 0.35 | 0.10 |

Table 3.3 Physical Property of AA 5052-H32

| Physical Property | Value |
|---|---|
| Density | 2.68 g/cm³ |
| Melting Point | 605 °C |
| Thermal Expansion | 23.7 x10^-6 /K |
| Modulus of Elasticity | 70 GPa |
| Thermal Conductivity | 138 W/m.K |
| Electrical Resistivity | 0.0495 x10^-6 Ω .m |

Table 3.4 Mechanical Property of AA 5052-H32

| | Ultimate tensile strength (MPa) | Yield strength (MPa) | Elongation (%) |
|---|---|---|---|
| min | 215 | 160 | - |
| max | 265 | - | 10 |

### 3.2 Polymers

Polymers are largely used in the production of a wide range of materials found in many applications in daily life due to properties such as being low cost, light weight and also ease of process (Singh & Dubey 2009). While polymers are light and some of

them exhibit high levels of ductility, they are not strong enough in order to classify them as high strength structural materials. They can be combined with high strength fibers and become structural materials with high strength, stiffness-to-weight ratios and these are becoming increasingly important in aerospace. By achieving these properties, the importance of polymers in the automotive and aerospace industries increases and make their usage common (Campbell, 2006).

Polymers can be classified into two categories based on their thermal processing behavior as thermoplastics and thermosets (Campbell, 2006). In addition, there is a useful chemical difference between these two groups to classify them. Thermoplastics contain essentially linear or lightly branched polymer molecules; on the other hand, thermosets are cross-linked materials, consisting of an extensive three-dimensional network of covalent chemical bonding. The classification of polymers is shown in Figure 3.3. (Menczel & Prime 2008).

Thermoplastics can be softened and melted under the application of heat and it is possible to process them either in the heat-softened state (e.g. by thermoforming) or in the liquid state (e.g. by extrusion and injection molding). This property is in contrast to the thermosets, the other class of polymers, which cannot be melted by the application of heat. Thermoplastic polymers have an advantage for the manufacturing industry that they can be processed repeatedly by the application of heat and can be recycled directly in order to produce new products. In the manufacturing industry, the common processes used for producing thermoplastic parts are blow molding, injection molding and thermoforming (Mallick 2010).

Thermosets do not melt when heated in contrast to thermoplastics but under sufficiently high temperature, decompose irreversibly. Generally, thermoset plastics are stronger, harder, more brittle than thermoplastics and cannot be recycled from wastes or produced parts. Thermoset plastics include polymers that cross-link together during the curing process to form an irreversible chemical bond. The cross-linking process eliminates the risk of the product remelting when heat is applied to parts

produced by thermosets and this property makes them ideal materials for high-heat applications such as electronics and appliances (Modor, nd; Globalspec, nd).

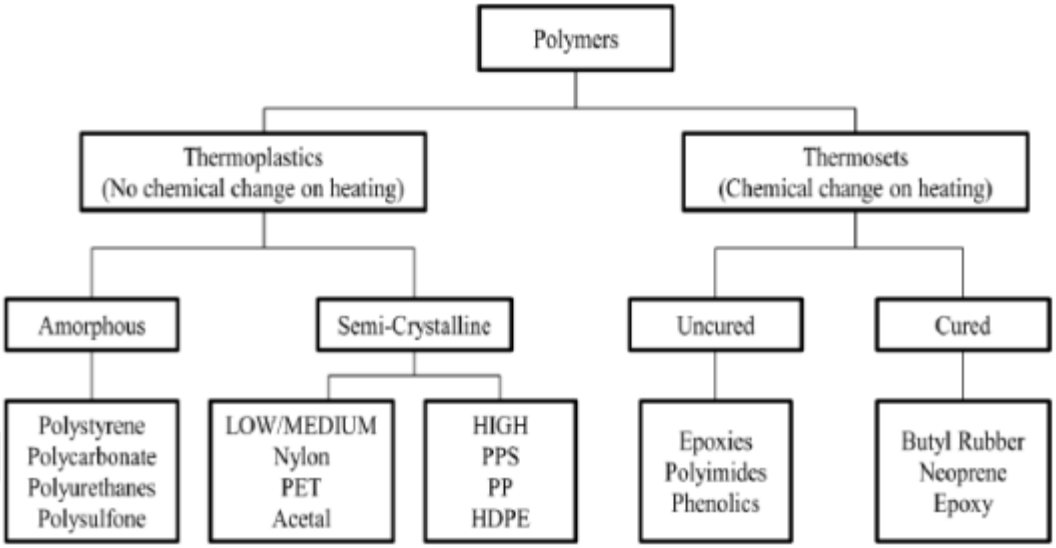


Figure 3.3 Classification of polymers (Zakut, 2012)

### *3.2.1 Polycarbonate*

Polycarbonate (PC) is a typical amorphous polymer (thereby displaying excellent mechanical properties and high dimensional stability) and plays an important role as an one of the most widely used engineering thermoplastics with the properties of transparency, excellent toughness, thermal stability and a very good dimensional stability. Polycarbonate has a glass transition temperature of about 150 °C so it softens gradually above this point and flows above about 300 °C and it protects its rigidity up to 140°C and toughness down to -20°C (Polycarbonate, nd).

The main properties of polycarbonates are given below:

- Easy to fabricate & machine,
- Low coefficient of thermal expansion,
- Excellent strength retention at elevated temperatures,
- High tensile, shear, and flexural strength,
- High modulus of elasticity,
- Low deformation under load,
- Good creep and cold flow resistance (Ips, Polycarbonate n.d.).

In addition to the given properties, one of the biggest advantages of polycarbonate is its impact strength. Figure 3.4 shows comparison of polycarbonate impact strength with some plastics. It is a very durable material and unlike most thermoplastics, it can undergo large plastic deformation without cracking and breaking in the structure. The diagram given below compares the impact strength of polycarbonate to other commonly used engineering plastics (Polymertechnology, nd; Polycarbanate, nd).

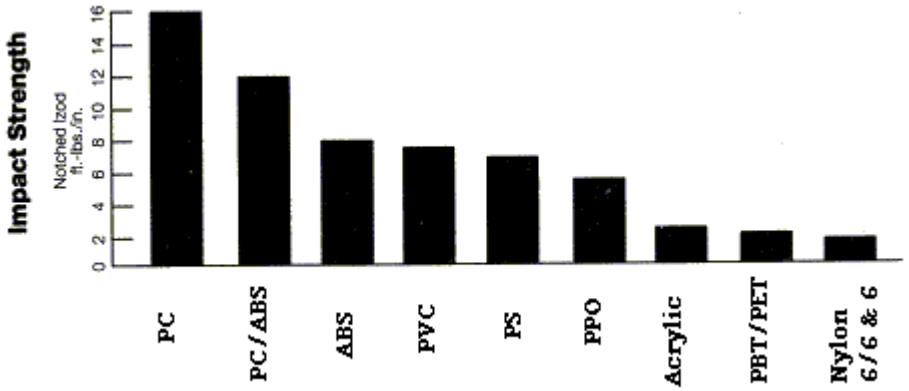


Figure 3.4 Comparison of PC Impact Strength with other plastics (Polymertechnology, nd)

Polycarbonate is used in many industries as given below:

- Automotive industry,
- Electric & Electronics,
- Home appliances,
- Glazing,
- Business machines,
- Medical applications,
- Lighting,
- General Industries / Packaging (Polycarbanate PC, nd; Polycarbanate, nd).

In this study, 4 mm thick polycarbonate sheet was used in the welding applications. The length and width of the PC sheets are 100 mm and 25 mm, respectively. Figure 3.5 shows the mechanical, physical and thermal properties of polycarbonate material.

Table 3.5 Properties of polycarbonate material (Polycarbonate properties, nd)

| PROPERTY TYPE | UNITS | VALUE |
|---|---|---|
| **PHYSICAL** | | |
| Density | $g/cm^3$ | 1.20 |
| Water Absorption | % | 0.20 |
| Water Absorption at Saturation | % | 0.40 |
| **MECHANICAL** | | |
| Yield Stress | MPa | > 60 |
| Yield Strain | % | 6 |
| Tensile Modulus | GPa | 2.2 -2.3 |
| Flexural Yield Strength | MPa | 89.6 |
| Flexural Modulus | GPa | 2.41 |
| Hardness, Rockwell R | | 126 |
| **THERMAL** | | |
| Thermal Conductivity | W/m-K | 0.187 |
| Melt Temperature | °C | 288-316 |
| Heat Deflection Temperature | °C | 143 |
| Typical Mold Temperature | °C | 82 - 121 |

### *3.2.2 Polypropylene GF%30*

Polypropylene (PP) is one of the most widely used thermoplastic polymers in a variety of commercial applications such as automotive industry, textile industry, packaging industry, fibers, films, filaments, home appliances, medical equipment and consumer products. It is known as one of the fastest growing and widespreading classes of commodity thermoplastics. Especially in the home appliances industry such as washing machines, dishwashers, refrigerators and ovens, polypropylene can be an alternative material for metal, glass, engineering plastics such as ABS, polycarbonate and nylon (Rodgers, 2004).

In this study, 4 mm thick polypropylene GF%30 sheet material was used in welding applications with the dimensions of 100 mm length and 25 mm width. The properties of this material are given in Figure 3.6.

Table 3.6 Properties of polypropylene GF%30 (Polypropylene properties, nd)

| PROPERTY TYPE | UNITS | VALUE |
|---|---|---|
| PHYSICAL | | |
| Density | $g/cm^3$ | 1.12 |
| MECHANICAL | | |
| Tensile modulus | MPa | 6600 |
| Stress at break | MPa | 95 |
| Strain at break | % | 2.3 |
| Charpy impact strength, +23°C | kJ/m² | 48 |
| Charpy impact strength, -30°C | kJ/m² | 44 |
| Charpy notched impact strength, +23°C | kJ/m² | 18 |
| Charpy notched impact strength, -30°C | kJ/m² | 20 |
| THERMAL | | |
| Melting Temperature | °C | 170 |
| Temp. of deflection under load, 1.80 MPa | °C | 148 |
| Temp. of deflection under load, 8.00 MPa | °C | 122 |

### 3.3 Friction Stir Spot Welding Apparatus Design and Manufacturing

In the friction stir spot welding applications, achieving a correct tool design and selection of suitable welding method is critical in order to attain a quality weld. Because of this, many studies have been conducted in the past related to tool design with the subject headings being the tool geometry optimization, effect of tool design on mechanical properties of weld quality, etc. In addition to tool design's effect on the weld quality, it is a popular subject for researchers working with FSSW since the tool design is related to tool performance, load bearing ability, load application capacity, tool life time and process cost.

In this study, similar and hybrid joint of aluminum and polymers were planned to weld using FSSW. The materials that are planned to use in hybrid joint trials have different melting temperatures and it was determined that the pre-heat step is necessary in the welds of dissimilar materials in order to tolerate temperature difference between polymer and aluminum. For that reason, there was a necessity of designing two different apparatus for similar and hybrid weld applications in terms of pre-heat step or one apparatus that can be used for both similar and hybrid weld

applications. In the step of apparatus design, refill friction stir spot welding method and friction stir spot welding with refilling by friction forming process (FSSW-FFP) have been taken as the reference method. In the scope of design studies, one welding apparatus was designed that includes two versions related to material weld combinations have a common use for both similar and hybrid joints. The first version of the apparatus, which was planned to use in similar material friction stir spot welding, includes only one step that is a creation of dome structure. The second version of the apparatus was planned to use in dissimilar materials friction stir spot welding and it has two steps that are creation of dome structure step and refilling step by friction forming process under pre-heat.

At the beginning of welding apparatus design, there were two problems to use refill friction stir spot welding method in the weld applications. First one is that RFSSW has a special welding tool that needs two vertical independent rotational motions and it is not possible to provide these motions with a milling machine. The second problem is that, there is no available RFSSW machine that works conformably with the tool. Under these conditions, a simple way that enables to use a conventional milling machine for this method in welding was searched. Venukumar & Muthukumaran (2014), have studied the failure modes and fatigue behavior of conventional and refilled stir spot welds. In this study, the simple way of refill FSSW method including friction forming process, can be performed by using a milling machine, which was described as schematically shown in Figure 3.5 below. In this method, the first step is creating a bush structure using filler plate with the same technique with FSSW. In the second step, bush structure is abolished with friction forming process. With this way, there is no keyhole in the weld zone and RFSSW is applied easily (Venukumar et al., 2013). It has been inspired from this method in the design study.

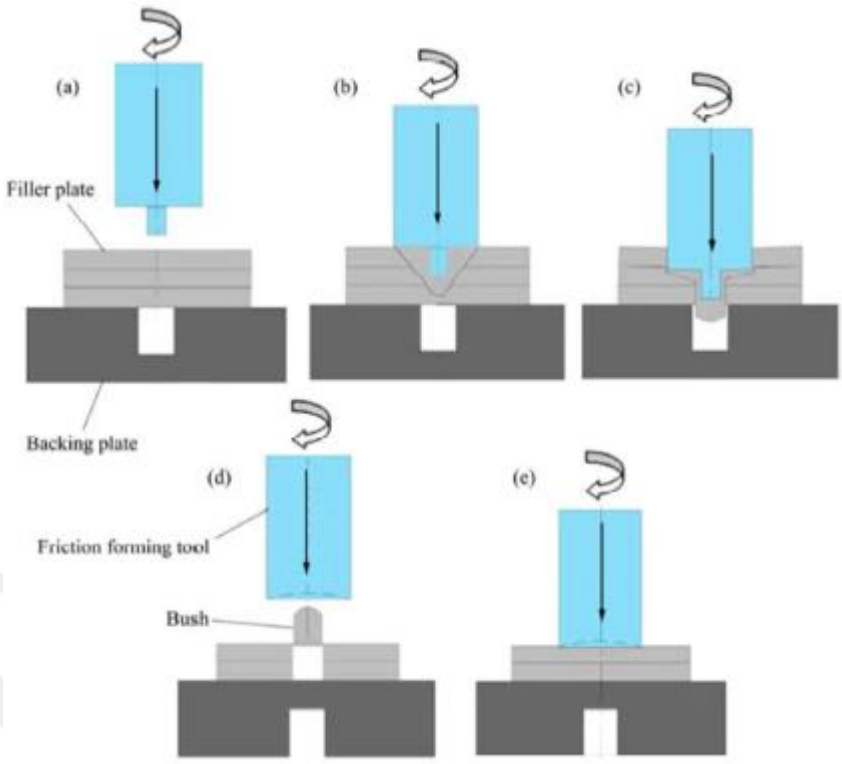


Figure 3.5 Schematic illustration of the FSSW-FFP (Venukumar et al., 2013)

The first version of the weld apparatus includes only the first step that is creation of the dome (bush) structure as given Figure 3.6. The first step of both versions of the welding apparatus is the same that produces the dome structure in the bottom surface of the weld joint as shown in Figure 3.6.

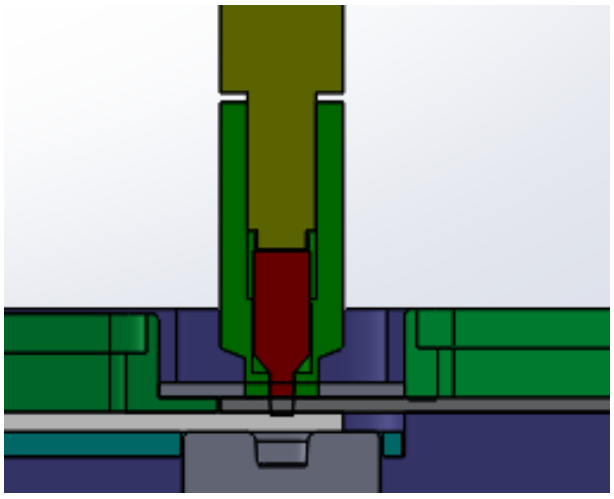

Figure 3.6 Schematic illustration of step-1 of both versions

The second version of the weld apparatus includes two steps that are creation of the dome structure step and friction forming process step respectively. The first step is the same with first version as stated before. The second step of second version includes differences in terms of pre-heat application. For the dissimilar material welds such as AA 5052-H32 and polycarbonate, pre-heat process kit is used as shown in Figure 3.7 in the second step.

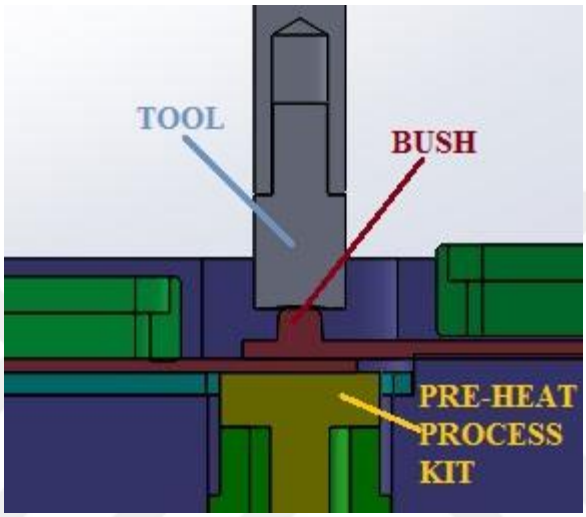


Figure 3.7 Schematic illustration of step-2 of second version includes pre-heat

At the beginning of the study, it was decided to use a milling machine for welding applications and that the apparatus should be suitable for hybrid weld applications of aluminum and polymers. In addition to these parameters given above, there are a few design parameters before creating three-dimensional model of apparatus which can be given as follows;

- The apparatus should be designed in accordance with refill welding method and using filler sheet,
- Plunge of shoulder and pin should be observed in the welding process if desired,
- The removing of samples after weld process should be easy in case of polymer sheets adhesion to main block,
- The apparatus should be suitable for placing and clamping of the weld samples easily,

- The apparatus should include pre-heat components and they should assemble or remove from the main block easily.

The welding apparatus versions comprise parts that are given below respectively;

- Main Block
- Main Block Additional Plate
- Cylindrical Weld Extrusion Block
- Shoulder-Milling Machine Interconnection Part
- Shoulder
- Pin
- Fixing Part - Right Side
- Fixing Part – Left Side
- Pre-Heat Process Kit

The first step of the welding process is common for both two versions of the welding apparatus. The manufactured first step of the apparatus is shown as in Figure 3.8.

Figure 3.8 Illustration of manufactured first step of the apparatus (Personal archive, 2017)

The first common step of the welding apparatus can be used for both similar and dissimilar materials. Firstly, welding apparatus is placed and fastened on the table of the milling machine. Two workpieces are put respectively in the rectangular channel of the apparatus, and then the filler plate is put on above the top work piece. Finally, these pieces are fastened from both right and left sides of the welding apparatus by

fixing parts. Figure 3.9 shows the prepared first step of the welding apparatus before using.

Figure 3.9 Illustration of the first step of the welding apparatus (Personal archive, 2017)

In the first step, weld application is carried out like normal FSSW. Firstly, the tool starts to rotate at a constant speed, and then the pin plunges into the filler plate and goes down within the limit of the plunge depth. In this stage, material is pushed into the gap, which is the top surface of cylindrical weld extrusion block, and this provides the creation of a dome protrusion at the bottom surface of the welded sheets as shown in Figure 3.10.

Figure 3.10 Illustration of dome protrusion shape on the welded sheets (bottom view) (Personal archive, 2017)

The second step of hybrid joint apparatus includes pre-heat process kit as shown in Figure 3.11 below. In this step, the dissimilar materials, which are welded in previous step, are placed into the welding apparatus. The heat are given to welded joint from bottom surface of material having a higher melting temperature by pre-heat kit, and then friction forming process starts in order to flatten dome structure after the predefined temperature has achieved in the weld region.

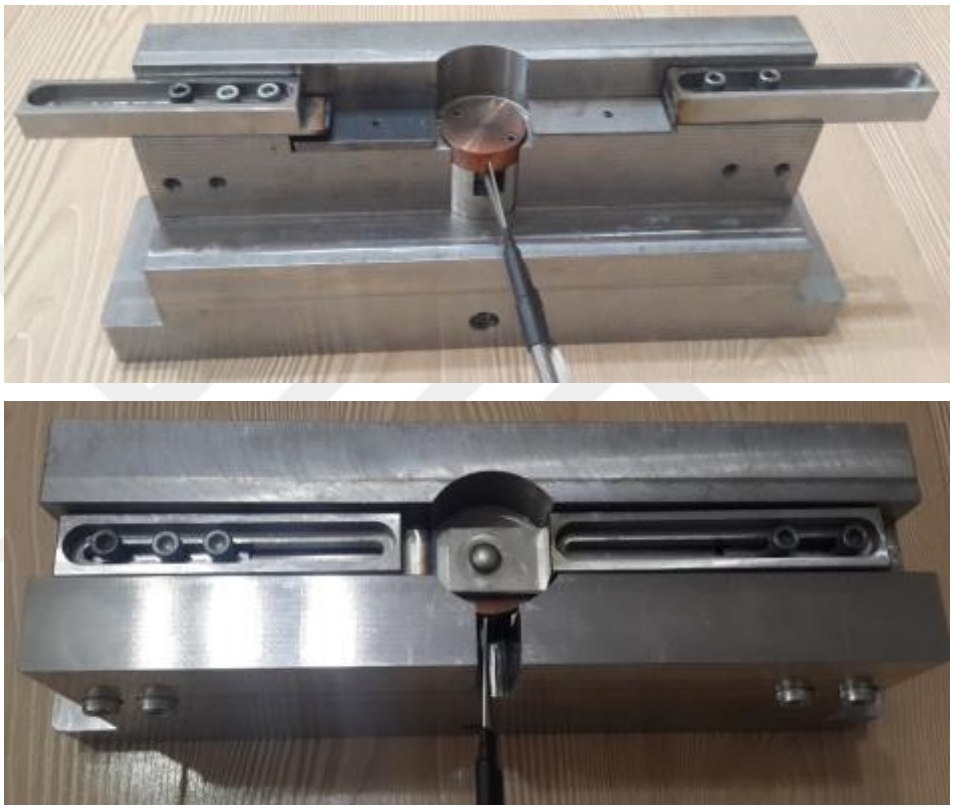

Figure 3.11 Illustration of the manufacture of the second step for the second version of the apparatus (Personal archive, 2017)

### *3.3.1 Main Block*

The main block is the biggest part and main structure of the friction stir spot welding apparatus for both versions. The welding and welding sheets are placed and clamped on it. In the welding process, this part is put on the platform of the milling machine and fixed by clamping. There are holes on it in order to fasten fixing parts and the main block additional part. Figure 3.12 shows the three dimensional model of main block.

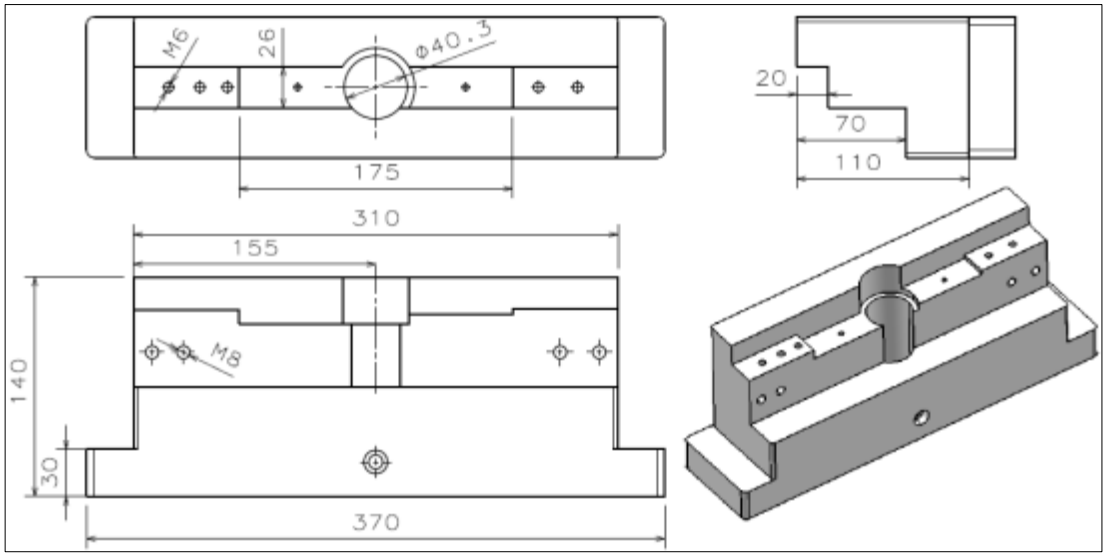


Figure 3.12 Three-dimensional model of main block

The main block was manufactured from 4140 high tensile steel in a CNC machine and Figure 3.13 shows the manufactured main block of the apparatus.

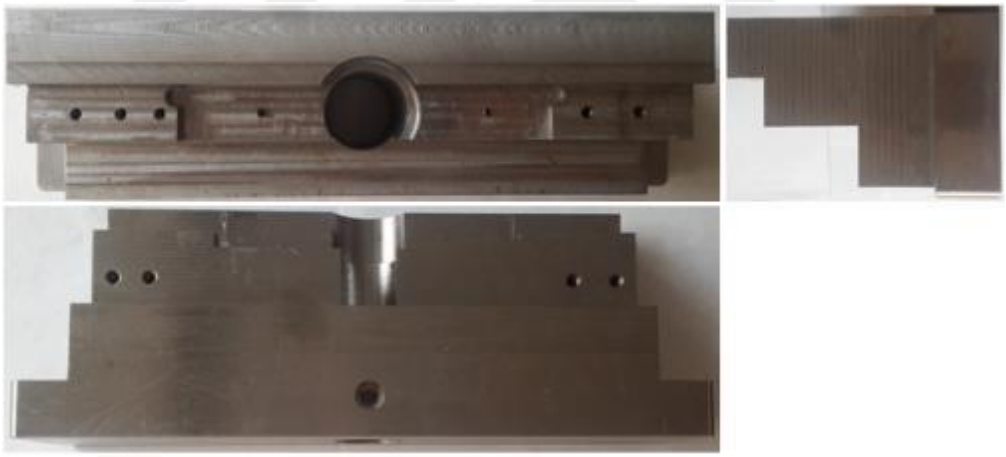

Figure 3.13 Manufactured main block (Personal archive, 2017)

### *3.3.2 Main Block Addition Part*

The additional part is a mountable and removable component of the apparatus in accordance with various conditions. In the design of welding apparatus, there were two design parameters for necessity of the main block additional part. The first parameter is to have ability of observing shoulder plunge motion during welding process. The second one is to remove welded samples easily from the welding

apparatus in case of polymer or aluminum sheets adhesion to main block. Due to these design parameters, this part was designed as mountable and removable as shown in Figure 3.14.

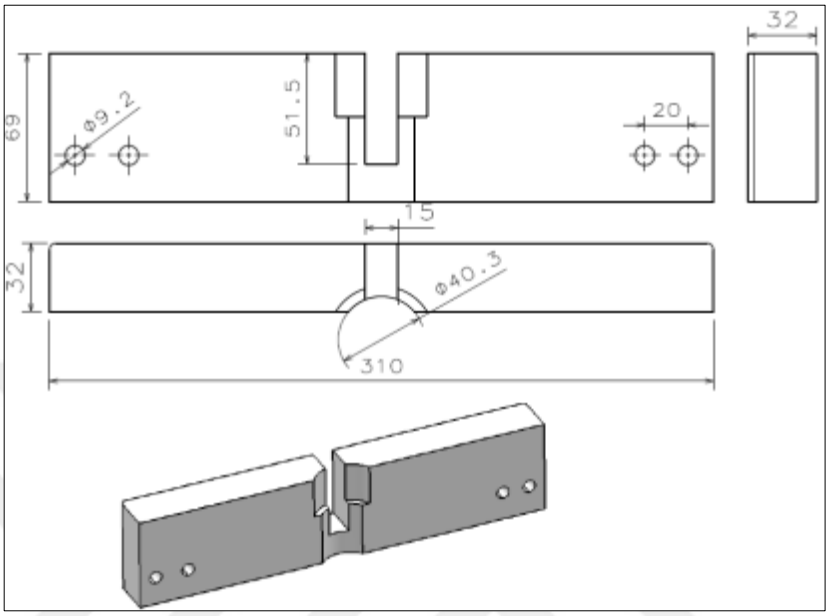


Figure 3.14 Three-dimensional model of main block additional part

Main block additional plate was manufactured from 4140 high tensile steel material and Figure 3.15 shows the manufactured part.

Figure 3.15 Manufactured main block additional part (Personal archive, 2017)

### *3.3.3 Cylindrical Weld Extrusion Block*

This part was designed in order to provide volume to filler and weld material that are pushed downward caused by the plunge motion of the shoulder and supports the

welding samples from bottom as a backing plate. There is a hole at the top surface of the part that has a role of taking in the pushed material caused by the shoulder plunge motion and in this way a protrusion with the shape of dome is created.

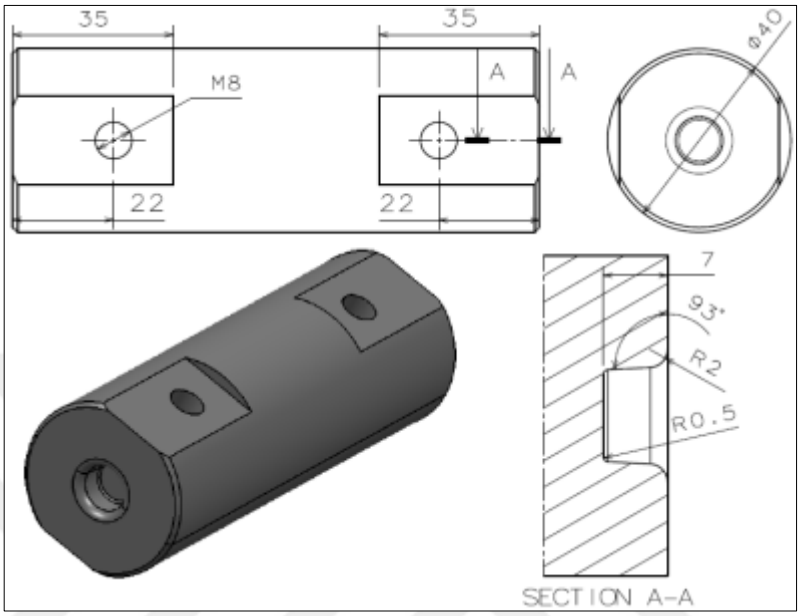


Figure 3.16 Three-dimensional model of cylindrical weld extrusion block

Cylindrical weld extrusion block was manufactured from 4140 high tensile steel material and the produced part is shown in Figure 3.17.

Figure 3.17 Manufactured cylindrical weld extrusion block (Personal archive, 2017)

### *3.3.4 Shoulder-Milling Machine Interconnection Part*

This interconnection part was designed in order to connect the shoulder to the milling machine. There is a metric 12 screw on the bottom side of the part and it is assembled to the inside of the shoulder by this screw.

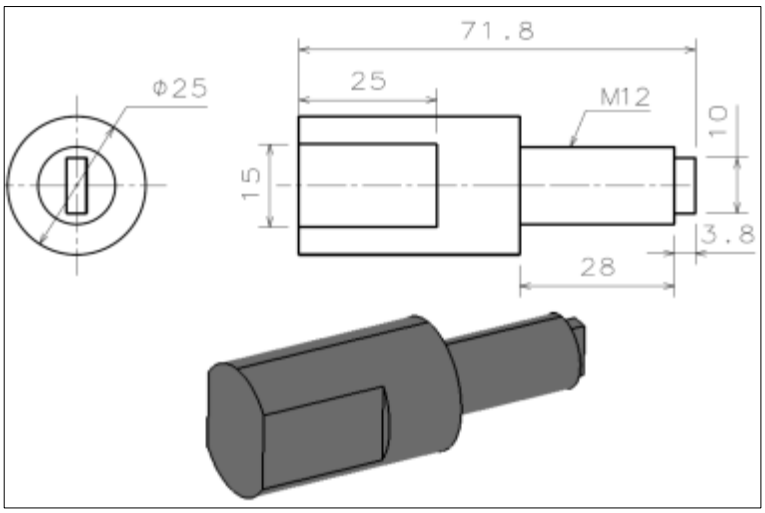


Figure 3.18 Three-dimensional model of shoulder-milling machine interconnection part

Shoulder-milling machine interconnection part was manufactured from 4140 high tensile steel and Figure 3.19 shows the produced part.

Figure 3.19 Produced shoulder-milling machine interconnection part (Personal archive, 2017)

### *3.3.5 Shoulder*

Shoulder is one of the most important parts of friction stir spot welding apparatus that plays the role of creating the frictional heat caused by rotational speed and plunge motion. There is a 5 mm diameter hole at the bottom and a metric 12 screw in it. In addition, there is a 3° tilt angle toward center so as to create sharp edges at the bottom surface of the shoulder. The aim of the tilt angle is to create concave shape on the bottom surface of shoulder and to remove the contact of the filler plate after the shoulder plunges into upper sheet.

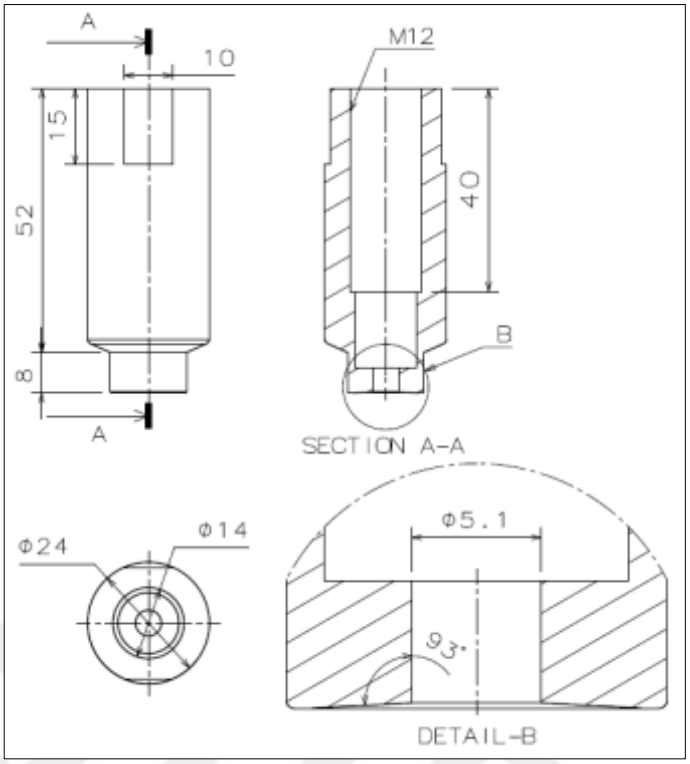


Figure 3.20 Three-dimensional model of shoulder

### *3.3.6 Pin*

The pin was designed so as to be assembled in the shoulder and the dimensions of the pin are given below. Figure 3.21 shows the three dimensional design of pin.

- The pin length is 5.3 mm (the length that is measured from the bottom surface of the shoulder),
- The diameter is M5 thread screw with a 5° tilt angle.

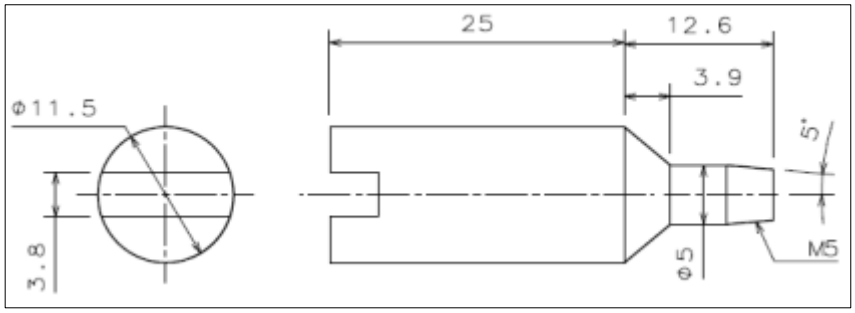


Figure 3.21 Three-dimensional model of pin

The pin was manufactured from 2344 hot worked steel and tempered at 50 rockwell hardness in order to prevent abrasion of the pin surface. Figure 3.22 shows the produced pin.

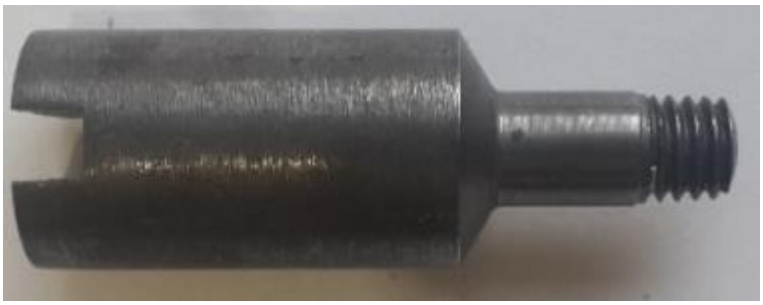

Figure 3.22 Produced pin (Personal archive, 2017)

### 3.3.7 Fixing Parts

The fixing parts are necessary in order to fasten welding sheets to the main block. There are two different fixing parts that are placed at the right and left sides of the main block, respectively. Figure 3.23 shows three dimensional model of fixing ports.

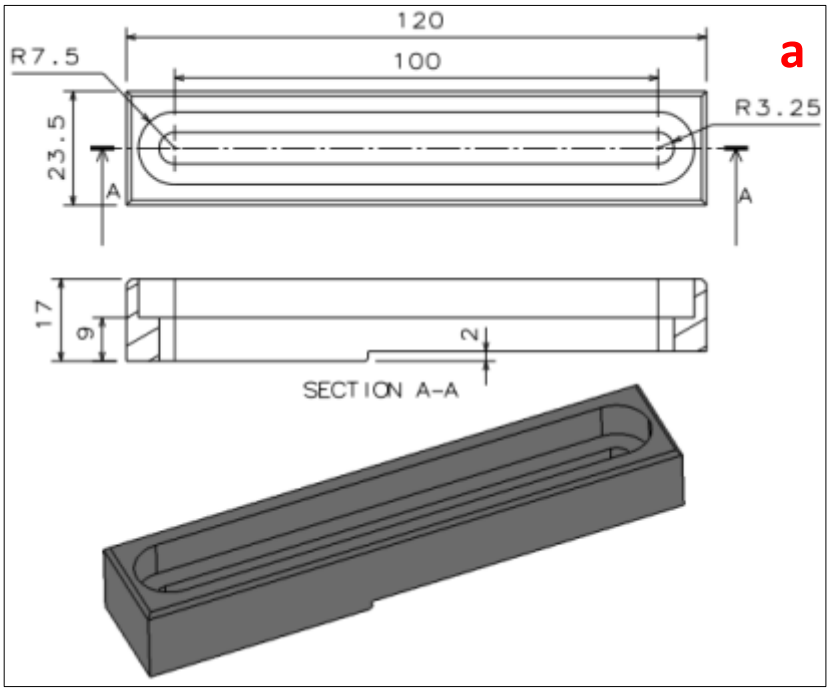

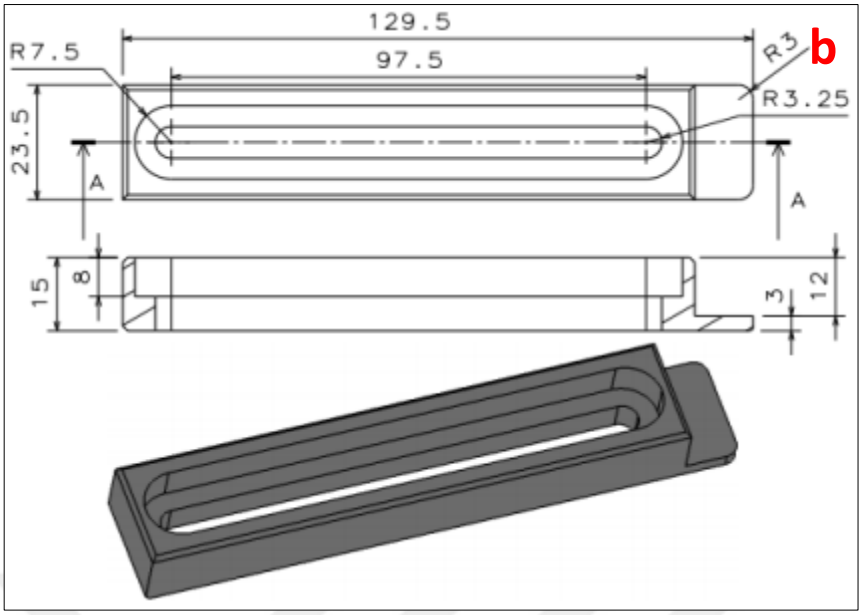


Figure 3.23 Three-dimensional model of right (a) and left (b) fixing parts

The fixing parts were manufactured from AISI 1040 carbon steel and Figure 3.24 shows the produced fixing parts.


Figure 3.24 Produced right (a) and left (b) fixing parts (Personal archive, 2017)

### 3.3.8 Pre-Heat Process Kit

The pre-heat process kit is necessary in the second step of the hybrid friction stir spot welding operations in order to heat aluminum sheet and tolerate temperature

difference between aluminum and polymers. This kit consists of a cylindrical heater part, a spiral resistance, a thermocouple, a heat control unit, an external cover part and fasteners.

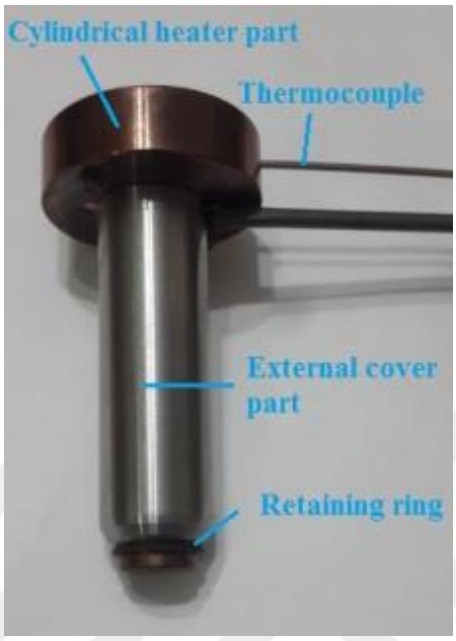


Figure 3.25 Manufactured pre-heat process kit (Personal archive, 2017)

The cylindrical heater contacts with aluminum sheet in order to heat it before starting the second step of the hybrid weld operation. The function of this part is to take the heat from the spiral resistance and transmit it to the bottom welding sheet. The material used is copper-beryllium alloy for cylindrical heater part.

The spiral resistance surrounds the bottom cylindrical section of the copper-beryllium alloy heater part. The role of this part is to provide heat to the system. The pre-heat process kit includes thermocouple that is necessary for controlling the top surface temperature of the heater part and the measured temperature is demonstrated by the heat control unit shown in Figure 3.26. Before starting to friction forming process in the second step, the heat control unit is used to check whether the pre-set temperature is reached on the bottom surface of aluminum sheet (at the same time, upper surface temperature of cylindrical heater part).

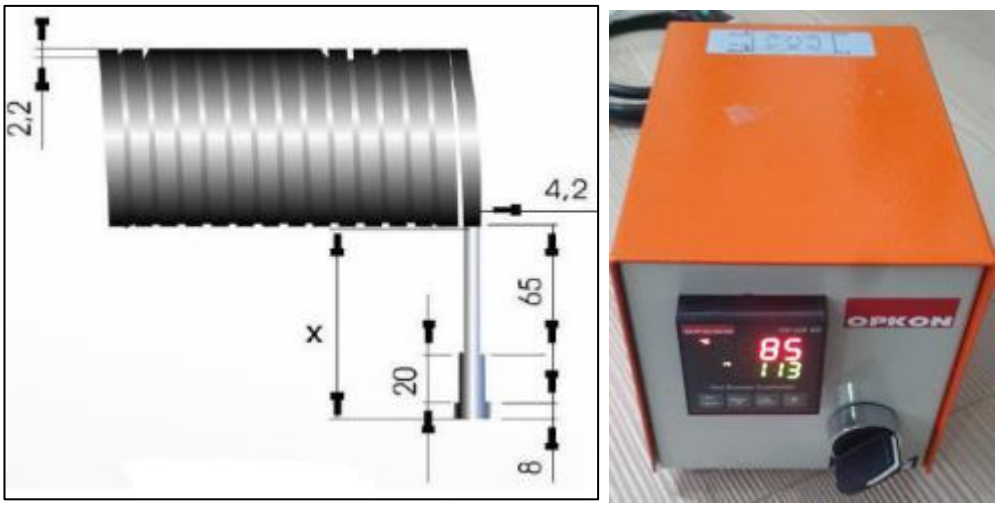


Figure 3.26 Spiral resistance and control unit (Personal archive, 2017)

### 3.3.9 Mounting part for pre-heat kit

This part is necessary for mounting of the pre-heat kit. There are four threaded holes on this part to fasten pre-heat process kit on mounting part.

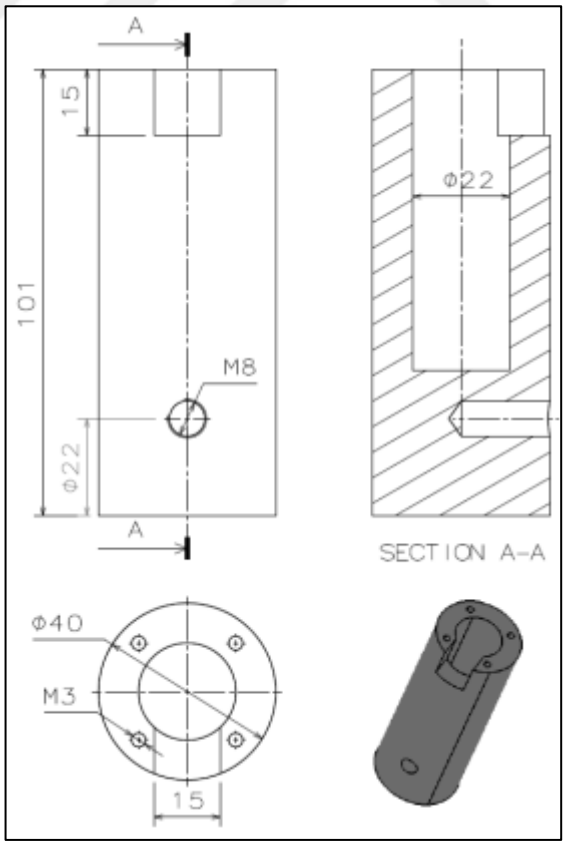


3.27 Three-dimensional model of mounting part for pre-heat kit

This part was manufactured from AISI 1040 carbon steel and Figure 3.28 shows the produced mounting part for pre-heat kit.

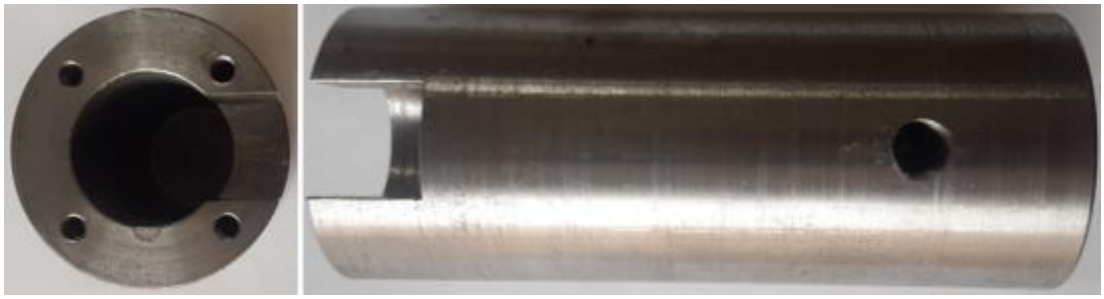

Figure 3.28 Manufactured mounting part for pre-heat kit (Personal archive, 2017)

## 3.4 Friction Stir Spot Welding Parameters

The welding parameters were defined according to previous studies carried out in the past and trial welds of aluminum and polymers. The defined welding parameters are given below respectively.

### *3.4.1 Rotational Speed*

In the friction stir spot welding process, the rotational speed is one of the most important parameters for weld quality and strength as stated in the previous sections. At the beginning, a few trial weld applications were carried out with different rotational speeds, and then the optimal speed for each combination was selected. The defined rotational speeds are given below for each welding combination:

- 1250 Rpm for AA 5052-H32 - AA 5052-H32 weld combination,
- 800 Rpm for PC – PC weld combination,
- 1000 Rpm for PP 30% GF - PP 30% GF weld combination,
- 800 Rpm for PC - AA 5052-H32 weld combination,
- 800 Rpm for AA 5052-H32 - PC weld combination,
- 400 Rpm for AA 5052-H32 - PP 30% GF weld combination.

### *3.4.2 Pin Geometry and Length*

The pin geometry was designed as circular with M5 thread according to previous studies in the literature and the length of it was defined as 5.3 mm based on sheet thickness. There is a 5° title angle toward the end of the pin in order to provide easy plunge into the weld materials. The pin length and geometry is the same for all combinations of similar and hybrid welds.

### *3.4.3 Shoulder Diameter and Geometry*

The shoulder geometry was designed as circular with 15 mm diameter according to previous studies in the literature. At the bottom surface of the shoulder there is a 3° tilt angle toward the center so as to create sharp edges at the bottom surface of the shoulder. This way, the contact between the upper sheet and the filler plate can be removed and it is known from previous studies that concave shoulder surface is better for weld strength.

### *3.4.4 Plunge Rate*

The plunge rate is one of the most significant parameters that affects the quality and strength of the weld joint. It differs according to material type and other parameters in the FSSW applications. In this study, the plunges rates used are as below for each weld combination.

- 50 mm / min for AA 5052-H32 - AA 5052-H32 weld combination,
- 10 mm / min for PC – PC weld combination,
- 10 mm / min for PP 30% GF - PP 30% GF weld combination,

### *3.4.5 Plunge Depth*

The plunge depth can be defined as the length of the plunge that is measured after the shoulder of the FSSW tool contacts the upper weld specimen and it is one of the critical parameters in FSSW studies in terms of mechanical properties and the quality

of the joint. For that reason, in the literature there are a lot of different studies related to its effect on mechanical properties of the weld. In this study, because of using filler plate in the welding method, shoulder plunges into the filler plate in weld applications. For that reason, plunge depth was measured from once the shoulder contacts filler plate.

Yoon et al. (2012), have investigated the influences of tool plunge depth and plunge speed on friction spot joining of AA 5054-O aluminum alloy plates with the thicknesses of 1.4 mm and 1.0 mm. In the study, the plunge speed of the tool was changed in a range of 100−500 mm/min under a constant rotation speed of 500 rpm. In addition, the plunge depth was ranged between 1.6 mm to 2.2 mm. They have analyzed the influence of tool plunge depth on the surface appearance, macrostructure and average maximum tensile shear of welded aluminum plates. It was observed that the increase of the tool plunge depth causes the increase in the amount of the burr and at the same time decrease in the thickness at the central weld zone of the lower plate as shown in Figure 3.29.

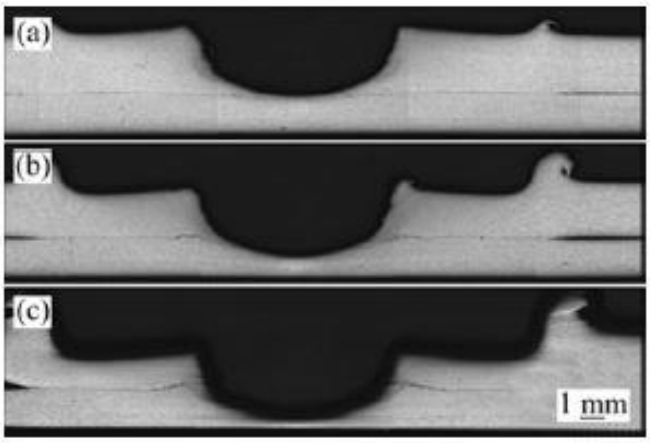


Figure 3.29 Influence of the tool plunge depth on macrostructure (a) 1.6 mm; (b) 2.0 mm; (c) 2.2 mm

Yoon et al. (2012) have showed that the plunge depth is a significant parameter in terms of controlling the surface appearance of joint as shown in Figure 3.30. Tensile shear tests showed that the increase of the tool plunge depth resulted in better tensile shear loads as shown in Figure 3.31 (Yoon et al., 2012).

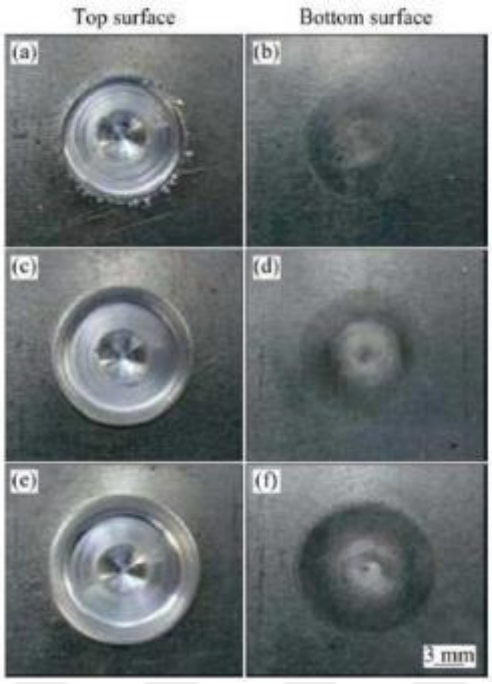


Figure 3.30 Influence of the tool plunge depth on surface appearance (a), (b) 1.6 mm; (c), (d) 2.0 mm; (e), (f) 2.2 mm

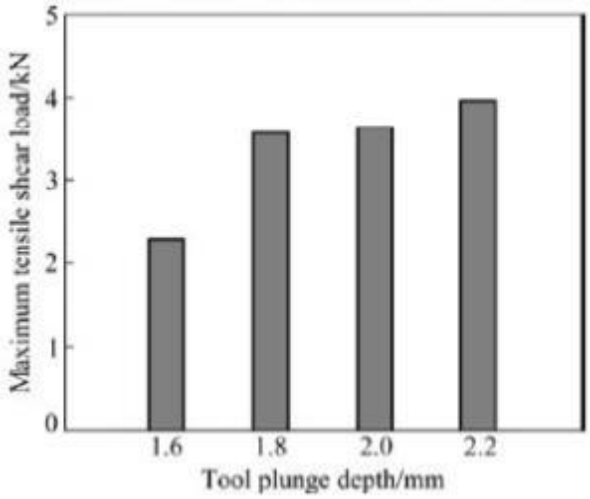


Figure 3.31 Influence of the tool plunge depth on average maximum tensile shear load

The plunge depth was defined according to weld material combinations and material thicknesses. At the beginning of the weld application, before taking weld samples which will be used in the mechanical tests, trial welds have been conducted in order to decide the optimum plunge depth for each type of weld combination. The plunge depth was calculated and determined after the shoulder bottom surface contacts the filler plate top surface.

- The plunge depths are 3 mm, 3.5 mm and 4 mm for AA 5052-H32 - AA 5052-H32 weld combination,
- The plunge depths are 5 mm, 5.5 mm and 6 mm for PC – PC weld combination,
- The plunge depths are 5 mm, 5.5 mm and 6 mm for PP 30% GF - PP 30% GF weld combination,

### 3.5 Mechanical Tests and Evaluation

The quality of the friction stir spot welded samples is measured by evaluating the mechanical properties of the joint. There are several mechanical tests that are generally used for joint evaluation such as lap shear and cross-tension and also microhardness determination and fatigue tests are utilized. In the scope of this study, for aluminum weld evaluation, lap shear test and microhardness measurement were used and for PC, PP GF%30 weld evaluation lap shear test was used. For each plunge depth value, a total of four samples were welded for aluminum weld combinations. Three of them were used for the lap shear tests and one of them was used for microhardness measurement and macrostructure evaluation.

#### 3.5.1 Lap Shear Test

In the lap shear test of all samples, Shimadzu AG-X tensile testing device was used and the weld samples were tested with 1 mm/sec pulling speed. Before starting the tests, the support parts were added to welded samples to provide correct test conditions as shown in Figure 3.32.

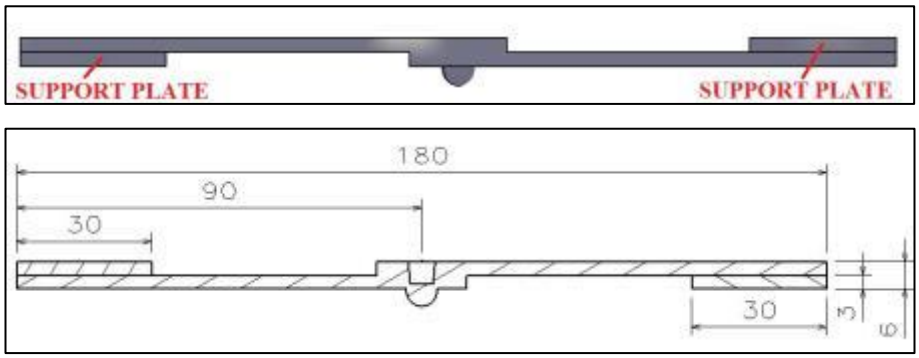


Figure 3.32 Illustration of lap shear test specimen

### 3.5.2 Microhardness Measurement

The microhardness measurements of aluminum sheets alloys were performed in accordance with TS EN ISO 6507-1 using Duramin manuel micro/macro hardness tester as shown in Figure 3.33.

Figure 3.33 Duramin micro/macro hardness tester (Personal archive, 2017)

### *3.5.3 Macrostructure Investigation*

The macrostructure evaluation was used in the analyzing of aluminum weld samples. In the investigation of microstructure and the macrostructure process, welded samples are cross-sectioned and generally the weld region are investigated in terms of SZ, TMAZ and HAZ. In this study, the dome structure's geometry and dimensions were analyzed differently.

# CHAPTER FOUR
# RESULTS AND DISCUSSION

## 4.1 Investigation of Mechanical Properties of AA 5052-H32 - AA 5052-H32 FSSW Combination

Aluminum similar friction stir spot welding was performed with constant rotational speed of 1250 rpm and three different plunge depths as 3, 3.5mm, 4mm were applied. In these weld applications, 3mm thick AA 5052-H32 aluminum sheets were used and the weld configuration was as shown in Figure 4.1. Aluminum sheets were overlapped 20 mm and the 30mm length of filler plate was used.

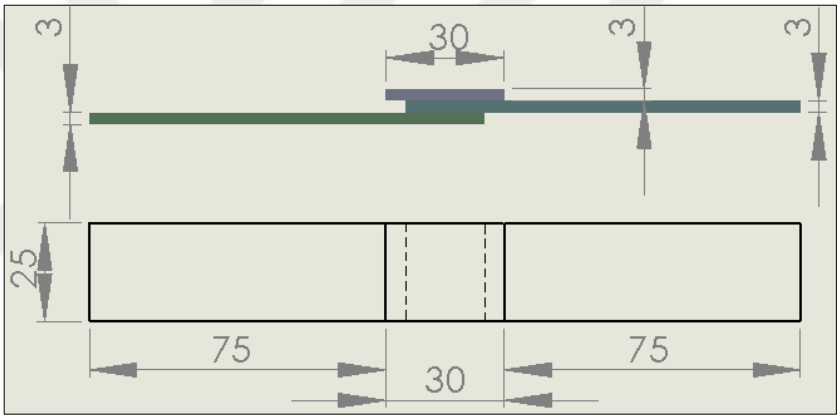


Figure 4.1 Aluminum similar weld configuration

The aluminum sheets were located and fastened into the welding apparatus as given in Figure 4.2 before starting the weld process and in pre-trial weld applications, the weld processes were observed.

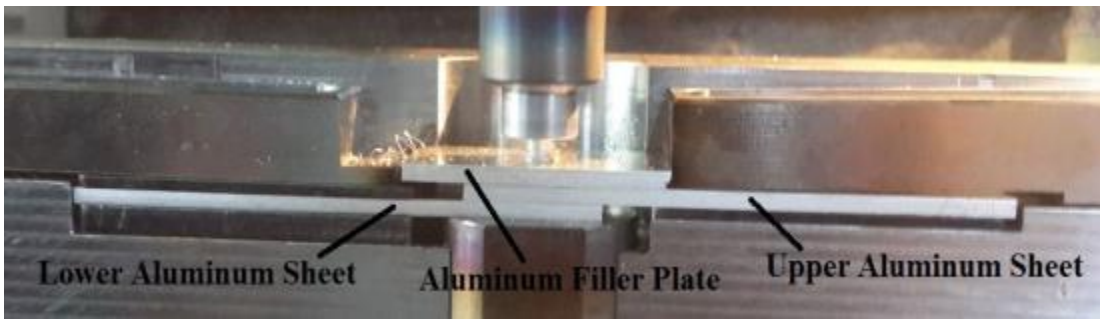


Figure 4.2 The position of aluminum sheets in the welding apparatus (Personal archive, 2017)

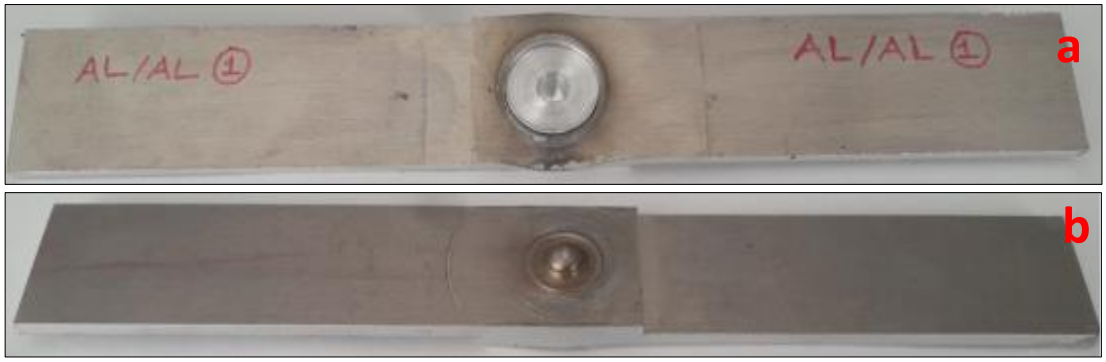


Figure 4.3 Welded aluminum sheets (a) top wiev (b) bottom view (Personal archive, 2017)

### *4.1.1 Lap Shear Test of AA 5052-H32 - AA 5052-H32 FSSW Combination*

The lap shear test results of aluminum weld samples, which have a 3 mm plunge depth are given in Figure 4.4 below. The measured maximum forces are 2425N, 2534.9 N, 2787.5 N, respectively.

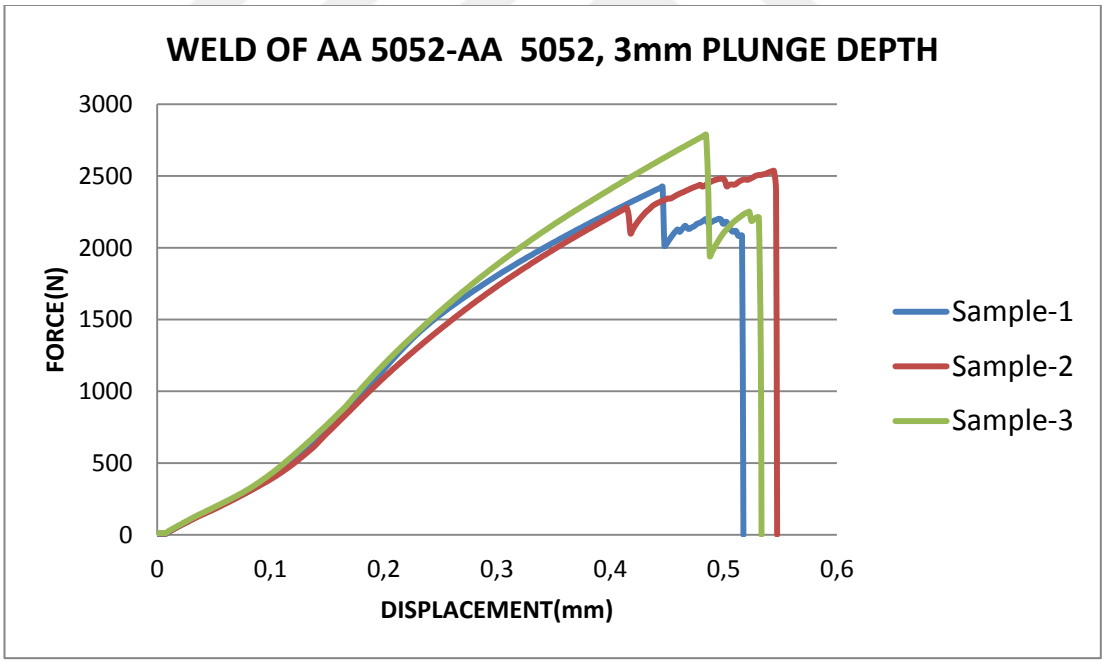


Figure 4.4 Lap shear test results of aluminum sheets – 3 mm plunge depth

The lap shear test results of aluminum weld samples, which have a 3.5 mm plunge depth are given in Figure 4.5. The measured maximum forces are 2885 N, 2602.9 N, 2468.5 N, respectively.

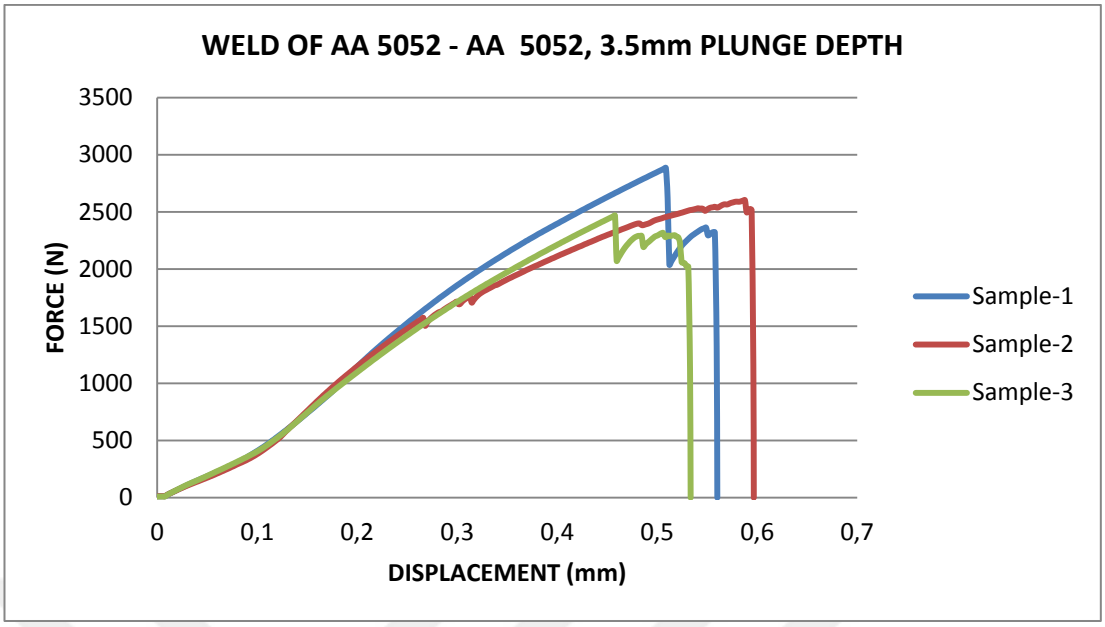


Figure 4.5 Lap shear test results of aluminum sheets – 3.5 mm plunge depth

The lap shear test results of aluminum samples, which have a 4 mm plunge depth are given in Figure 4.6. The measured maximum forces are 3628.2 N, 5164.4 N, 3066.7 N, respectively.

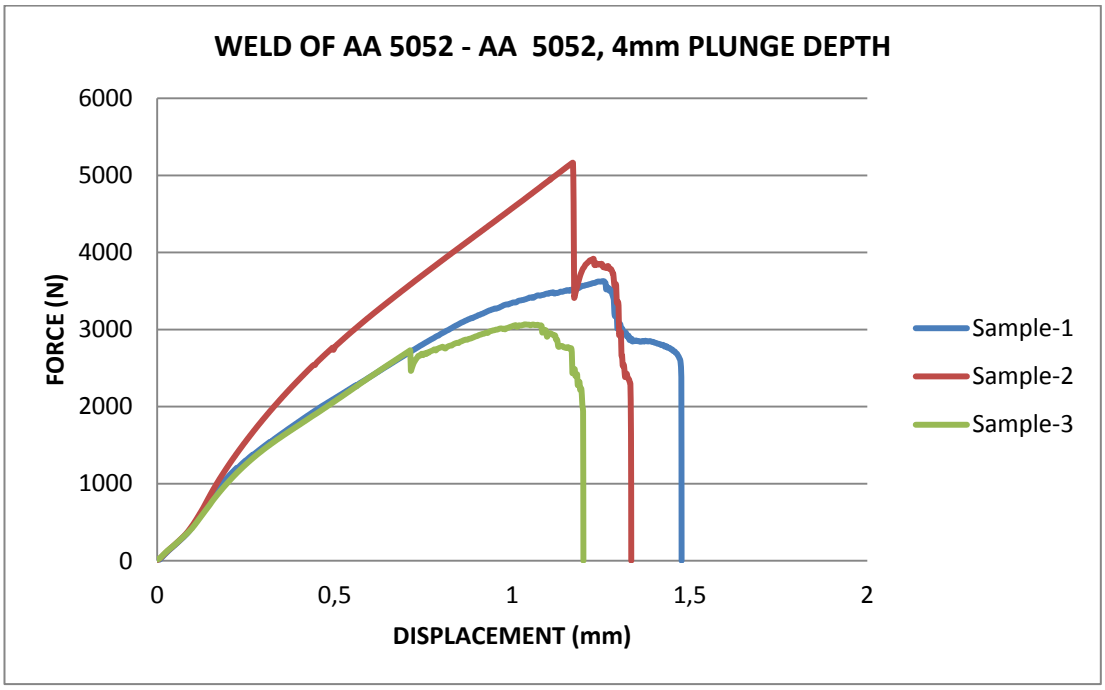


Figure 4.6 Lap shear test results of aluminum sheets – 4 mm plunge depth

Table 4.1 summarizes the measured maximum forces in the lap shear tests of all welded samples. For each plunge depth test results, the average maximum force values were calculated. When these average force values are evaluated it is seen from the table that, increasing the plunge depth has resulted in an increasing in the maximum measured force during the lap shear test.

Table 4.1 Measured maximum forces of aluminum alloys

| | Maximum Forces (N) | | | |
|---|---|---|---|---|
| Sample Definition | Sample-1 | Sample-2 | Sample-2 | Average |
| 3mm Plunge Depth Samples | 2425 | 2534.9 | 2787.5 | 2582.4 |
| 3.5mm Plunge Depth Samples | 2885 | 2602.9 | 2468.5 | 2652.1 |
| 4mm Plunge Depth Samples | 3628.2 | 5164.4 | 3066.7 | 3953 |

### *4.1.2 Microhardness Measurement of AA 5052-H32 - AA 5052-H32 FSSW Combination*

The microhardness values were measured 1 mm above from the joint interface of upper and lower aluminum sheets for three aluminum welded samples that have different plunge depths. The measurement lines were marked before the tests as shown in Figure 4.7 and the measurements were performed at intervals of 1mm from left side to the right side line.

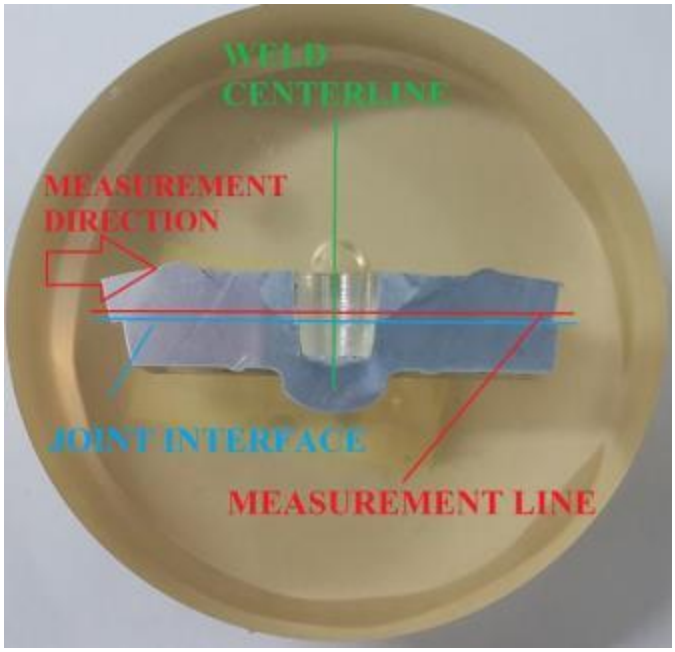


Figure 4.7 Illustration of microhardness measurement sample (Personal archive, 2017)

Figure 4.8 shows measurement values of microhardness measurements for each weld sample and their microhardness distribution along the line.

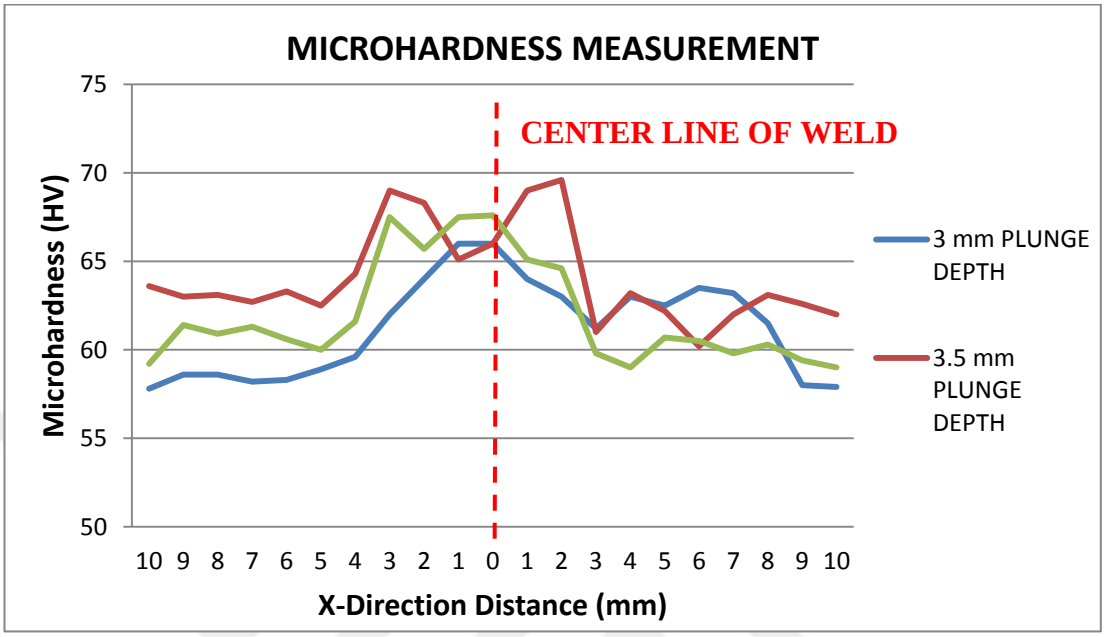


Figure 4.8 Illustration of microhardness measurement values

Microhardness measurement results show that the microhardness values increase towards the weld stir zone. The chart lines of microhardness measurement results are similar for different plunge depths and show symmetry according to center line of weld.

### *4.1.3 Macrostructure Investigation of AA 5052-H32 - AA 5052-H32 FSSW Combination*

In the scope of evaluating the mechanical properties of aluminum alloy joints, the cross-section appearances of the welded samples were analyzed considering to the different plunge depths. Three welded samples were cut by waterjet cutting machine and prepared. The macrostructure of all aluminum welded samples were investigated in terms of three measurement parameters as shown in Figure 4.9.

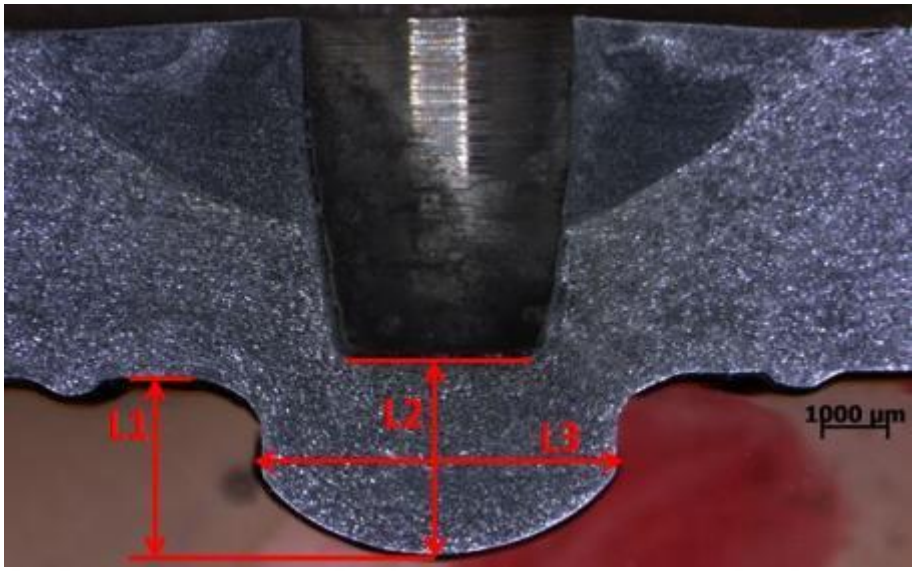


Figure 4.9 Illustration of macrostructure parameters

These dimensional parameters were measured from the scaled images using a special computer aided programme for all samples, respectively. The aim of analyzing these parameters is to investigate how the dome structure changes according to different plunge depths and how the shear test results change according to dome structure and parameters. Length-1 (L1) parameter identifies the dome height from bottom surface of the lower aluminum sheet. Similarly, length-2 (L2) parameter identifies the dome height from the bottom point of the weld keyhole. Length-3 (L3) describes the width of the dome structure.

Firstly, Figure 4.10 shows the macrostructure view and measured dimensional parameters of the welded aluminum sheets, which have a 3 mm plunge depth. The measured values are given in Table 4.2.

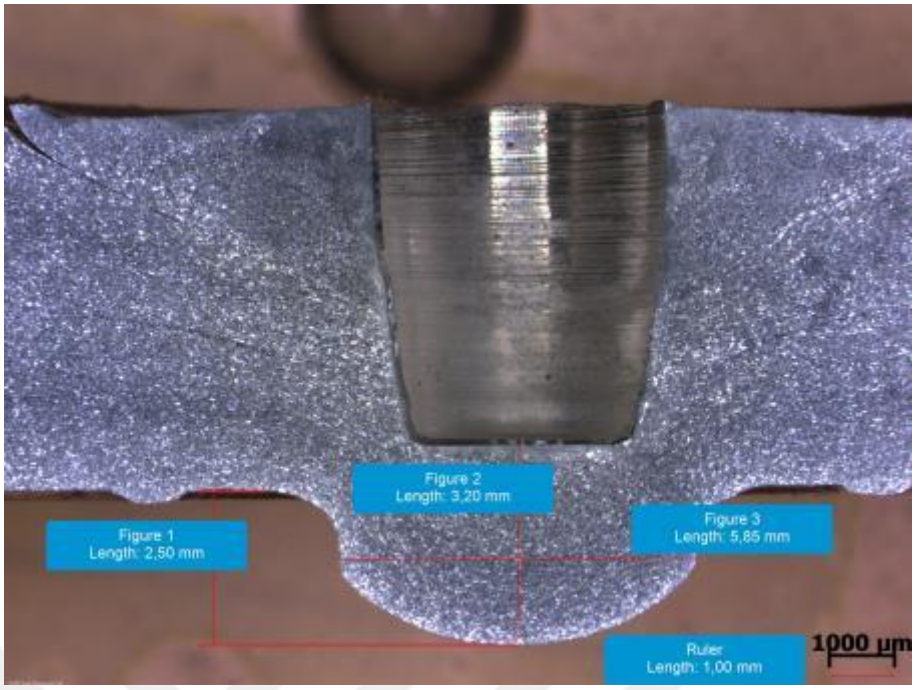


Figure 4.10 Illustration of measured parameters of welded sample and macrostructure view– 3mm plunge depth

Figure 4.11 shows the macrostructure view and measured dimensional parameters of the welded aluminum sheets, which have a 3.5 mm plunge depth.

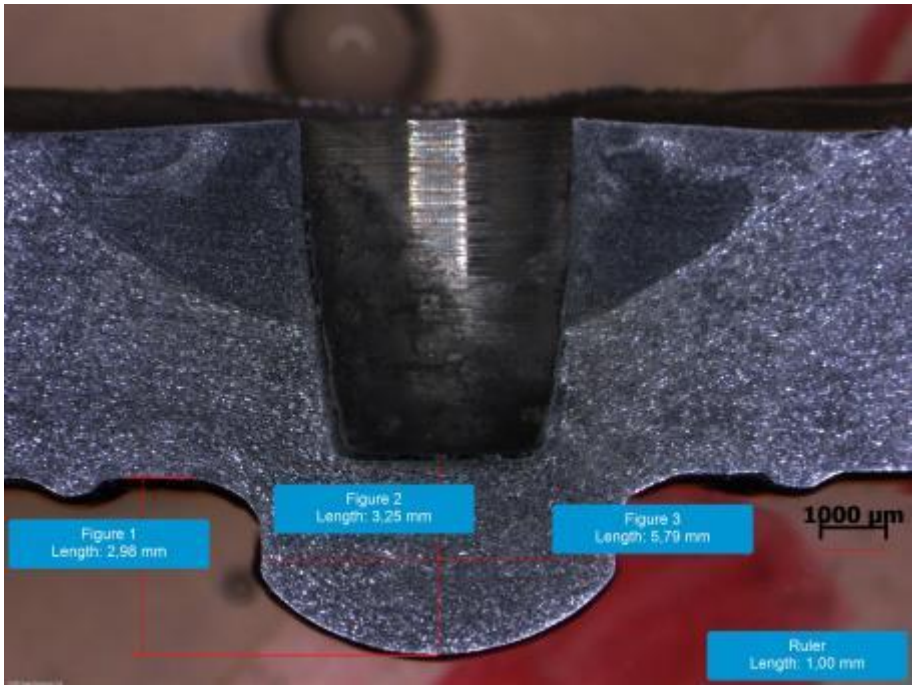


Figure 4.11 Illustration of measured parameters of welded sample and macrostructure views – 3.5mm plunge depth

Finally, Figure 4.12 shows the macrostructure view and measured dimensional parameters of the welded aluminum sheets, which have a 4 mm plunge depth.

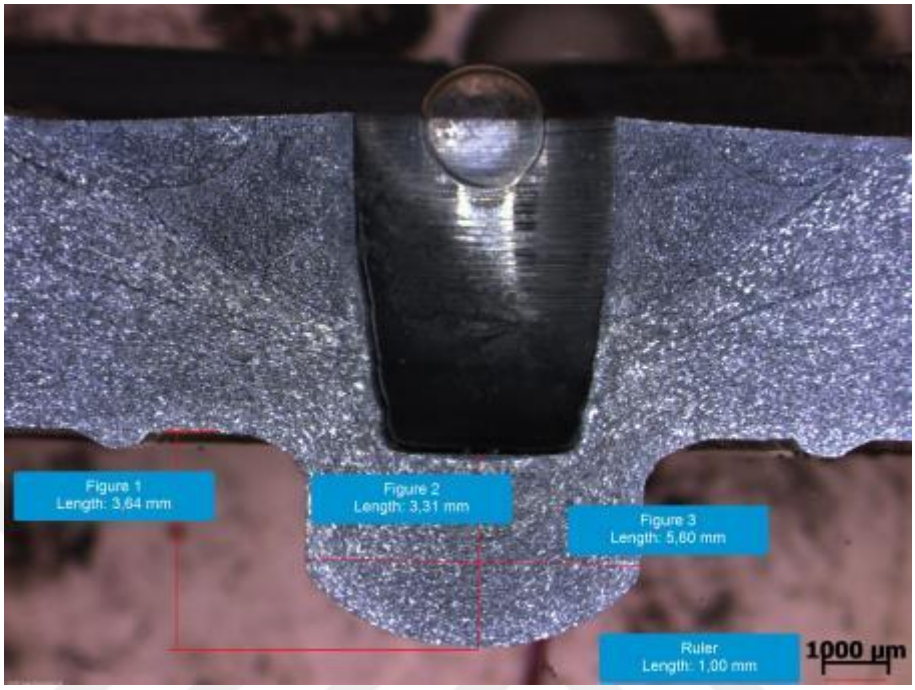


Figure 4.12 Illustration of measured parameters of welded sample and macrostructure view – 4mm plunge depth

Table 4.2 summarizes the measured values. It can be observed from the table that when the plunge depth increases the dome height increases in parallel and the dome structure width reduces.

Table 4.2 Measured parameters

| **Sample Definition** | **L1 (mm)** | **L2 (mm)** | **L3 (mm)** |
|---|---|---|---|
| AA Welded Sample - 3mm Plunge Depth | 2.50 | 3.20 | 5.85 |
| AA Welded Sample - 3.5mm Plunge Depth | 2.98 | 3.25 | 5.79 |
| AA Welded Sample - 4mm Plunge Depth | 3.64 | 3.31 | 5.60 |

In the analysis of the macrostructure of the welded samples, the stir zone of each type of welded samples was analyzed in terms of the stir zone area. Firstly, stir zones were defined in the cross-sectional views of the samples and then area of the bordered SZ were calculated from scaled images using a computer aided programme.

The first sample welded with 3 mm plunge depth has a 5.10 mm² area of stir zone.

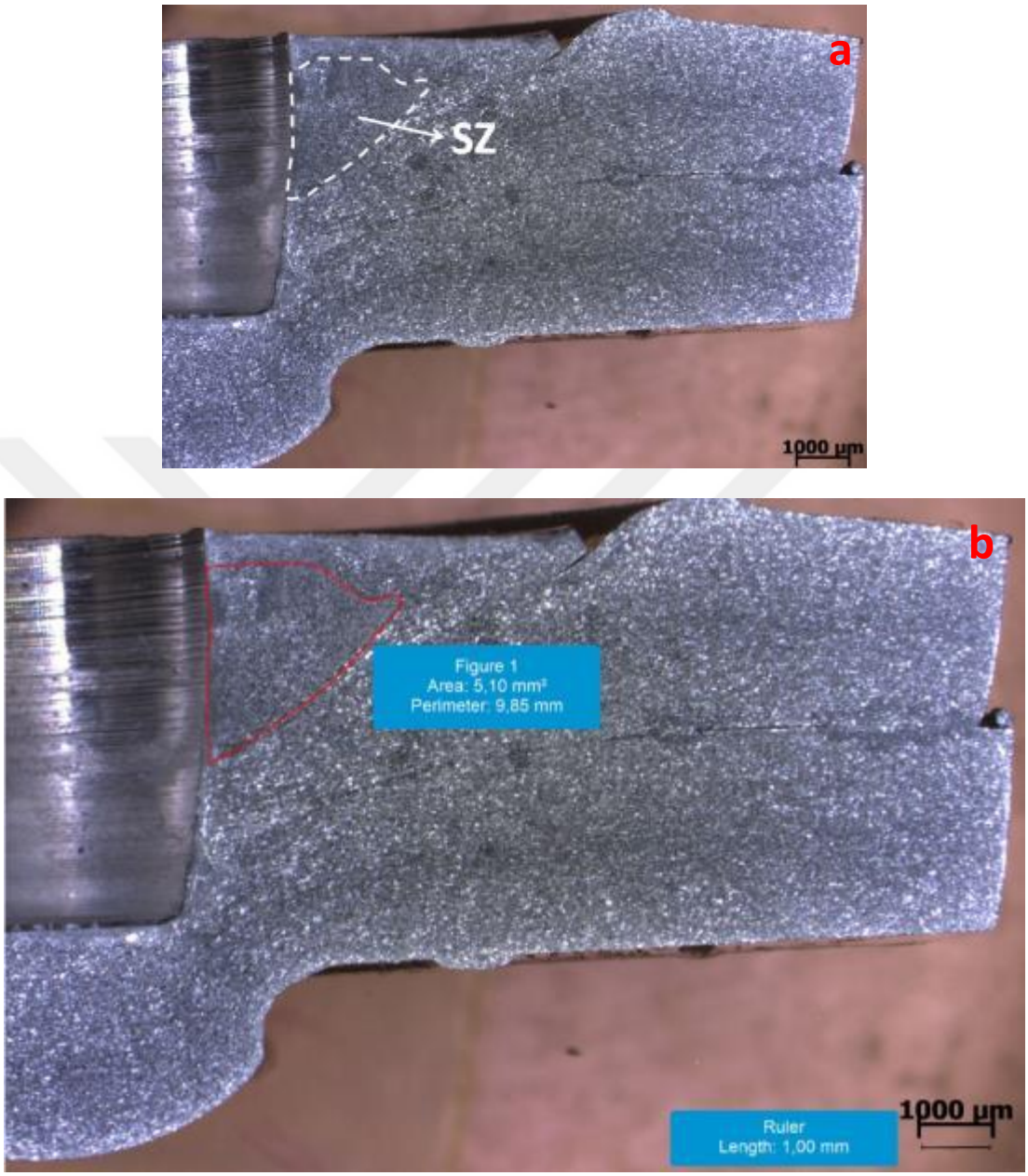


Figure 4.13 Illustration of (a) stir zone border lines and stir zone measured area – aluminum sample 3 mm plunge depth

The second sample welded with 3.5 mm plunge depth has a 6.14 mm² area of stir zone.


Figure 4.14 Illustration of (a) stir zone border lines and stir zone measured area – aluminum sample 3.5 mm plunge depth

The last aluminum sample welded with 4 mm plunge depth has a 7.05 mm² area of stir zone.


Figure 4.15 Illustration of (a) stir zone border lines and stir zone measured area – aluminum sample 4 mm plunge depth

When the stir zone areas are compared, it can be argued that increasing the plunge depth causes a rise of stir zone area.

## 4.2 Investigation of the Mechanical Properties of PC – PC FSSW Combination

4 mm thick PC sheets were welded with constant rotational speed of 800 rpm and at three different plunge depths as 5, 5.5 mm, 6 mm. Figure 4.16 shows the weld configuration of the PC sheets and the position of 4mm thick filler plate.

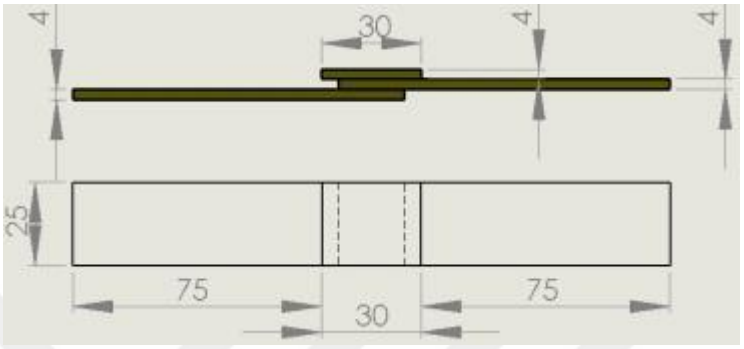


Figure 4.16 PC sheets weld configuration

FSSW process of the PC sheets is the same as the aluminum sheets. PC sheets were placed and fastened onto welding apparatus as shown in Figure 4.17. For each plunge depth value, three samples were welded as given in Figure 4.18 for the shear laps tests.

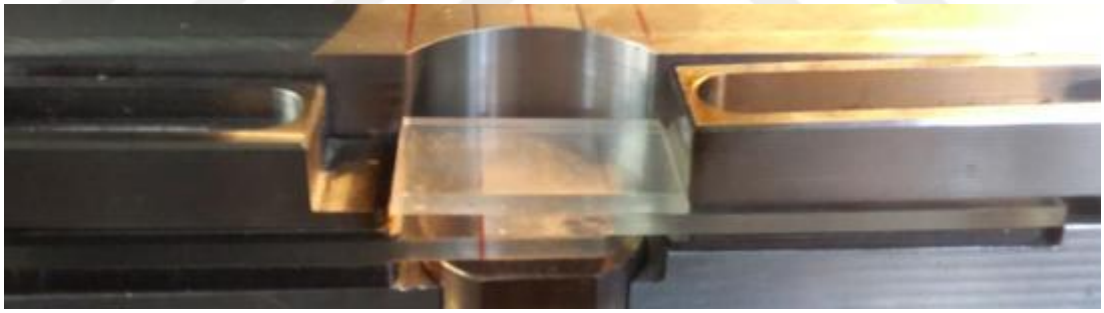

Figure 4.17 The position of PC sheets in the welding apparatus (Personal archive, 2017)

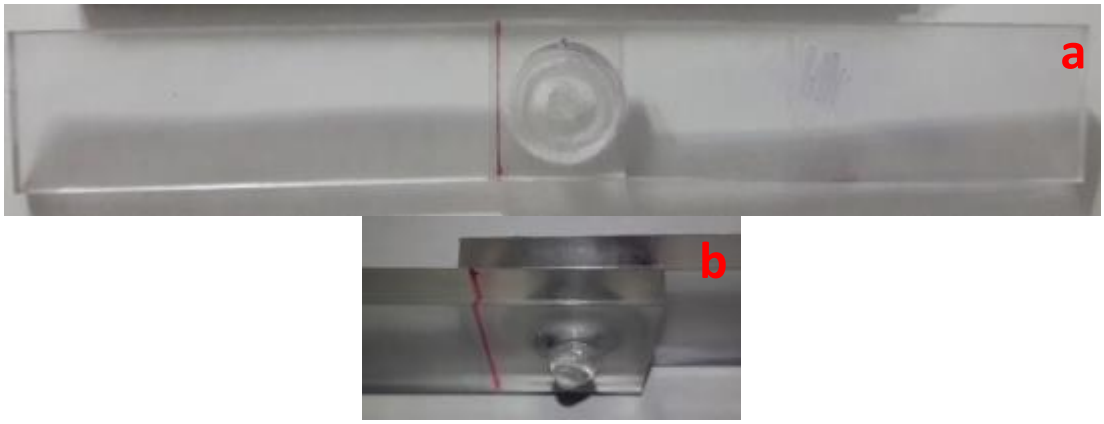


Figure.4.18 Welded PC sheets (a) top wiev (b) bottom view (Personal archive, 2017)

### *4.2.1 Lap Shear Test of PC-PC FSSW Combination*

The lap shear test of all welded PC samples was carried out with 1 mm/sec pulling speed. The shear test results of PC weld samples, which have 5 mm plunge depth are given in Figure 4.19. Maximum measured forces are 1246.8 N, 1124.6 N, 1152 N, respectively.

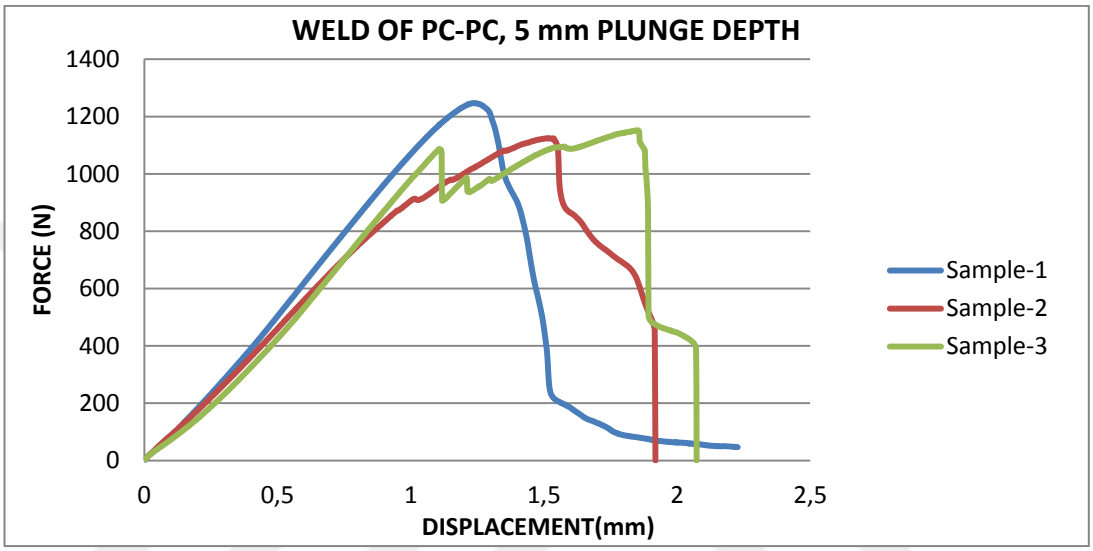


Figure 4.19 Lap shear test results of PC sheets – 5 mm plunge depth

The lap shear test results of PC weld samples, which have 5.5 mm plunge depth are given in Figure 4.20. Measured maximum forces are 1318.3 N, 1236.9 N and 1274 N respectively.

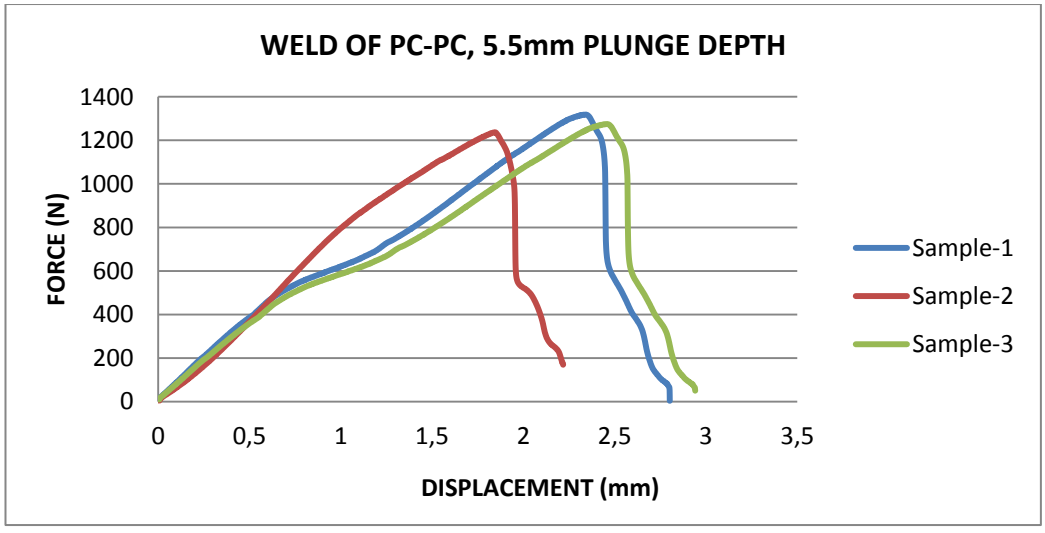


Figure 4.20 Lap shear test results of PC sheets – 5.5 mm plunge depth

The lap shear test results of PC weld samples, which have a 6 mm plunge depth are shown in Figure 4.21.

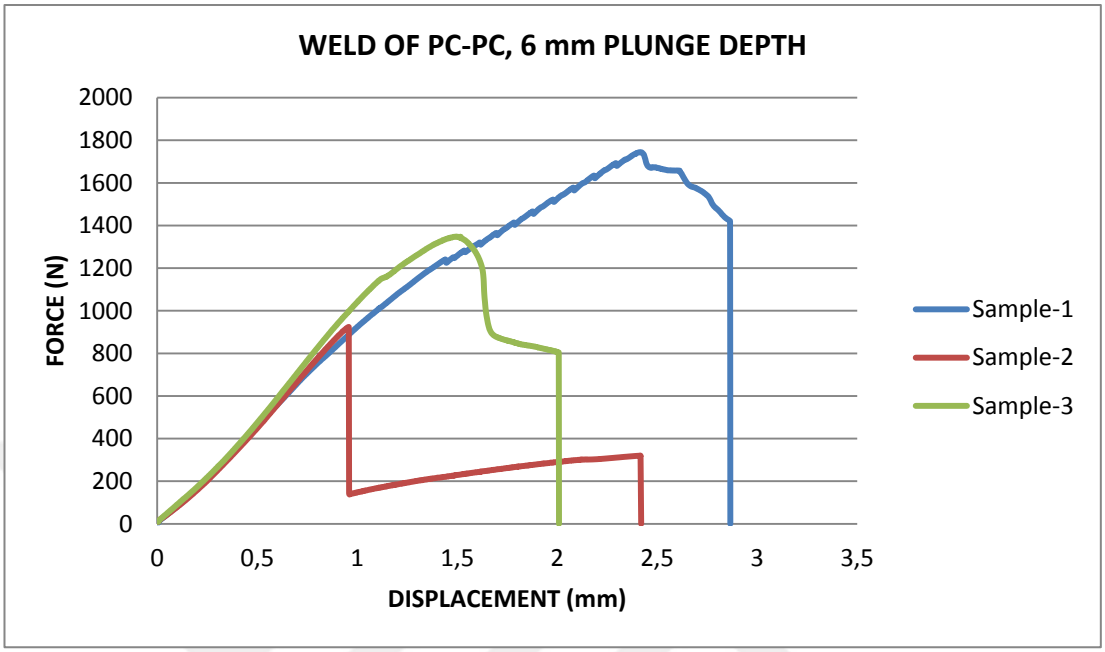


Figure 4.21 Lap shear test results of PC sheets – 6 mm plunge depth

Table 4.3 summarizes the measured maximum forces for welded polycarbonate sheets. As it is seen from the table, with the increasing plunge depth, the maximum average force in lap shear tensile test increases.

Table 4.3 Measured maximum forces of PC

| | Maximum Forces (N) | | | |
|---|---|---|---|---|
| Sample Definition | Sample-1 | Sample-2 | Sample-3 | Average |
| 5mm Plunge Depth Samples | 1246,8 | 1124,6 | 1152 | 1174,5 |
| 5.5mm Plunge Depth Samples | 1318,3 | 1236,9 | 1274 | 1276,4 |
| 6mm Plunge Depth Samples | 1744,7 | 924 | 1347,9 | 1338,9 |

## 4.3 Investigation of the Mechanical Properties of PP 30% GF - PP 30% GF FSSW Combination

4 mm thick PP 30% GF sheets were welded with a constant rotational speed of 1000 rpm and three different plunge depths as 5 mm, 5.5 mm, 6 mm. The PP sheets were placed and fastened to welding apparatus similar to previous applications and the weld configuration was the same with FSSW of polycarbonate sheets.

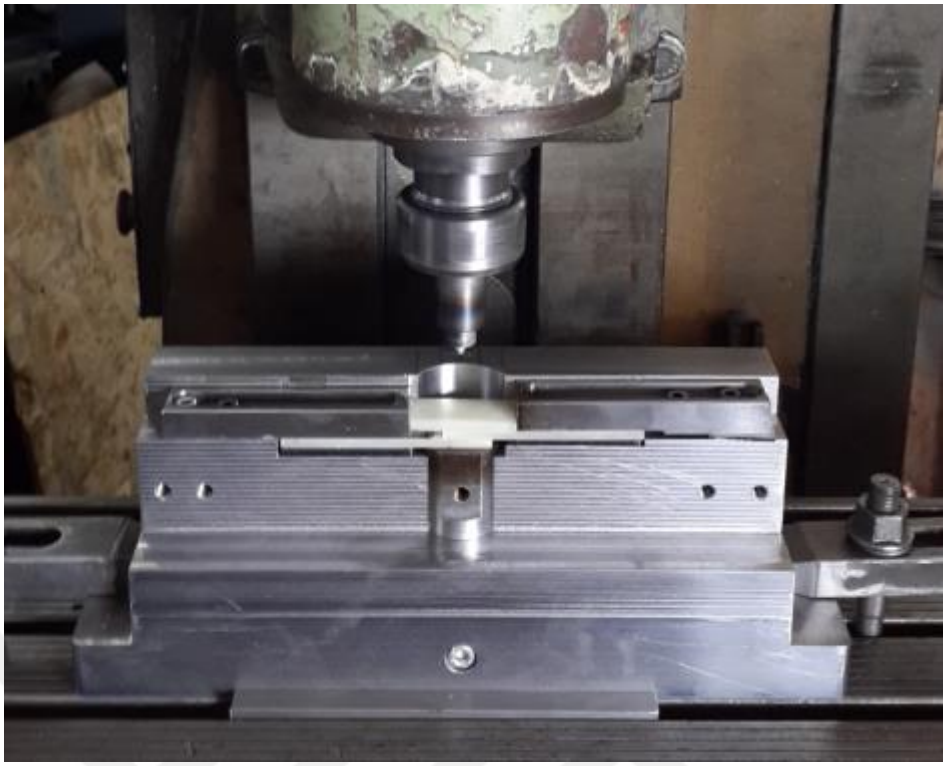

Figure 4.22 The position of PP 30% GF sheets in the welding apparatus (Personal archive, 2017)

For each combination, three samples were welded for lap shear test. Figure 4.23 shows a sample of welded PC sheets using FSSW.

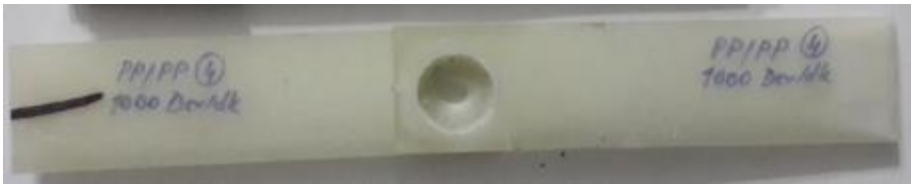

Figure 4.23 Welded PP GF%30 sheets (Personal archive, 2017)

### *4.3.1 Shear Lap Test of PP 30% GF - PP 30% FSSW Combination*

The shear lap test of all welded PP 30% GF samples were tested with 1 mm/sec pulling speed. The shear test results of PP 30% GF weld samples, which have a 5 mm plunge depth are given in Figure 4.24. Maximum measured forces are 644.8 N, 356.5 N, 524 N, respectively.

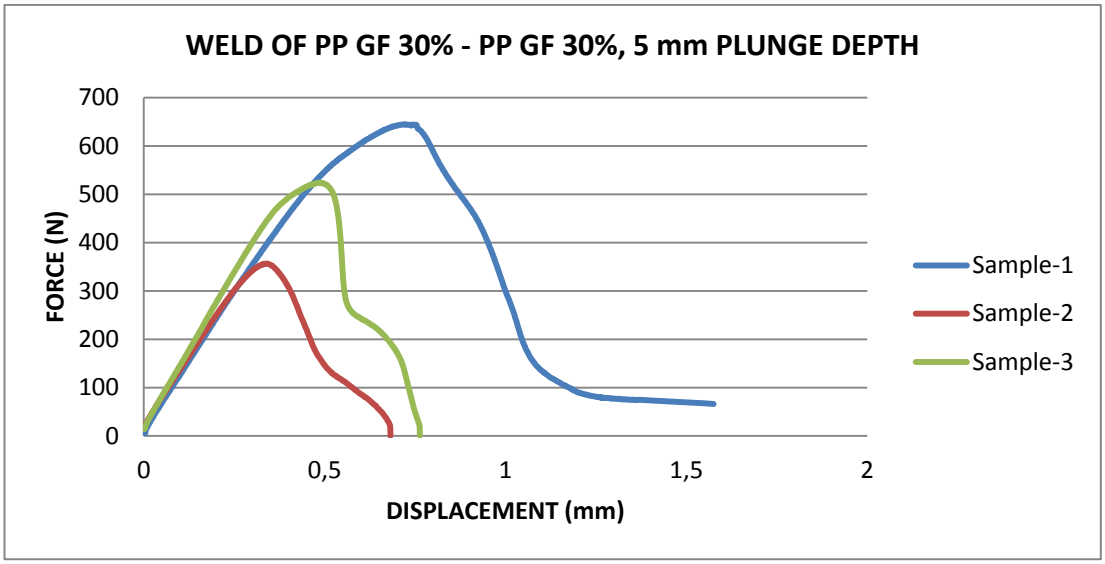


Figure 4.24 Lap shear test results of PP GF%30 sheets – 5 mm plunge depth

The shear test results of PP 30% GF weld samples, which have a 5.5 mm plunge depth are shown in Figure 4.25. Maximum measured forces are 569.4 N, 710 N, 632.5 N, respectively.

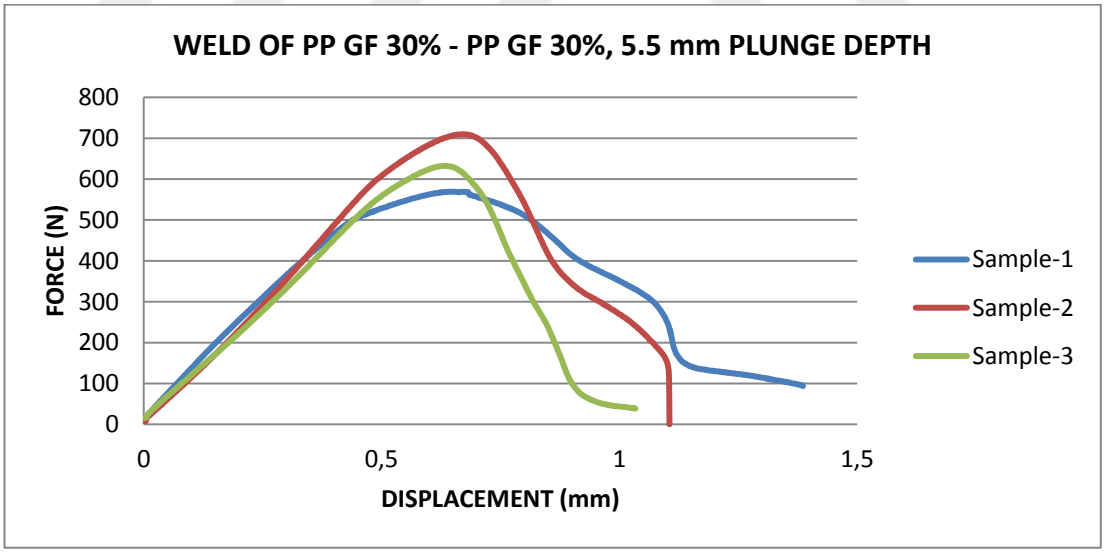


Figure 4.25 Lap shear test results of PP GF%30 sheets – 5.5 mm plunge depth

The shear test results of PP 30% GF weld samples, which have a 6 mm plunge depth are given below. Maximum measured forces are 434.4 N, 496 N, and 505 N, respectively.

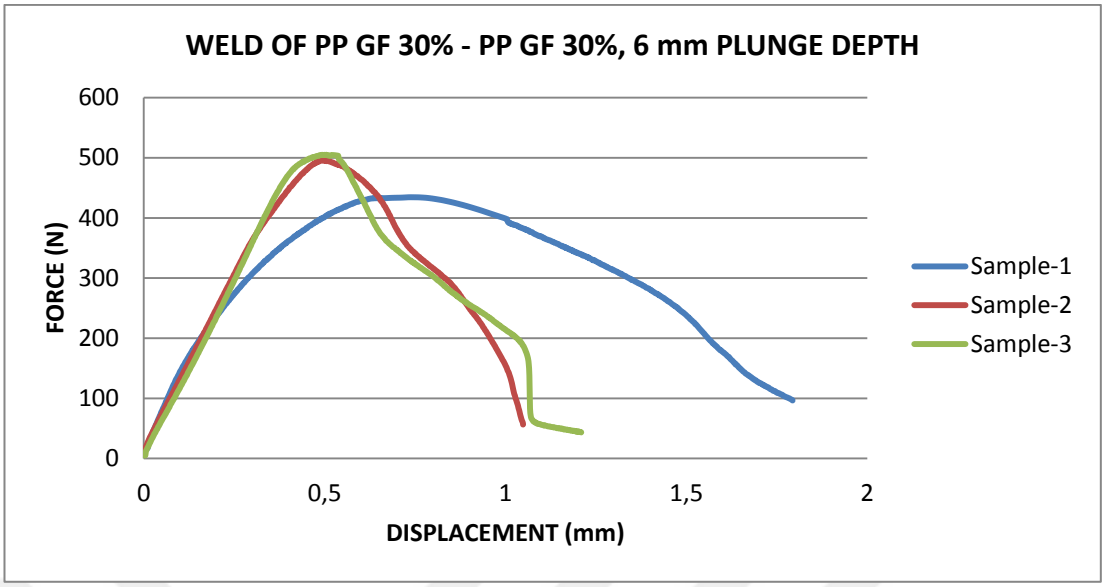


Figure 4.26 Lap shear test results of PP GF%30 sheets – 6 mm plunge depth

Table 4.4 summarizes the measured maximum forces for welded PP GF%30. Maximum measured force has been obtained in 5.5 plunge depth in this welding combination.

Table. 4.4 Measured maximum forces of PP GF%30

| | Maximum Forces (N) | | | |
|---|---|---|---|---|
| Sample Definition | Sample-1 | Sample-2 | Sample-3 | Average |
| Samples - 5mm Plunge Depth | 644.8 | 356.5 | 524 | 508.4 |
| Samples - 5.5mm Plunge Depth | 569.4 | 710 | 632.5 | 637.3 |
| Samples - 6mm Plunge Depth | 434.4 | 496 | 505 | 478.5 |

## 4.4 PC – AA 5052-H32 FSSW Combination

The hybrid joint of 4 mm thick polycarbonate sheet and 3 mm thick AA-5052-H32 sheet was tried and the weld application was carried out with two different weld parameter conditions. The first set of weld parameters are as given below;

- 800 rpm rotational speed,
- 4 mm plunge depth,
- 16 mm/min plunge rate.

In this trial, PC sheet was placed under the aluminum sheet and aluminum filler plate was used. In the weld process, the maximum temperature was measured as approximately 340 °C using an infrared thermometer.

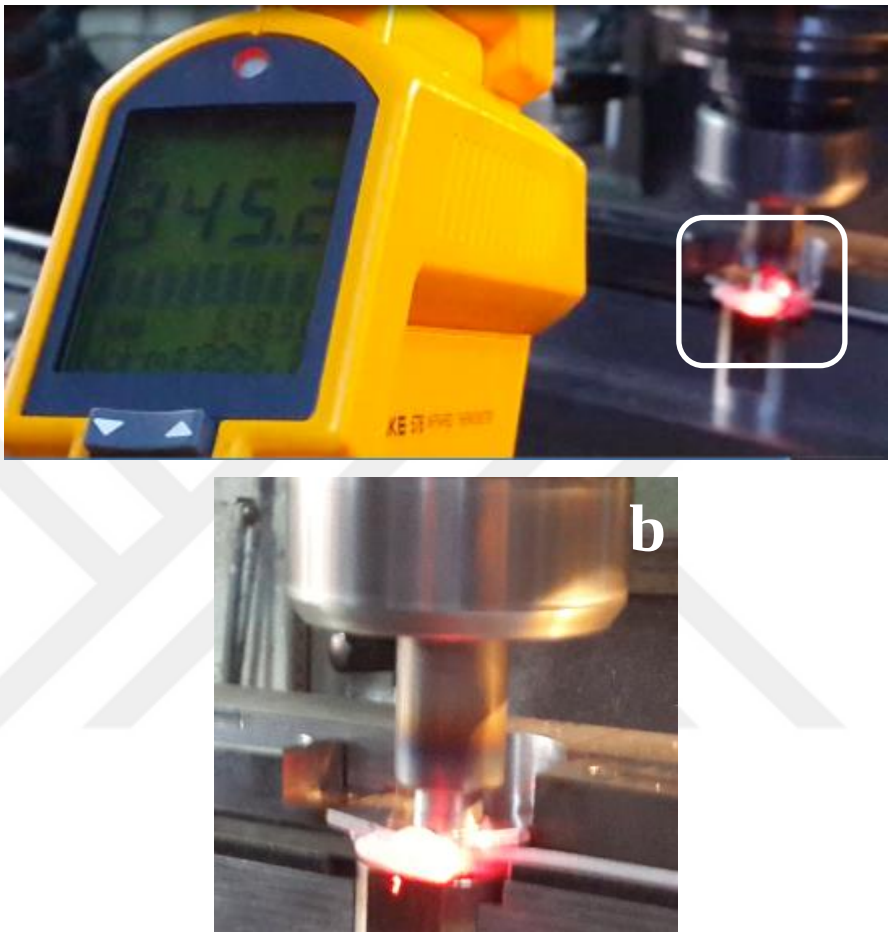


Figure 4.27 (a) The measured maximum temperature, (b) measurement region (Personal archive, 2017)

During the weld process, the polycarbonate sheet melted because the maximum temperature of weld region was higher than the melting temperature of the PC material. For that reason, a successful hybrid joint was not obtained, Figure 4.28 shows the weld sample of this trial.

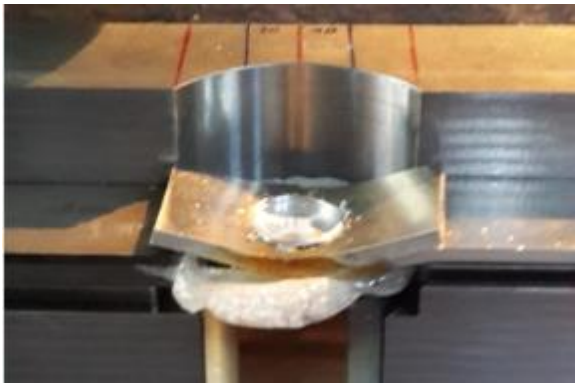

Figure.4.28 The first trial sample of PC – aluminum sheet (Personal archive, 2017)

In the second weld trial, below stated weld parameters were used and the maximum temperature was measured as approximately 300 °C. Similar to the first trial, a successful hybrid joint was not obtained and Figure 4.29 shows the weld sample of the second weld trial.

- 400 rpm rotational speed,
- 4 mm plunge depth,
- 16 mm/min plunge rate.

Figure 4.29The second trial sample of PC – aluminum sheet (Personal archive, 2017)

### 4.5 Investigation of PP 30% GF - AA 5052-H32 FSSW Combination

The hybrid joint of 4 mm thick PP 30% GF sheet and 3 mm thick AA 5052-H32 sheet was tried and the parameters were as given below;

- 400 rpm rotational speed,
- 4 mm plunge depth,
- 16 mm/min plunge rate.

In this trial, PP 30% GF sheet was placed under the aluminum sheet and aluminum filler plate was used as similar to previous hybrid joint application. The maximum temperature was measured as approximately 240 °C in the weld region using an infrared thermometer. During the weld process, the PP 30% GF sheet melted because the maximum temperature of weld region was higher than the melting temperature of the material. For that reason, a successful hybrid joint was not obtained, Figure 4.30 shows the weld sample of this trial.

Figure 4.30 The welded sample of PP 30% GF - aluminum sheet (Personal archive, 2017)

# CHAPTER FIVE
# CONCLUSIONS

In the scope of this study, the results given below have been obtained after experimental studies.

1. A new version of overlap friction stir spot welding of AA 5052-H32, PC and PP GF30% has been carried out successfully as a similar joint.

2. Hybrid joint of the aluminum and polymers was not carried out using FSSW because of the melting temperature differences of the materials. However, this study, which has a new version of friction stir spot welding method and a special welding apparatus can be used as a reference for other similar studies related to hybrid joints.

3. In FSSW of aluminum and polycarbonate sheets, it was found out that when the plunge depth increases, the dome structure height and the tensile shear strength increase relatedly.

4. It is found that the dimensions of dome structure, namely the height and width, are related to plunge depth.

5. Stir zone area is related to plunge depth of FSSW. In aluminum sheet weld applications, it is observed that increasing the plunge depth causes a larger stir zone area.

6. The designed welding apparatus was used successfully for similar material welding. This welding apparatus and the welding method can be used as reference for other studies.

For the future studies, this method and the welding apparatus can be used for the joining of other similar materials and to evaluate the effect of different welding parameters such as rotational speed, plunge rate etc. on mechanical properties by

taking this study as a reference. In this study, polymers have melted and deformed because of the high welding temperature during friction stir spot welding. In hybrid joint of aluminum alloys and polymers, friction stir spot welding of different materials, which have a little difference in melting temperature can be carried out.

## REFERENCES


Aalco, Aluminum Alloy 5052 - H32 Sheet and Tread plate (n.d.).Retrieved May 27, 2017, from [http://www.aalco.co.uk/datasheets/Aluminum-Alloy-5052-H32-Sheet-and-Tread plate_138.ashx]

Allen, C. & Arbegast, W.(2005). Evaluation of Friction Spot Welds in Aluminum Alloys. SAE Technical Paper. 01-1252.

Arıcı, A., & Mert, Ş. (2008). Friction Stir Spot Welding of Polypropylene. *Journal of Reinforced Plastics and Composites*, 27, 2001-2004.

Awang, M. (2007). *Simulation of Friction Stir Spot Welding (FSSW) Process: Study of Friction Phenomena*. PhD Thesis, West Virginia University, Morgantown, West Virginia.

Badarinarayan, H.,Shi, Y., Li, X., Okamoto, K. (2009). Effect of Tool Geometry on Hook Formation and Static Strength of Friction Stir Spot Welded Aluminum 5754-O Sheets. *International Journal of Machine Tools&Manufacture 49*, 814–823.

Bakavos, D., & Prangnell, P., B. (2009). Effect Of Reduced or Zero Pin Length and Anvil Insulation On Friction Stir Spot Welding Thin Gauge 6111 Automotive Sheet. *Science and Technology of Welding and Joining*, 14, 442-456.

Bakavos, D., Chen, Y., Babout, L., Prangnell P. (2011). Material Interactions in a Novel Pinless Tool Approach to Friction Stir Spot Welding Thin Aluminum Sheet. *The Minerals, Metals & Materials Society*, 42A, 1266-1282.

Bilici, M., K., & Yükler, A., I. (2012). Influence Of Tool Geometry and Process Parameters On Macrostructure and Static Strength In Friction Stir Spot Welded Polyethylene Sheets. *Materials and Design 33*, 145–152.

BPF, Polycarbonate PC (n.d.). Retrieved May 30, 2017, from http://www.bpf.co.uk/plastipedia/polymers/Polycarbonate.aspx.

Campbell, F., C. (2006). Aluminum. *Manufacturing Technology for Aerospace Structural Materials*. (15-90). Great Britain: Elsevier Ltd, from www.elsevier.com.

Cole, G.,S., & Sherman, A., M. (1995). Lightweight Materials for Automotive Applications. *Materials Characterization, 35*:3-9.

Davis, J., R. (2001). Aluminum and Aluminum Alloys. *Alloying: Understanding the Basics*, (351-416). ASM İnternational, from www.asminternational.org.

Er, O. (2010). *Elektrik Direnç ve Sürtünme Karıştırma Nokta Kaynaklı Alüminyum Alaşımı Bağlantıların Mekanik Özelliklerinin İncelenmesi*. Yüksek Lisans Tezi, Mersin Üniversitesi, Mersin.

Gean, A., Westgate, S., A., Kucza, J., C., Ehrstrom, J., C. (1999). Static and Fatigue Behavior of Spot-Welded 5182-0 Aluminum Alloy Sheet. *Welding Journal, 78*, 81-86.

Gonçalves, J., Santos, J., F., Canto, L., B., Amancio-Filho, S., T. (2015). Frictionspotweldingofcarbon fiber-reinforcedpolyamide66laminate. *Materials Letters159*, 506–509.

Globalspec, Properties of Thermoset Plastics (n.d.). Retrieved June 2, 2017, from http://www.globalspec.com/reference/25161/203279/html-head-chapter-1-properties-of-thermoset-plastics.

Hancock, R. (2004). *Welding Journal*. (2004), 40-43.

IPS, Polycarbonate (n.d.). Retrieved May 24,2017, International Polymer Solutions Inc. 5 Studebaker, from Irvine, CA 92618.

Iwashita, T. (2003). *Method and Apparatus For Joining*. US Patent Issued. Retrieved August 5, 2003.

Jambhale, S., Kumar, S., Kumar, S. (2015). Effect of Process Parameters & Tool Geometries on Properties of Friction Stir Spot Welds: A Review. *Universal Journal of Engineering Science* 3(1): 6-11.

Jeon, C.,S., Hong, S., T., Kwon, Y., J., Cho, H., H., Han, H., N. (2012). Material properties of friction stir spot welded joints of dissimilar aluminum alloys. *Trans. Nonferrous Met. Soc. China 2*, 605−613.

Khan, M., I., Kuntz, M., L., Su, P., Gerlich, A., North, T., Zhou, Y. (2007). Resistance and friction stir spot welding of DP600: a comparative study. *Science and Technology of Welding and Joining*. *12*, 175-182.

Lambiase, F., Paoletti, A., Di Ilio, A. (2015). Mechanical behaviour of friction stir spot welds of polycarbonate sheets. *Int J Adv Manuf Technol 80*:301–314.

Leon de M. & Shin S. H., (2016). Material flow behaviours during friction stir spot welding of lightweight alloys using pin and pinless tools. *Science and Technology of Welding and Joining*, 21:2, 140-146.

Mallick, P.K. (2010) *Materials, design and manufacturing for lightweight vehicles (1-174).* Woodhead Publishing Limitied. Materials for lightweight automotive structures. Newyork: CRC Press.

Martinsen, K.,S., Hu, J., Carlson, B., E. (2015). Joining of dissimilar materials. *CIRP Annals - Manufacturing Technology 64*, 679–699.

MatWeb, Aluminum 5052-H32 (n.d.). Retrieved June 7, 2017, from http://www.matweb.com/search/datasheet_print.aspx?matguid=96d768abc51e4157a1b8f95856c49028.

Menczel J., D. & Prime R., B. (Eds). (2008). Thermal Analysis of Polymers, Fundamentals and Applications. New Jersey.

Mert, Ş., & Mert, S. (2013). Sürtünme Karıştırma Nokta Kaynak Yönteminin İncelenmesi. *Journal of Advanced Technology Sciences, 2* (1), 26-35.

Miller, W.S., Zhuang, L., Bottema, J., Wittebrood, A.J., De Smet, P., Haszler P., et al. (2000). Recent development in aluminium alloys for the automotive industry. *Materials Science and Engineering* A280, 37–49.

Mishra, R., S., & Mahoney, M., W. (2007). Introduction. *Friction Stir Welding and Processing,* (1-5). Mahoney: ASM İnternational, www.asminternational.org.

Modor Plastics, Thermoset Vs. Thermoplastics (n.d.). Retrieved June 13, 2017, from http://www.modorplastics.com/thermoset-vs-thermoplastics.

Okamoto, K., Hunt, F. & Hirano, S. (2005). Development of Friction Stir Welding Technique and Machine for Aluminum Sheet Metal Assembly- Friction Stir Welding of Aluminum for Automotive Applications. SAE Technical Paper 2005-01-1254.

Önol A., T. (2010). *Microstructural Characterizaton and Mechanical Property Determination of Overlap Friction Stir Welding of Alüminum and Copper*. M. Sc. Thesis, Dokuz Eylül University, İzmir.

Pabandi, H., K., Movahedi, M., Kokabi, A., H. (2017). A New Refill Friction Spot Welding Process For Aluminum/Polymer Composite Hybrid Structures. *Composite Structures, 174,* 59-69.

Piccini, J., M., & Svoboda, H., G. (2015). Effect of the tool penetration depth in Friction Stir Spot Welding (FSSW) of dissimilar aluminum alloys. *Procedia Materials Science 8*, 868 – 877.

Polycarbanate (n.d.). Retrieved May 25,2017, from http://www.extatico.es/extaticodoc/POLICARBONATO.pdf.

Polycarbonate Properties (n.d.). Retrieved May 25,2017, from http://www.gplastics.com/pdf/polycarbonate.pdf

Polymertechnology, A Guideto Polycarbonatein General (n.d.). Retrieved May 25,2017, from http://www.ptsllc.com/intro/polycarb_intro.aspx.

Polypropylene Properties (n.d.). Retrieved May 25,2017, from http://www.campusplastics.com

Rodgers B. (Ed.). (2004). Rubber Compounding Chemistry and Applications. Newyork: Marcel Dekker Press.

Sakano, R., Murakami, K., Yamashita,K., Hyoe, T., Fujimoto, M., Inuzuka, M. et al., (2001). *Proceedings of the Third International Symposium of Friction Stir Welding*. Kobe, Japan.

Schwartz, M. (2011). *Innovations in Materials Manufacturing, Fabrication and Enviromental Safety.* Taylor & Francis Group. Newyork: CRC Press.

Singh, J. & Dubey, R.C., (2009). Organic Polymer Chemistry, Global Media, India, 1-2.

Sudağ, M. (2011). *Alüminyum Alaşımı Malzemelerin Sürtünme Karıştırma Nokta Kaynağı ile Birleştirilmesi ve Dayanım Özelliklerinin Araştırılması*. Yüksek Lisans Tezi, Gazi Üniversitesi, Ankara.

Thornton, P., H., Krause, A., R., Davies, R., G. (1996). The Aluminum Spot Weld. *Welding Journal*, 75, 101-108.

Tier, M., D., Rosendoa, T., S., dos Santos, J., F., Huberb, N., Mazzaferroc, J., A., Mazzaferro, C., P., et al. (2013). *Journal of Materials Processing Technology 213*, 997– 1005.

Tozaki, Y., Uematsub, Y., Tokajib, K. (2010). A newly developed tool without probe for friction stir spot welding and its performance. *Journal of Materials Processing Technology 210*, 844–851.

Tozaki,Y., Uematsb, Y., Tokaji, K. (2007). Effect of Tool Geometry on Microstructure and Static Strength in Friction Stir Spot Welded Aluminium Alloys. *International Journal of Machine Tools & Manufacture 47*, 2230–2236.

Venukumar, S., Muthukumaran, S., Yalagi S., G., Kailas, S., V. (2014). Failure modes and fatigue behavior of conventional and refilled friction stir spot welds in AA 6061-T6 sheets. *International Journal of Fatigue 61*, 93-100.

Venukumar, S., Yalagi, S., Muthukumaran S. (2013). Comparison of microstructure and mechanical properties of conventional and refilled friction stir spot welds in AA 6061-T6 using filler plate. *Trans. Nonferrous Met. Soc. China 23*, 2833−2842.

Venukumara, S., Babya, B., Muthukumaran, S., Kailasb, S., V. (2014). Microstructural and mechanical properties of walking friction stir spot welded AA 6061-T6 sheets. *Procedia Materials Science 6*, 656 – 665.

Wang, D., A., & Lee, S., C. (2007). Microstructures and failure mechanisms of friction stir spot welds of aluminum 6061-T6 sheets. *Journal of Materials Processing Technology 186*, 291–297.

Yang, X., W., Fu, T., Li, W., Y. (2014). Friction Stir Spot Welding: A Review on Joint Macro and Microstructure, Property, and Process Modelling. *Advances in Materials Science and Engineering*, 1-12.

Yoon, S., Kang, M., Kwon, Y., Hong, S., Park, D., Lee, K. Et al. (2012). Influences of Tool Plunge Speed and Tool Plunge Depth on Friction Spot Joining of AA5454-O Aluminum Alloy Plates With Different Thicknesses. *Trans. Nonferrous Met. Soc. China 2*, 629−633.

Zakut M. (2012). Effects of Huntite/Hydromagnesite on Capasity of Flame Retardancy, Mechanical and Physical Properties of Polypropylene. M. Sc. Thesis, İstanbul Technical University, İstanbul.

Zhang, Z., Yang, X., Zhang, J., Zhou, G., Xu, X., Zou, B. (2011). Effect of welding parameters on microstructure and mechanical properties of friction stir spot welded 5052 aluminum alloy. *Materials and Design 32*, 4461–4470.